1 CLASS VI PERMIT APPLICATION NARRATIVE

40 CFR 146.82(a)

TULARE COUNTY CARBON STORAGE PROJECT (TCCSP)

Facility Information

Facility (site) Name: Tulare County Carbon Storage Project (TCCSP)
Facility Operator: TCCSP, LLC.

Facility Contact: [redacted]

Project Location: [redacted] Tulare County, California

Injection Well Name and Coordinates:

Well Name	Latitude	Longitude
TCCSP_INJ-1	[redacted]	[redacted]
TCCSP_INJ-2	[redacted]	[redacted]

Table of Contents

List of Tables

List of Figures

List of Acronyms/Abbreviations

2D	2-Dimensional
3D	3-Dimensional
AoI	Area of Interest
AoR	Area of Review
bbl/d	Barrels per day
BHP	Bottom Hole Pressure
CCS	Carbon capture and storage
CO_2	Carbon dioxide
CMG	Computer Modelling Group
D_H	Hydraulic Diameter
DRM	Dynamic Reservoir Model
EoS	Equation of State
EPA	Environmental Protection Agency
f_D	Darcy's Friction Factor
ft	feet
g	Acceleration due to Gravity
GEM	General Equation of State
KB	Kelly Bushing
$k_{r,CO2}$	CO_2 Relative Permeability
kh	Permeability-Thickness Product
k_h	Absolute Horizontal Permeability
k_v	Absolute Vertical Permeability
$k_{r,w}$	Water Relative Permeability
mg/L	milligrams per liter

MIP	Mercury Intrusion Porosimetry
MIT	Mechanical Integrity Testing
MMt	Millions of Metric tons
MMtpa	Millions of Metric tons per annum
ΔP	Pressure Drop
ΔP_{TH}	Threshold Pressure
PISC	Post-Injection Site Care
P_{grid}	Grid Block Pressure
pH	Potential Hydrogen
ppm	Parts per Million
psi	Pounds per square inch
psia	Pounds per square inch, absolute
ρ	Fluid Density
ρ_i	Injection Zone Fluid Density
ρ_u	Underground Source for Drinking Water Fluid Density
RCA	Routine Core Analysis
R_e	Reynolds Number
SCA	Specialized Core Analysis
SEM	Static Earth Model
S_{grmax}	Maximum Residual Gas Saturation
SS	Subsea
S_{wconn}	Connate Water Saturation
S_{wirr}	Irreducible Water Saturation
T_{grid}	Grid Block Temperature
TVD	True Vertical Depth
UIC	Underground Injection Control
USDW	Underground Source of Drinking Water
U.S. DOE	United States Department of Energy
U.S. EPA	United States Environmental Protection Agency
v	Fluid Velocity
z_i	Injection Zone Top Depth
z_u	Underground Source for Drinking Water Bottom Depth

1.1 Project Background and Contact Information

GSDT Submission - Project Background and Contact Information

GSDT Module: Project Information Tracking
Tab(s): General Information tab; Facility Information and Owner/Operator Information tab

Please use the checkbox(es) to verify the following information was submitted to the GSDT:
☒ Required project and facility details ***[40 CFR 146.82(a)(1)]***

1.1.1 Project Background

TCCSP, LLC. proposes to construct an industrial-scale carbon capture and storage (CCS) hub located in Tulare County, California (**Figure 1-1**). Regional and site-specific geological characterization indicates that the subsurface geology of the Southern San Joaquin basin is comprised of high-quality storage reservoirs and confining units that can achieve large-scale CO_2 storage of at least [redacted] million metric tons of CO_2 over a [redacted] injection period. The Tulare County Carbon Storage Project (TCCSP) aims to capture CO_2 emissions from the [redacted], located in [redacted], California. The project has been designed to inject a total of [redacted] of CO_2 per year into the [redacted]. The current project plan includes developing a CO_2 storage terminal at or near [redacted] to support operational storage and offloading of CO_2 to meet injection rate requirements. TCCSP, LLC.'s current project design includes potential emitters offloading pipeline- and injection-grade CO_2 at the TCCSP terminal. The CO_2 transport infrastructure will comprise nearly [redacted] miles of 12-inch trunk line to transport CO_2 from the [redacted] CO_2 terminal to the injection site. TCCSP, LLC. proposes to construct two CO_2 injection wells, [redacted] to ensure safe, secure, and long-term CO_2 storage and to comply with 40 CFR 146.90.

TCCSP, LLC. has conducted a thorough evaluation of the regional, local, and site-specific geology, legacy well infrastructure, injection site design, and project planning to support the development of this UIC Class VI application with the U.S. Environmental Protection Agency (EPA) Region 09. Subsurface data were acquired to evaluate the subsurface storage complex and include two-dimensional seismic data, legacy oil/gas well logs and core, subsurface well test data, groundwater well data, and published technical literature. These subsurface data were used to generate a static geologic model to characterize subsurface reservoirs and confining units and assess the viability of CO_2 storage. The three-dimensional static earth models were implemented in dynamic reservoir simulations to evaluate the CO_2 plume behavior for [redacted] post-injection, to confirm plume stabilization with further discussion in the **Area of Review and Corrective Action Plan**.

There are several notable surface features near the project area. **Figure 1-1** shows the location of all surface bodies of water, the town of [redacted] numerous roads, including [redacted] and land containing residential and commercial buildings. Commercial buildings in the TCCSP project area are predominantly comprised of dairies. **Figure 1-1** also shows the location of the

[redacted]

1.1.2 Partners and Collaborators

TCCSP is owned and operated by TCCSP, LLC. [redacted] will be the primary CO_2 sources for TCCSP. Both primary sources are [redacted] California, approximately [redacted] of the proposed TCCSP storage site.

Table 1-1. Partners and Collaborators.

Partner	Role	Contact Information
TCCSP, LLC.	Project owner and operator	[redacted]
[redacted]	Primary CO_2 Source	[redacted]
[redacted]	Primary CO_2 Source	[redacted]

1.1.3 State, Local, and Tribal Contacts

TCCSP, LLC. has been working with the following state and county level offices to develop this project:

California Department of Conservation Geologic Energy Management Division (CalGEM)
Point of Contact: [redacted]
Phone: [redacted]
Email: [redacted]@conservation.ca.gov

Tulare County Resource Management Agency
Point of Contact: [redacted]
Email: [redacted]@tularecounty.ca.gov

The TCCSP project area does not interact with any tribal lands. Contact information for local tribes in Tulare County are provided below.

(1) Santa Rosa Rancheria Tachi Yokut Tribe
Chairperson: [redacted]
Address: [redacted]
Phone: [redacted]
Email: not listed

(2) Tule River Indian Tribe
Chairperson: [redacted]
Address: [redacted]
Phone: [redacted]
Email: [redacted]

1.1.4 Project Timeframe

TCCSP, LLC. plans to inject CO_2 for [redacted], followed by a post-injection monitoring period of [redacted]. The post-injection timeframe has been chosen after evaluating the results of the dynamic reservoir modeling. Additional details on the post-injection timeframe can be found in the **Post-Injection Site Care and Site Closure Plan.**

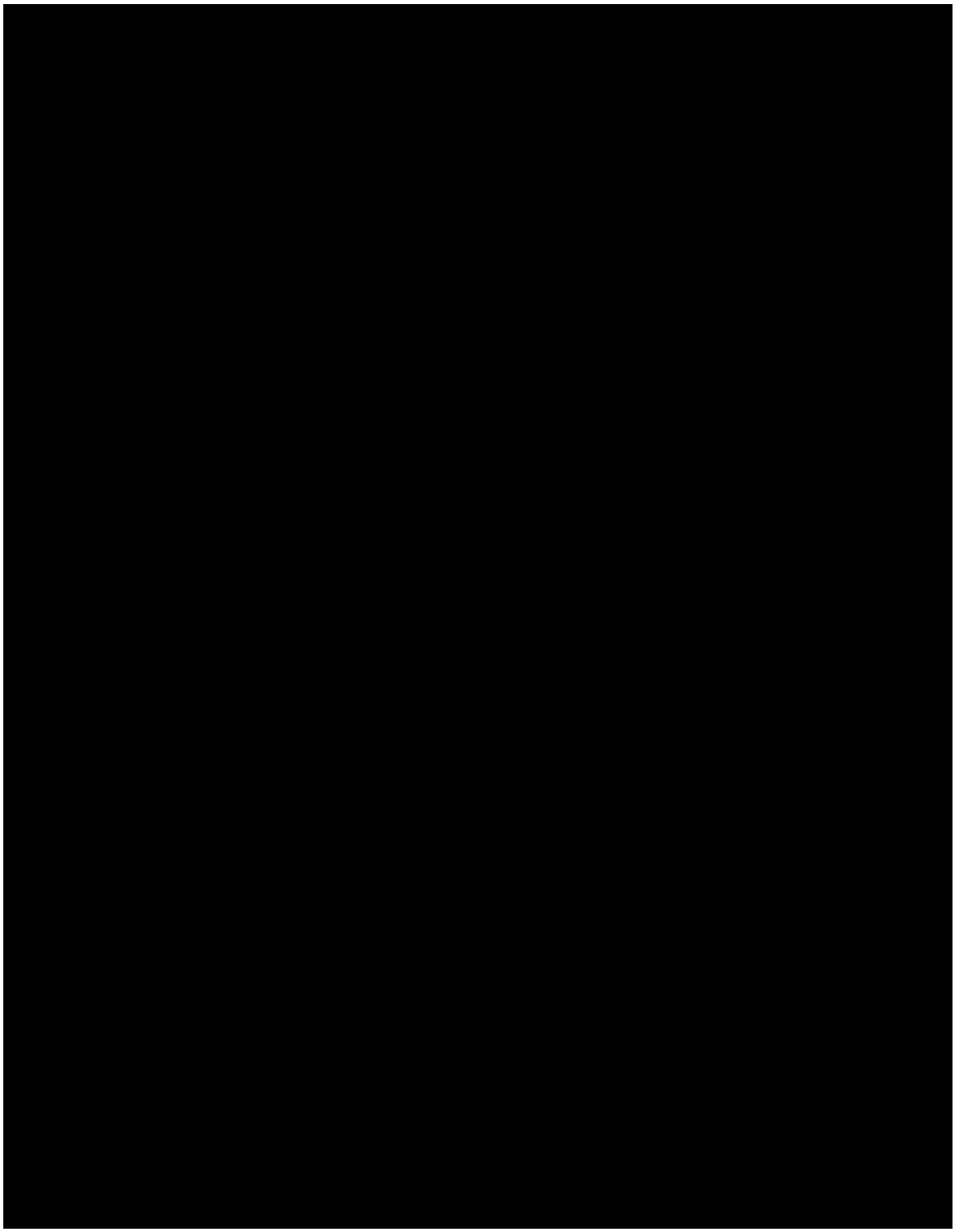

Figure 1-1. Location map of the Tulare County Carbon Storage Project (TCCSP) site located in Tulare County, California. The TCCSP_INJ-1 and TCCSP_INJ-2 CO_2 injection wells are located [redacted].

1.1.5 Proposed Injection Mass and CO_2 Source

TCCSP, LLC. plans to inject [redacted] of CO_2 over [redacted] at the TCCSP site using two injection wells, TCCSP_INJ-1 and TCCSP_INJ-2, at a combined yearly injection rate of [redacted]. Constant injection rates of [redacted] and [redacted] were assigned to the TCCSP_INJ-1 and TCCSP_INJ-2, respectively. TCCSP_INJ-1 will inject into the [redacted] for the entire [redacted] injection period. TCCSP_INJ-2 targets the [redacted] of injection and the [redacted].

CO_2 Sources

The CO_2 for injection and storage at TCCSP is anticipated to be sourced from multiple industrial sources. A base amount of [redacted] will be sourced from the [redacted], California (**Figure 1-1**). CO_2 produced at [redacted]. Combined, these [redacted]. [redacted] CO_2 is currently being captured at food-grade specification levels, and its nominal composition will remain similar for geologic storage. Please see the **Appendix** for the latest available data on the CO_2 stream from [redacted].

TCCSP, LLC. is negotiating with potential CO_2 emitters that have expressed interest in collaborating to geologically sequester their CO_2. TCCSP, LLC. has established a minimum injection specification of the CO_2 stream listed as listed in **Table 1-2**. TCCSP, LLC. does not bear liability or responsibility of emitters to deliver CO_2 to [redacted] at the minimum design specification noted in **Table 1-2**. However, TCCSP, LLC. will ensure the CO_2 transported to the injection site and thereafter injected at TCCSP will meet the physical and chemical specifications noted in **Table 1-2**. One potential non-named emitter has entered into an agreement with TCCSP, LLC, for [redacted] of specification-grade CO_2, with day-one capacity to be brought to [redacted]. TCCSP, LLC. is in negotiations with other potential emitters in Tulare and Kern counties for an additional [redacted] to bring the total annual injection mass to [redacted] There are no agreements in place with emitters other than [redacted]. TCCSP, LLC. will confirm to the Region 09 UIC Director that the CO_2 sourced from these emitters will conform to the minimum design specifications listed in **Table 1-2**. TCCSP, LLC. will also provide the exact location of the source relative to the storage facility, as well as details on the proposed mode of CO_2 transportation from each emitter facility to the storage facility.

Table 1-2. Minimum desired CO_2 stream specification at TCCSP.

Component[1]	Specification	Unit
[redacted]		

A master gathering manifold located at or near [redacted] will be used to combine the CO_2 streams from [redacted] as well as other potential emitters into a single stream that will be transported to the storage site via a [redacted] (**Figure 1-1**). [redacted] and monitor their physical and chemical characteristics to comply with 40 CFR 146.90(a). Please see section **7.3** of the **Testing and Monitoring Plan** for additional details on CO_2 stream sampling and analysis. Once the CO_2 sources and the physical and chemical characteristics of the CO_2 transported to the CO_2 gathering station in [redacted] for sequestration are determined, TCCSP, LLC. will computationally model fluid mixing during capture and the thermodynamics of mixed streams at the CO_2 gathering station. Based on the results of this mixing model, TCCSP, LLC. will review **Table 1-2** to confirm the final stream specification and modify the computational model and design bases as necessary.

As shown in **Table 1-2**, the CO_2 stream specification is that of [redacted]. This specification has been established to minimize the effect of impurities on phase behavior of CO_2 and maximize the compatibility of construction materials with CO_2 stream. Therefore, fluid flow computational modeling conducted for TCCSP [redacted] to model the area of review as discussed in the **Area of Review and Corrective Action Plan**. TCCSP, LLC. will compare the phase behavior of [redacted], based on the stream specification derived from agreements with emitters and the requisite thermodynamic modeling of mixing streams noted above. If noticeable changes are observed, the current computational models will be updated and/or additional sensitivity analyses will be conducted with CO_2 stream specification as a parameter to reflect the physical and chemical characteristics of the CO_2 stream on TCCSP's project design.

During project startup, TCCSP, LLC. will gather a [redacted] to evaluate physical and chemical data as discussed in section **7.3. Carbon Dioxide Stream Analysis** of the **Testing and Monitoring Plan**. [redacted].

1.1.6 Injection Depth Waiver

No injection depth waiver is currently sought in this application.

1.1.7 Aquifer Exemption

No aquifer exemption is currently sought in this application.

1.1.8 Applicable Permit Information Under 40 CFR 144.31(e)(1) through (6)

Table 1-3 provides information on activities conducted by TCCSP, LLC. for this project which require it to obtain permits under the Resource Conservation and Recovery Act (RCRA), Underground Injection Control (UIC), the National Pollution Discharge Elimination system (NPDES) program under the Clean Water Act (CWA), or the Prevention of Significant Deterioration (PSD) program under the Clean Air Act.

Table 1-3. Permit Information Required under 40 CFR144.31(e)(1).

Regulation	Jurisdiction	Agency	Relevant Permits
Resource Conservation and Recovery Act (RCRA)	Federal	Federal – U.S. Environmental Protection Agency (U.S. EPA) – Region 09	Not Anticipated
Underground Injection Control (UIC) Program	Federal	Federal – U.S. Environmental Protection Agency (U.S. EPA) – Region 09	Class VI Injection Well Permits
National Pollutant Discharge Elimination System (NPDES) – Clean Water Act (CWA)	State	Central Valley Regional Water Quality Control Board	[redacted]
Prevention of Significant Deterioration (PSD) – Clean Air Act (CAA)	State	San Joaquin Valley Air Pollution Control District	

1.1.9 Contact Details for TCCSP, LLC.

Facility (site) Name: Tulare County Carbon Storage Project (TCCSP)
Facility Operator: TCCSP, LLC.
Facility Contact: [redacted]
Project Location: [redacted] Tulare County, California

Well Name	Latitude	Longitude
TCCSP_INJ-1	[redacted]	[redacted]
TCCSP_INJ-2	[redacted]	[redacted]

1.1.9.1 Applicable SIC Codes

Per 40 CFR 144.31(e)(3), applicable SIC codes are listed below:

[redacted]

Name: TCCSP, LLC.
Address: [redacted]
Telephone number: [redacted]
Ownership status: Limited liability corporation
Nature of the entity (Federal, State, private, public): Private

1.1.9.2 Other permit information required under 40 CFR 144.31(e)(6)

The TCCSP project related activities conducted by TCCSP, LLC. are listed in **Table 1-4**. **Table 1-5** summarizes the project related applicable permits.

Table 1-4. Activities conducted by TCCSP, LLC. and applicable permits as noted in 40 CFR 144.31(e)(6).

Regulation	Jurisdiction	Agency	Relevant Permits
Drilling Permits	Federal, State	Federal – U.S. Environmental Protection Agency (U.S. EPA) State – California Geologic Energy Management Division (CalGEM)	[redacted]
Nonattainment Program under CAA	State	San Joaquin Valley Air Pollution Control District	
California Endangered Species Act	State	California Department of Fish and Wildlife (CDFW)	Incidental take permit not anticipated
Water Quality Certification under Section 401 of the CWA	State	Central Valley Regional Water Quality Control Board	Not anticipated
Valid Access Agreements	County, Township/City	Tulare County Resource Management Agency (RMA)	In discussion
Encroachment Permits	County, Township/City	Tulare County Resource Management Agency (RMA)	In discussion

Table 1-5. Applicable permits and construction approvals as noted in 40 CFR 144.31(e)(6).

Permit	Jurisdiction	Relevant Permits
Hazardous Waste Management Program under RCRA	State	[redacted]
U.S. EPA UIC Program under SDWA	Federal	Class VI Injection Well Permits

Permit	Jurisdiction	Relevant Permits
National Pollutant Discharge Elimination System (NPDES) – Clean Water Act (CWA)	State	[redacted]
Prevention of Significant Deterioration (PSD) – Clean Air Act (CAA)	State	Not anticipated
Nonattainment Program under – Clean Air Act (CAA)	State	[redacted]
Dredge and Fill Permits under Section 404 of the - Clean Water Act (CWA)	State	Not anticipated

This project qualifies for review under CalGEM's California Environmental Quality Act (CEQA) process. TCCSP, LLC. is working on engaging an environmental services contractor to aid with this process. TCCSP, LLC. understands that the Tulare County RMA will serve as the lead CEQA agency.

1.2 Site Characterization

1.2.1 Regional Geology, Hydrogeology, and Local Structural Geology [40 CFR 146.82(a)(3)(vi)]

1.2.1.1 Regional Geologic Structures

The Tulare County Carbon Storage Project (TCCSP) is located nearly [redacted] of the [redacted] in Tulare County, California. The site is located within the Great Valley of California, which is a present-day alluvial plain divided into the Sacramento Basin to the north and the San Joaquin Basin (SJB) to the south. The SJB is separated from the Sacramento Basin to the north by the Stockton Fault and Stockton Arch and bounded south by the San Emigdio and Tehachapi mountains. The SJB is a northwest-trending asymmetric structural trough that comprises a wedge of sedimentary rocks up to 24,000 feet thick, deposited in a forearc setting. The SJB is surrounded by the Sierran magmatic arc to the east and the Coastal Ranges and San Andreas Fault Zone to the west as shown in **Figure 1-2** [1].

Scheirer and Magoon (2007) divided the SJB into three geographic zones including the northern, central, and southern zones, due to the locations of major changes in subsurface stratigraphy across the region [2]. The boundary between the northern and central areas is defined by the northern edge of marine deposition during the middle Miocene (~15 Ma), while the southern and central boundary reflects a facies change in the [redacted].

The basin has a steeply dipping southwest limb with a greater degree of structural deformation occurring near the San Andreas Fault Zone, a deep basin axis that trends northwest, and a more gently dipping northeast limb that progressively shallows to the east toward the Sierra Nevada Batholith (**Figure 1-2**). The SJB is floored by crystalline rocks overlain by a thick sequence of late Mesozoic-and Cenozoic-aged clastic sedimentary rocks. Sedimentary rocks within the basin were

initially deposited in a Mesozoic-aged forearc basin, which subsequently evolved into a successive ponded transform margin basin during the Cenozoic due to tectonic activity associated with the San Andreas Fault Zone [1,3]. The TCCSP site is located on the [redacted].

The Bakersfield Arch, located in central Kern County, further subdivides the southern SJB into the Buttonwillow sub-basin, also called the Tulare sub-basin, north of the arch, and the Maricopa (Tejon) sub-basin to the south, as shown **Figure 1-2** [4]. The Buttonwillow sub-basin is an asymmetrical depression, with a northwest-southeast structural gain and a major synclinal axis along the western margin of the sub-basin [4]. The TCCSP project site is located in the [redacted] of the SJB.

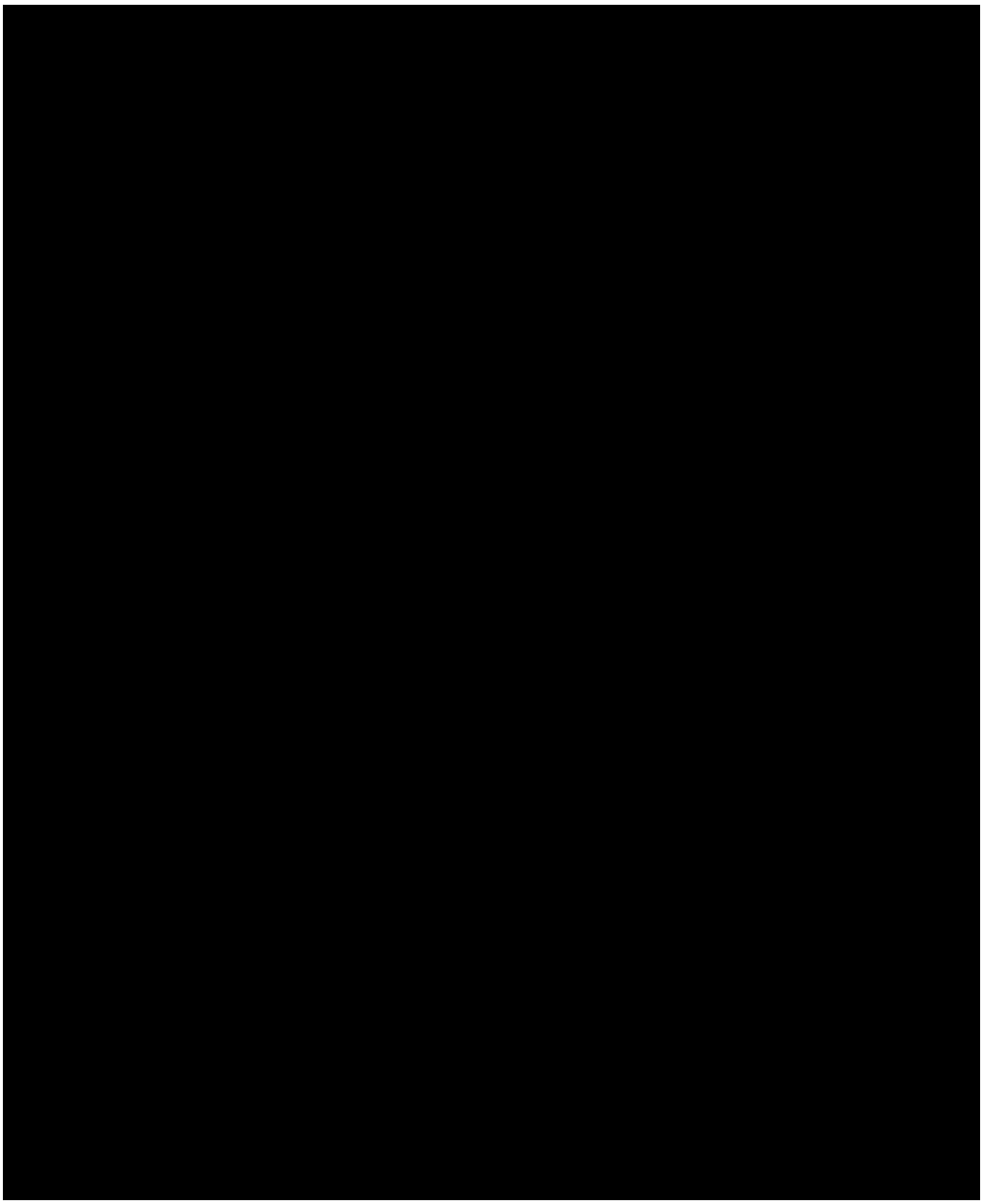

Figure 1-2. Location map of the San Joaquin Basin (SJB) showing the northern, central, and southern provinces. The star indicates the location of the TCCSP site. Modified from Magoon et al., (2009) [5].

1.2.2 Regional Lithostratigraphy and Megasequences

1.2.2.1 Regional Lithostratigraphy

The lithostratigraphy of the San Joquin basin (SJB) is complex, with each sub-basin (northern, central, and southern) featuring unique profiles, stratigraphic columns, and lithostratigraphic nomenclature. Lithostratigraphic units of the TCCSP area were identified and mapped based on regional cross-sections and stratigraphic framework [2,3,8]. The TCCSP project is located in the

[redacted] portion of the southern SJB and features geologic units and subsurface profiles of both the southern and central sub-basins. The lithostratigraphic columns used to conceptualize and build the TCCSP project are listed in **Figure 1-4**.

The regional and local subsurface stratigraphy at TCCSP comprises [redacted]. The TCCSP stratigraphic section is comprised of a mixed assemblage of [redacted] [8]. The following section features regional descriptions and characteristics of geologic units interpreted as present at or around the TCCSP site and within the interval of interest. The lithostratigraphic framework of the TCCSP project is introduced below, in ascending stratigraphic order (oldest to youngest).

[redacted]

The deepest clastic interval interpreted to be present at the TCCSP site is the [redacted], which immediately rests on top of the [redacted]. The [redacted] is a mixed assemblage of [redacted] within the TCCSP study area, with [redacted] [8]. The formation is interpreted to be deposited in a range of environments across the region, including [redacted].

[redacted]

The [redacted] overlies the [redacted] and is dominantly composed of [redacted] at the unit's base. Subsurface correlations sometimes combine the [redacted] with the [redacted] The interval transitions [redacted] and then predominantly [redacted] [8].

[redacted]

Within the study area, Bloch (1991) interpreted the [redacted] to rest atop the [redacted] and contain a [redacted], capped by an [redacted] [8]. The [redacted] was found to be predominantly [redacted], which transitions to [redacted] [2]. Bloch (1991) grouped the [redacted] with the [redacted] [8]. The [redacted] overlies the [redacted] at the project site but represents a [redacted] that caps the [redacted] of the project site.

[redacted]

The [redacted] is a major t[redacted]. The [redacted] is a [redacted] at the

base of the [redacted], with little published subsurface data or literature cover in the southern San Joaquin. However, in the northern SJB, the [redacted] [2]. In the northern province, the upper portion of the [redacted] [2]. [redacted] reaching [redacted] in the northern SJB [9]. The [redacted] is predominately a [redacted]. It transitions to [redacted] to the east.

[redacted]

The [redacted] along the southeastern margin of the southern SJB [1]. North of the Bakersfield Arch on the eastern basin flank, the [redacted] [2]. The [redacted] is predominantly [redacted]. It [redacted] to the [redacted] towards Tulare County, where it interfingers with [redacted]

[redacted]

The [redacted] is primarily divided into [redacted] near the study area, including the [redacted]. The [redacted] and demonstrates reservoir throughout the southern SJB, where it is [redacted] and [redacted] [8,10]. The [redacted] is a [redacted], sourced from the [redacted]. The interval outcrops [redacted] [10]. In the subsurface, the [redacted]. Within the TCCSP study area, the [redacted].

The [redacted] is a member of the [redacted] and [redacted] t [11]. The unit is a [redacted] [4]. Basinward, the [redacted] and undergoes a [redacted]. In outcrop, the [redacted] [10]. The [redacted] is a member of the [redacted] at the base of the interval and contains a [redacted] [10]. The [redacted] generally occupies a similar stratigraphic position within the transgressive sequence [redacted]. The basal section of the [redacted] [4,10]. The transition from [redacted]

[redacted] represents [redacted]. In the AoR, the [redacted]

The [redacted] was deposited following the [redacted] [4]. [redacted] [4]. The interval correlates stratigraphically with the [redacted] [2]. The [redacted] progressively [redacted].

The [redacted] that is overlain by the [redacted] [10]. The interval is predominantly [redacted] at the [redacted] [10]. The [redacted] b[redacted]. In more proximal positions, the [redacted].

[redacted]

The [redacted] is divided into [redacted]. Stratigraphic members of the [redacted] are described below.

[redacted]

The [redacted] and is capped by the [redacted]. The [redacted] [10]. The interval is generally [redacted] [4]. [redacted] [4]. The [redacted]. The [redacted] [4].

[redacted]

The [redacted] is a [redacted] with the [redacted] [8]. The [redacted], where it is a [redacted]. The interval is correlative with its [redacted] 10].

[redacted]

The [redacted] is overlain by a sequence of [redacted]. In well logs, the [redacted]. The [redacted]

[redacted]

The [redacted] overlies the [redacted] and [redacted] The [redacted] and, finally, the [redacted] [1]. Both the [redacted]. The [redacted] is the deepest Underground Source of Drinking Water (USDW) at the TCCSP site, and the [redacted]

Figure 1-3. Schematic sequence stratigraphic cross-section based on seismic reflection geometries showing lowstand, transgressive, and highstand systems tracts from the [redacted] Sequence Boundaries (SB). From Tye et al. (1993) [6].

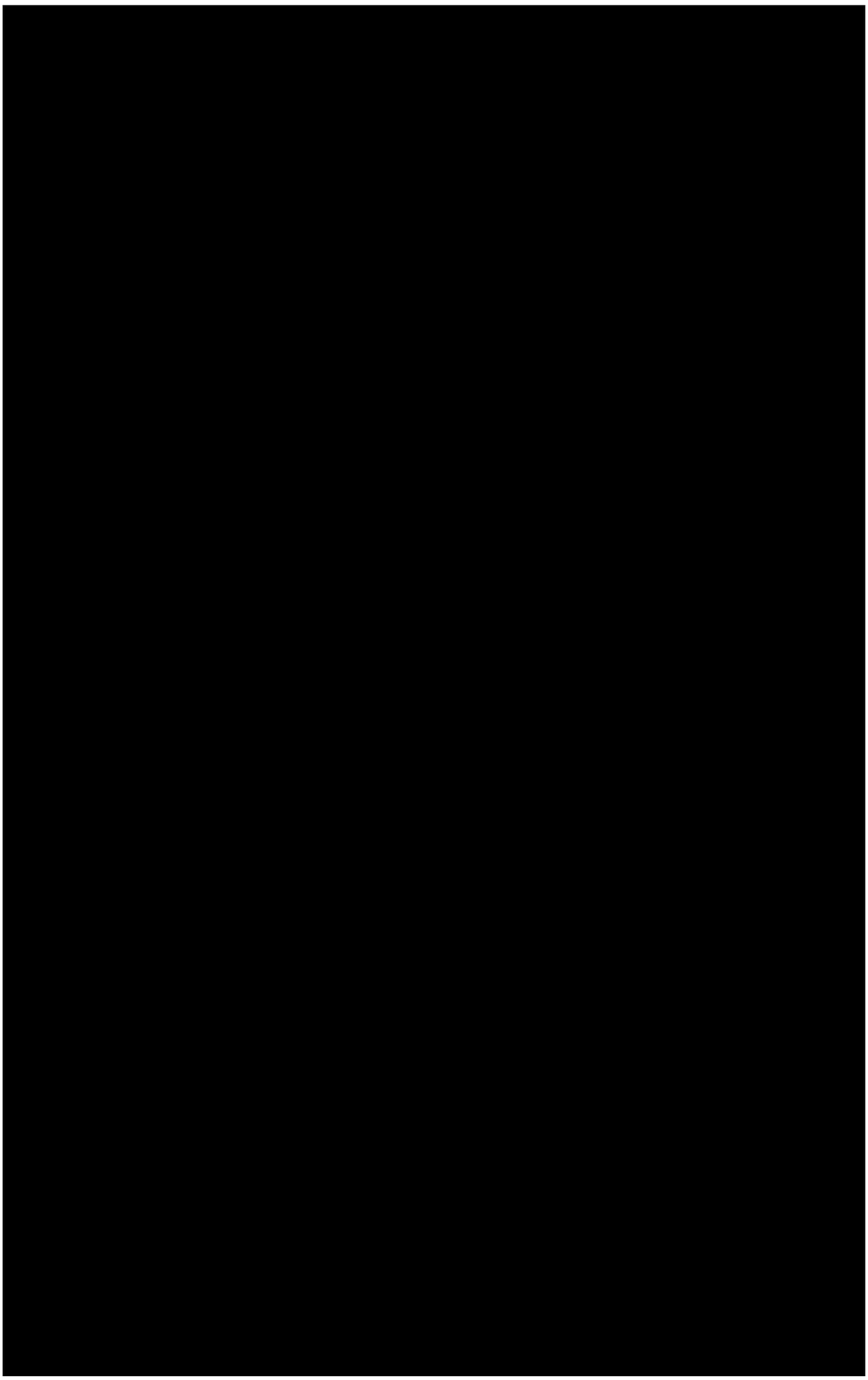

Figure 1-4. (Left) Regional chronostratigraphic column of the central and southern San Joaquin basin. The TCCSP site occurs in the [redacted] portion of the [redacted] San Joaquin basin and retains stratigraphic names of both the southern and central provinces. (Right) Type log from the [redacted] showing the subsurface stratigraphy. Modified from Scheirer and Magoon (2007) [2].

Figure 1-5. Diagrammatic stratigraphic cross-section showing stratigraphic relationships and well log correlations of [redacted] through the TCCSP site [3]. The [redacted] position along this cross-section is representative of the TCCSP site.

1.2.2.2 Regional Stratigraphic Megasequences

Sedimentary rocks within the SJB represent over [redacted] of deposition of a [redacted] column of marine and marginal-marine sediment in a ponded forearc to transform-margin basin setting, resulting from changes in accommodation space, sediment supply, global eustatic sea level change, basin subsidence/uplift, and climate change [3]. Basin-fill stratigraphy within the SJB has also been strongly influenced by the effects of tectonism on sedimentation. Large-scale tectonic megasequences coupled with changes in sea level have been interpreted and represent the transition from a forearc basin to a successive transform margin basin. [redacted] [2, 4]. [redacted] display more variable distribution patterns with sediment-source terranes located east, west, and south of the basin and were deposited during multiple tectonic episodes [4].

Stratigraphic nomenclature in the SJB is notoriously complex, with localized (often field-specific) informal naming mixed in with highly variable regional stratigraphic terminology. Johnson and Graham (2007) interpreted seven megasequences named after lithostratigraphic units and largely characterized the sedimentary basin-fill and stratigraphic architecture across the basin. Johnson

and Graham (2007) interpreted [redacted], named after key lithostratigraphic units, and bounded by major unconformities (e.g., [redacted]). These [redacted] recognized in some form basin-wide, representing major tectonic, climatic, and eustatic controls on basin fill. Numerous shorter-duration, higher-order cycles are nested within these [redacted], with variable preservation and stratigraphic expression basin-wide.

The [redacted] overlies the [redacted] and reflects forearc basin sedimentation deposited during widespread [redacted]. During this period, [redacted] and [redacted] sourced from the [redacted] were transported and deposited in the basin by [redacted]. The subsequent [redacted] was deposited next and represent the transition of the [redacted]. [redacted] were deposited, followed by a series of [redacted] and [redacted]

At [redacted] and a major basin reorganization initiated the [redacted], which deposited [redacted] in a deep and anoxic forearc basin. The [redacted] was deposited on top of the [redacted] during a period of renewed [redacted], which generated [redacted] with high reservoir quality and extensive lateral connectivity.

During the [redacted] was deposited as the [redacted] migrated to the [redacted] of the basin. [redacted] dominated the [redacted] SJB, while [redacted] were deposited to the [redacted]. Pronounced subsidence facilitated the deposition of the [redacted], which is the most [redacted] for the basin. The [redacted] to Recent [redacted] and was deposited in a [redacted] fill as the motion of the [redacted]. Along the basin margins, [redacted].

1.2.3 TCCSP CCS Complex

To properly evaluate CCS feasibility at the site and design a storage system capable of safe long-term containment of CO_2, the TCCSP_OBS-1 stratigraphic test well sought to collect data needed to validate the presence, subsurface extent, and chemical/physical characteristics of the following storage complex elements:

(1) Shallow freshwater aquifers and the deepest USDW aquifer
(2) Above zone monitoring intervals
(3) Regional confining units capable of sealing commercial quantities of CO_2 injectate
(4) Presence of intermediate baffling units or buffer zones
(5) Commercial-quality geologic reservoirs
(6) Sub-storage bottom seals.

Figure 1-6 depicts an overview of major geologic units interpreted to be present at the TCCSP site, TCCSP geologic units (as mapped and modeled), along with an overview of the storage system design components. A preliminary CCS assessment was conducted at the site prior to the formation of the TCCSP project, which identified the deepest USDW to likely be present within the [redacted] based on literature and well log analysis. The [redacted] was identified to be present at the site as an [redacted] which transitions up section to [redacted]. The unit was interpreted to feature several [redacted], of which the [redacted] to [redacted] occur as the [redacted], and therefore, was chosen as the primary confining zone, overlying all prospective TCCSP reservoirs.

The regionally extensive [redacted] were chosen as the primary CCS reservoir due to their [redacted]. The [redacted] interpreted to act as an [redacted].

The [redacted] was interpreted to be a [redacted] Limited information was available regarding the occurrence and reservoir profiles of [redacted] and sparse availability of literature within the [redacted]. The initial TCCSP stratigraphic framework and lithostratigraphic nomenclature of [redacted], as part of a regional cross-section depicting the units occurring across the TCCSP study area.

Initial mapping efforts during the planning stages of the TCCSP_OBS-1 well encountered [redacted]. To increase confidence, accuracy, and consistency of mapped TCCSP intervals, [redacted] in **Figure 1-6.** [redacted] Consistent interpretation and correlation of the [redacted], separated from the underlying [redacted]. The [redacted] was observed in [redacted] with

the [redacted]. The [redacted]. These units were [redacted]

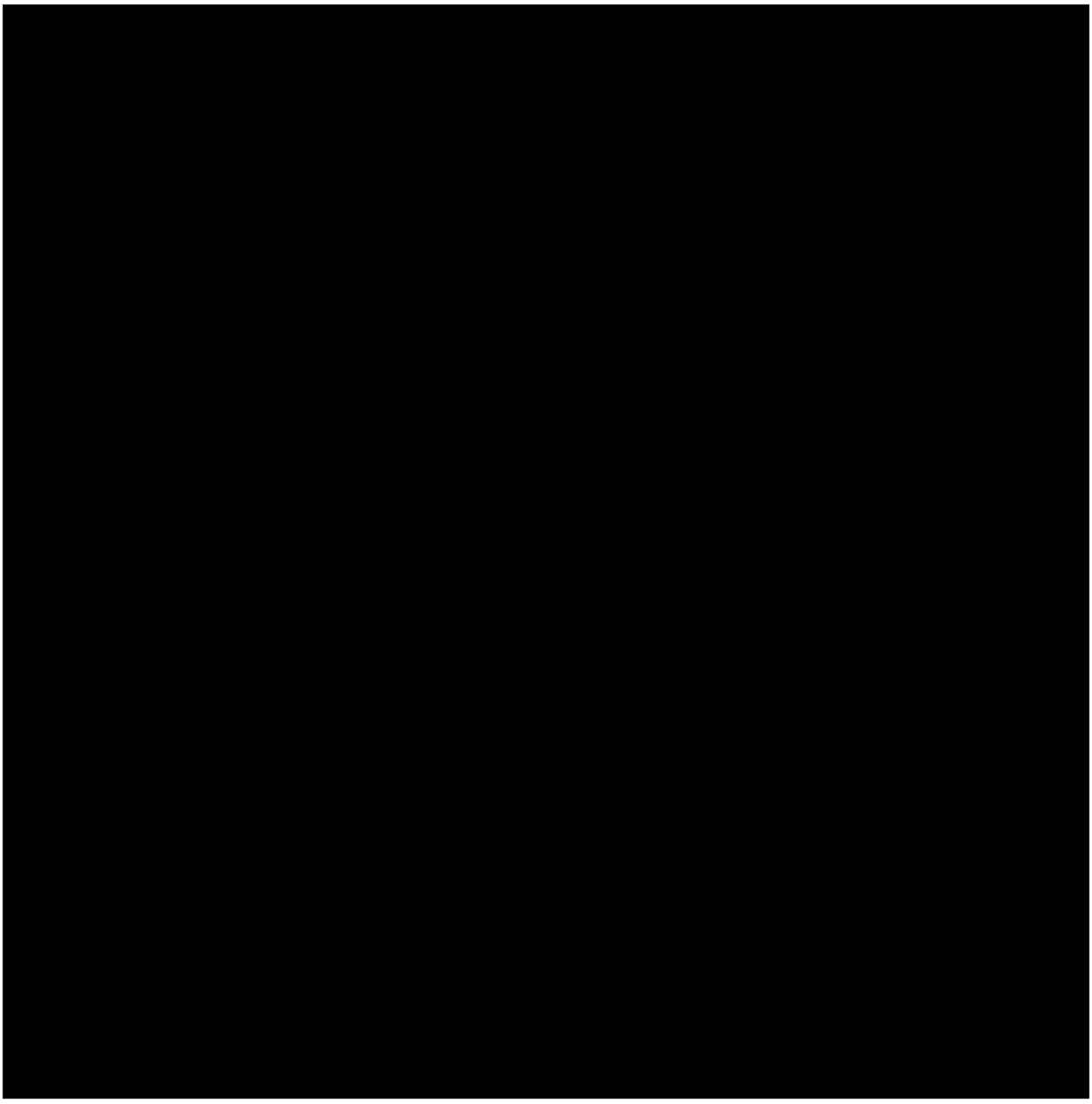

Figure 1-6. Stratigraphic chart showing the deepest USDW (dashed blue line), overburden, and the geologic storage zones.

1.2.4 Maps and Cross Sections of the AoR [40 CFR 146.82(a)(2), 146.82(a)(3)(i)]

Subsurface Database

Subsurface profiles of TCCSP confining and reservoir units were delineated within the project AoR and surrounding region ([redacted]) by completing a regional subsurface mapping investigation, leveraging insights gained from drilling a stratigraphic test well (TCCSP_OBS-1), along with data from [redacted] offset wells (**Figure 1-7**) and [redacted] 2D seismic lines (**Figure 1-8**). Information on historical wells utilized in TCCSP subsurface mapping and SEM development is available in **Appendix Table 1-2.**

Well-log based subsurface mapping was conducted in [redacted] and [redacted]. Correlations were based primarily on spontaneous potential (SP), gamma ray, and deep resistivity logs. Where available, supplementary data from neutron porosity, bulk density, and compressional sonic slowness logs were incorporated to refine stratigraphic interpretations. Initial regional geologic tops and profiles were revised based on insights gained from the geologic prognosis of TCCSP_OBS-1. The geologic prognosis and subsurface profiles of TCCSP_OBS-1 are summarized in **Figure 1-7** and **Table 1-6**. **Figure 1-7** features an offset well [redacted] and a geologic cross-section of the key formations used in the TCCSP static earth model (SEM). Geologic correlations were then further vetted and adjusted using subsea elevation and isopach maps during the development of the SEM.

A total of [redacted] 2D seismic lines were licensed from a private seismic data broker to complete a regional evaluation of TCCSP confining and reservoir units. The spatial distribution of licensed 2D seismic lines is depicted in **Figure 1-8**. Seismic lines were selected based on their quality, ensuring they had minimal acquisition gaps and processing artifacts. Selected lines were arranged to create a [redacted], so that [redacted] providing more complete coverage throughout the area of interest. Prior to geologic interpretation, a synthetic seismogram and sonic and density logs from the TCCSP_OBS-1 well were used to depth-tie the seismic lines. All seismic analysis was conducted in [redacted] software.

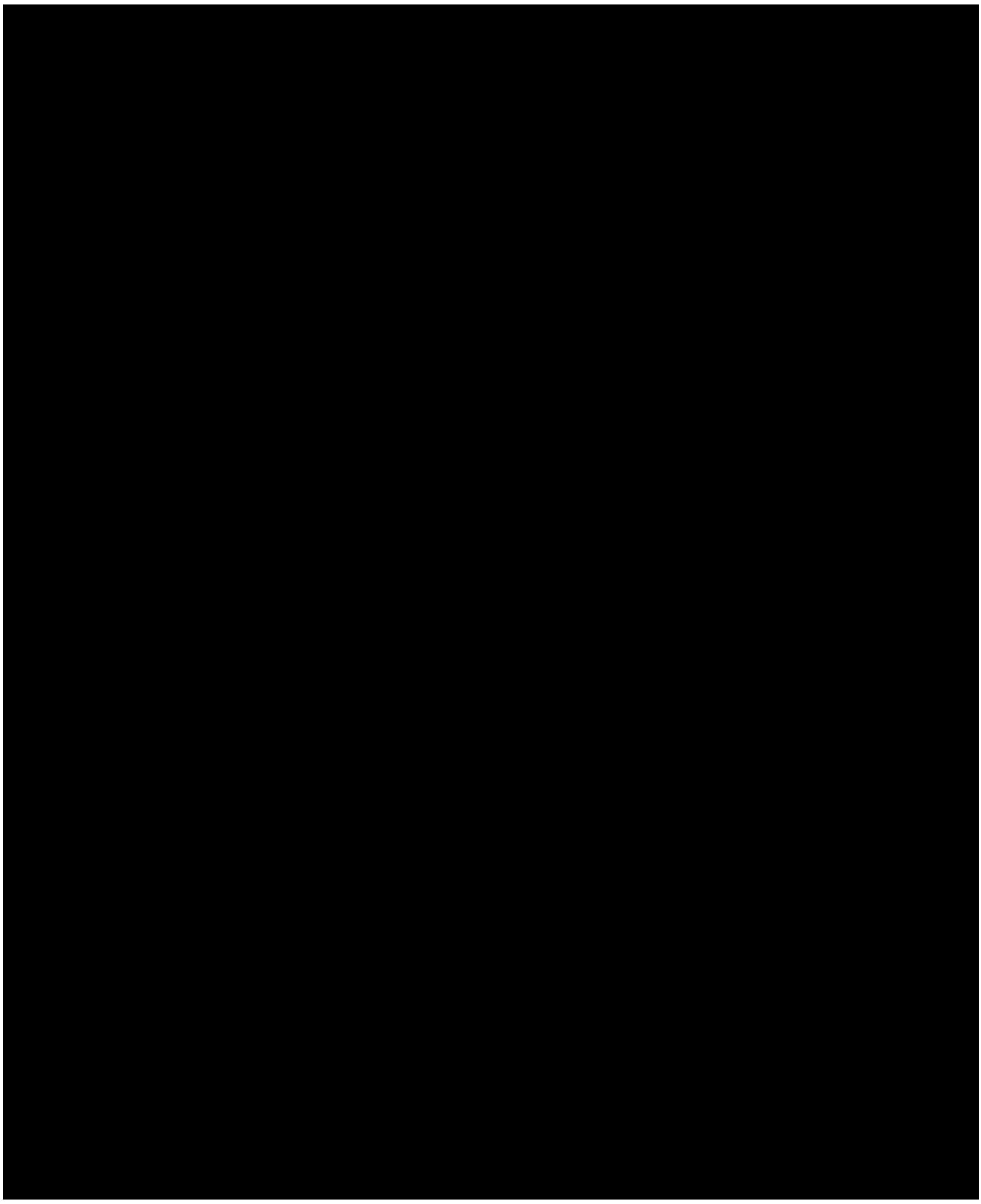

Figure 1-7. Basemap featuring wells used in the SEM structure and two key well-sections tied to the TCCSP_OBS-1 well. Black dots represent other wells where formation tops were also picked. The [redacted]. The purple boundary is [redacted] and corresponds to the footprint of the Static Earth Model (SEM). On the left is the [redacted], which was drilled to [redacted] and features [redacted] stratigraphic zones that were interpreted based on wells in the area. The geologic cross-section (A-B) in the bottom right [redacted]; in general, we can see here the relative thickness of these formations.

Table 1-6. Geologic description from the TCCSP_OBS-1 well.

Lithostratigraphic Unit or Zone	Significance	Unit Thickness	Actual Depth (ft. MD)	Observed Lithology
[redacted]				

Figure 1-8. Location of the [redacted] 2D seismic lines (orange lines) licensed relative to the [redacted] and the proposed TCCSP site (blue circle).

Geologic Cross-Sections and Maps

Figure 1-7 summarizes the wells utilized in geologic mapping and SEM construction and identifies the locations of two regional cross sections: a [redacted] section (**Figure 1-9**) illustrating lithostratigraphic continuity, and a [redacted] section (**Figure 1-10**). Collages of subsea elevation and thickness maps for all stratigraphic units represented in the SEM are shown in **Figure 1-11** and **Figure 1-12**, respectively.

Stratigraphic correlations and mapping were based on the regional framework of Bloch (1991) and Johnson and Graham (2007) [3,8]. The [redacted], located [redacted] of TCCSP_OBS-1 and [redacted], served as a key reference in these studies. Incorporated into the regional cross-section (**Figure 1-7**), the [redacted] was used as the type well for propagating stratigraphic picks across the study area.

Within the SEM, interpreted seismic and formation well tops indicate an average structural dip of [redacted], **Figure 1-11**. All reservoirs and confining zones are [redacted]

Regional mapping indicates that the [redacted] and its [redacted], with [redacted]. The unit averages [redacted] SEM footprint, **Figure 1-12**. At the [redacted] and [redacted] (**Figure 1-7**), isolated [redacted] These [redacted] as they are [redacted] to overlying or reservoir units.

The [redacted] averages about [redacted] in thickness across the study area. It is composed primarily of [redacted] that [redacted], while [redacted]. The [redacted]ns observed at TCCSP_OBS-1 generally continue along [redacted], where a [redacted] (**Figure 1-7**).

The [redacted] is encountered at [redacted] in the TCCSP_OBS-1 well and has an average thickness of [redacted] across the study area. To the [redacted], [redacted] **Figure 1-9**. Eastward [redacted].

The [redacted]) represents a [redacted] with an average thickness of [redacted]t across the study area. Based on SP log signatures, t[redacted], **Figure 1-9** and **Figure 1-10**. Basinward, however, [redacted]

The [redacted] has an average thickness of [redacted] across the study area. Its SP log response [redacted]e

[redacted], **Figure 1-9** and **Figure 1-10**.

The [redacted] averages [redacted] in thickness across the study area but [redacted] at the TCCSP_OBS-1 well. [redacted]st, based on current SP log correlations, **Figure 1-9**. In many wells, the interval contains [redacted].

The [redacted] and consists of a [redacted] across the study area, **Figure 1-9** and **Figure 1-10**. [redacted]. R[redacted]

[redacted] averages [redacted] in thickness and [redacted]. Seismic expression on 2D lines indicates that the [redacted], **Figure 1-9** and **Figure 1-10**. Despite this [redacted], with [redacted] near the TCCSP_OBS-1 well.

The [redacted] are [redacted], **Figure 1-9** and **Figure 1-10**. Based on [redacted] in **Figure 1-7**, the [redacted]. Seismic expressions for these units suggest that they tend to [redacted]. While the [redacted], it is interpreted as an [redacted] the TCCSP storage complex.

Figure 1-9. Southwest-to-Northeast well-section featuring the lithostratigraphic well top picks.

Figure 1-10. Northwest-to-southeast well-section featuring lithostratigraphic well top picks.

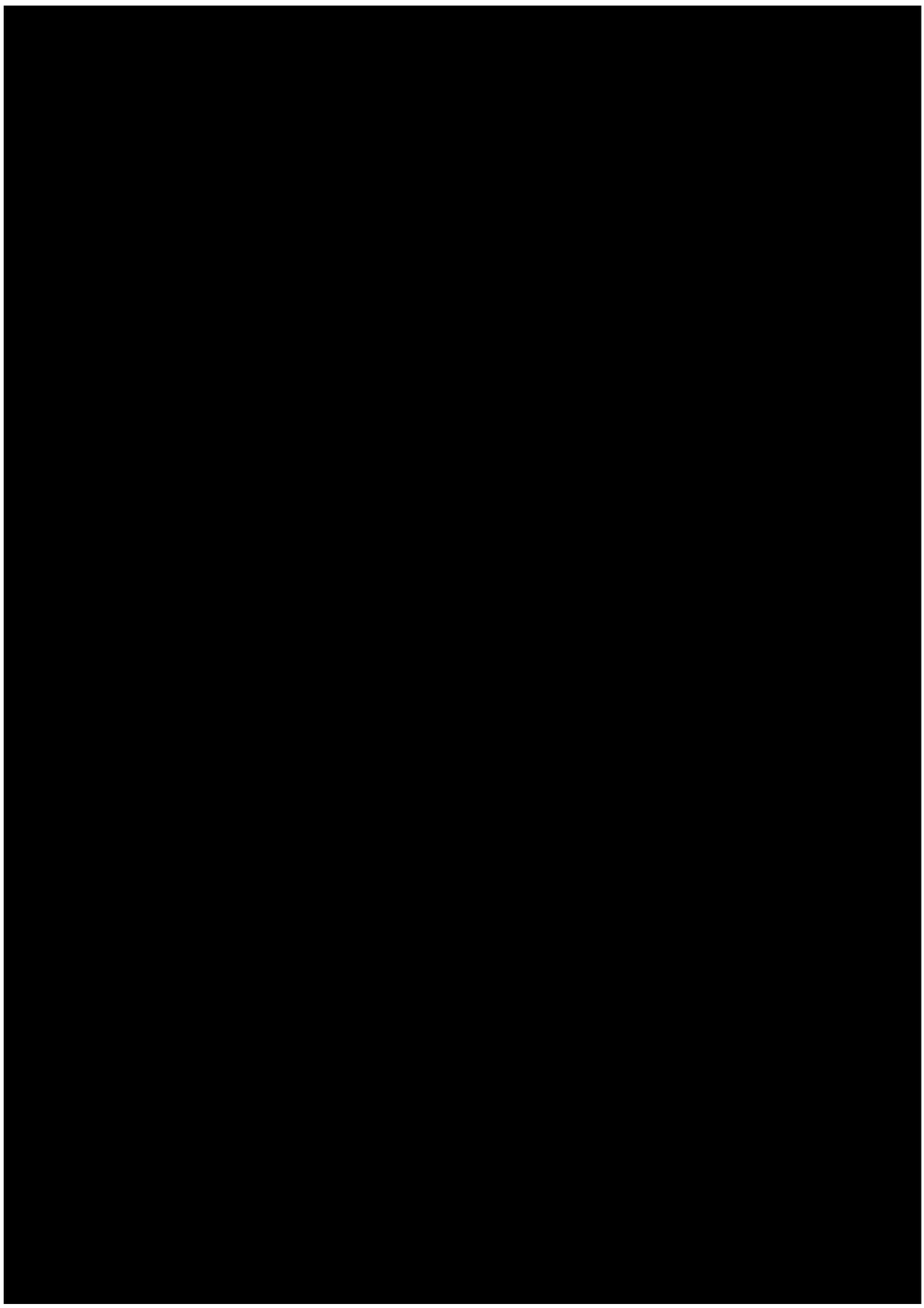

Figure 1-11. Structural maps depicting formation elevations across the [redacted] SEM area.

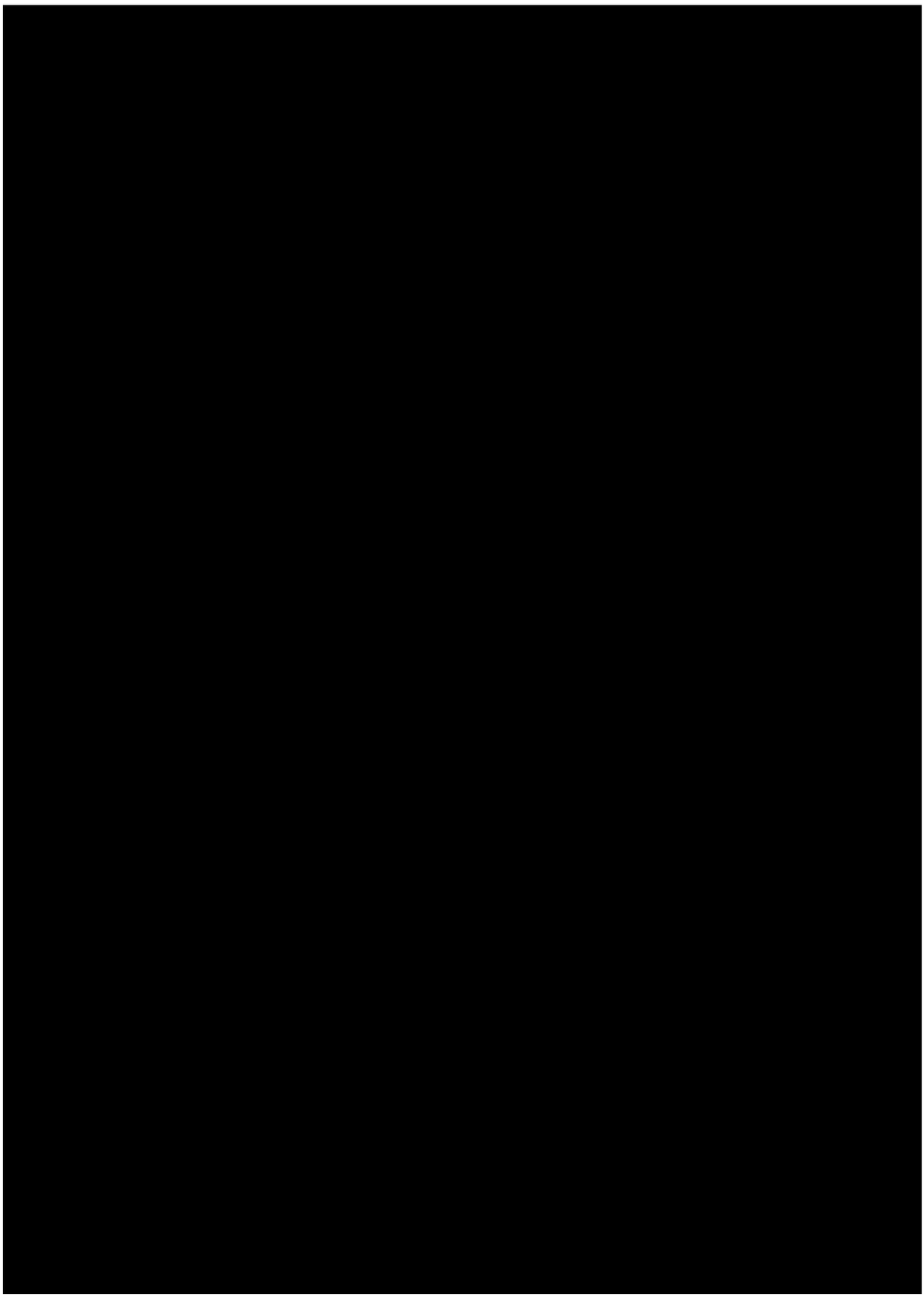

Figure 1-12. Maps depicting formation thicknesses across the [redacted] SEM area.

Figure 1-13. The TCCSP_OBS-1 well is posted in two-way travel time (TWT) against the nearest 2D seismic line. The lines run [redacted], and while they "capture" some dip, it is not the true dip direction of [redacted]. The [redacted] represents the top of the confining zone. The [redacted] represents the top of the target reservoir zone.

Figure 1-14. 2D seismic line along structural strike. The [redacted] represents the top of the confining zone. The [redacted] represents the top of the target reservoir zone. The TCCSP_OBS-1 well is projected onto this line and is located [redacted] to the [redacted].

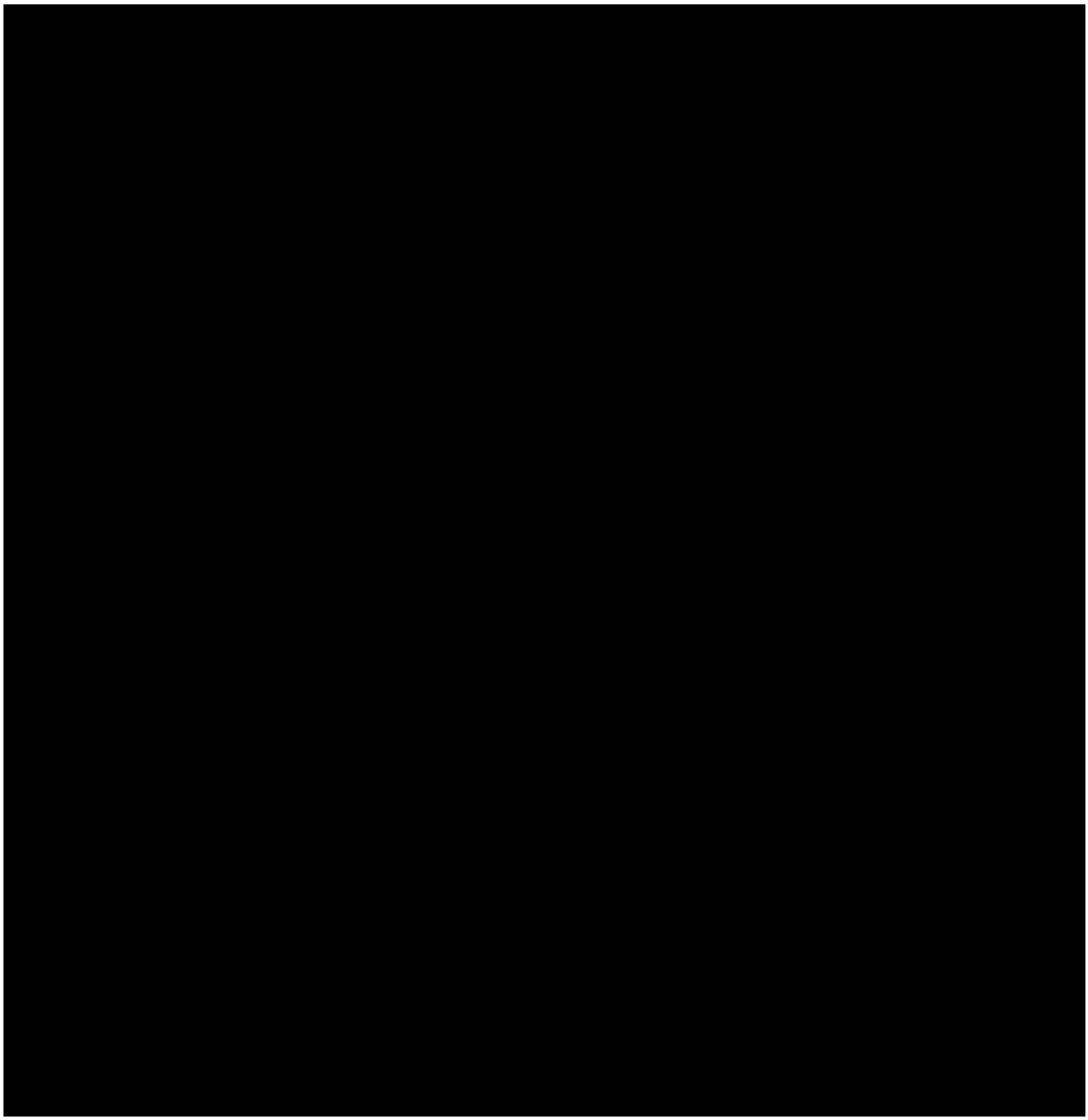

Figure 1-15. Top: An example of a 2D seismic line where reservoir pinch-outs are observed. Note that well trajectories are projected onto the 2D lines (they don't fall directly on the 2D line's plane). Bottom: Example of an interpreted 2D seismic line revealing

1.2.5 Faults and Fractures [40 CFR 146.82(a)(3)(ii)]

The prevalence of faults and fractures was evaluated within the TCCSP AoR and surrounding region using [redacted] historic 2D seismic lines, a resistivity borehole image logs (RBILs) from TCCSP_OBS-1, and publicly available geospatial shapefiles and geologic publications. RBIL analysis was conducted at the TCCSP_OBS-1 well to interpret the presence of sub-seismic faults and natural fractures across the TCCSP storage complex. 2D seismic lines were evaluated for the presence of larger seismic-scale faults.

Regional Faults

A review of regional literature shows that the TCCSP is situated along the [redacted]. Regionally, the east limb of the basin is [redacted] and is internally [redacted] with [redacted]. The structural configuration of the east limb is a product of the [redacted] and remained [redacted] [1].

The spatial distribution of all resolvable faults within and around the TCCSP AoR are depicted in **Figure 1-16**. Evaluation of 2D seismic, RBIL, and publicly available data found that [redacted] were observed to penetrate the TCCSP complex ([redacted] within the project AoR.

Regionally, very [redacted] TCCSP study area, as shown in **Figure 1-16.** The closest fault to the AoR is located [redacted] by the California Geological Survey. 2D seismic analysis identified a [redacted] of the TCCSP regional study area. This fault is situated approximately [redacted] of the TCCSP_OBS-1 well, exhibits a [redacted], and [redacted]. The [redacted]

[redacted] of the TCCSP AoR (**Figure 1-16**). These [redacted]. Therefore, these are interpreted to be [redacted] of the TCCSP storage complex.

The[redacted] will be verified and assessed further in future investigations using [redacted] (to be acquired as noted in the **Testing and Monitoring Plan)** and additional [redacted] (as noted in the **Pre-Operational Testing Program**).

Figure 1-16. Location of the [redacted] 2D seismic lines (orange lines) licensed and faults (brown lines) relative to the [redacted] and the proposed TCCSP site (blue circle).

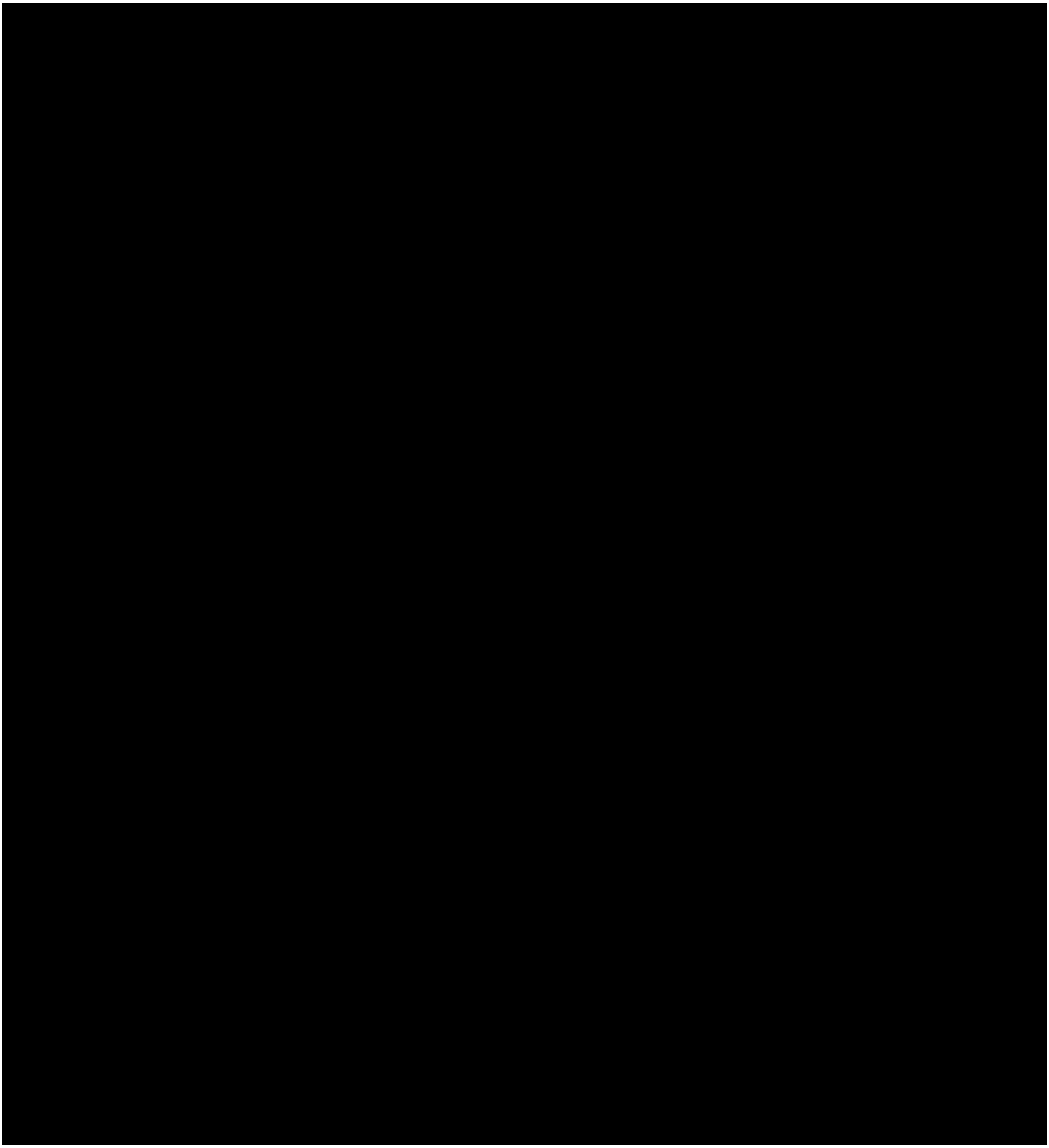

Figure 1-17. South–North seismic profile near the TCCSP site displaying [redacted] Top: Uninterpreted section. Bottom: Interpreted section.

Natural Fractures

To ensure safe, permanent storage of CO_2, the prevalence of natural fractures across the TCCSP storage complex was assessed using RBIL data collected at the TCCSP_OBS-1 well. The presence of natural fractures within relevant TCCSP geologic units, as observed at TCCSP_OBS-1, is summarized below.

[redacted]

Borehole image log analysis found the [redacted] to [redacted] natural fractures. The lack of natural fractures corroborates its safe and effective use as a primary confining zone for the TCCSP complex.

[redacted]

[redacted]. Due to its resistive nature coupled with the use of water-based mud, this fracture is interpreted to be [redacted].

[redacted]

The [redacted]. [redacted] observed within the [redacted].

[redacted]

RBIL analysis identified [redacted], all of which are [redacted]. Fractures were observed at depths of [redacted] and were interpreted to be [redacted] observed within the [redacted]

[redacted]

RBIL analysis found the [redacted], corroborating its use as a tight and impermeable intermediate seal to underlying reservoirs.

[redacted]

RBIL fracture analysis in the [redacted] indicated the [redacted] interpreted to be an [redacted]

[redacted]

RBIL analysis of the [redacted] revealed [redacted] natural fractures, corroborating its use as a secondary confining zone to the underlying [redacted].

[redacted]

RBIL fracture analysis in the [redacted] tal. A [redacted] .

[redacted]

In the [redacted], [redacted] which are interpreted to be likely [redacted] The [redacted] is interpreted to feature the [redacted] observed at TCCSP_OBS-1, as fractures [redacted]. Despite this occurrence over a [redacted], which are not interpreted to [redacted] to the TCCSP project.

1.2.6 Injection and Confining Zone Details [40 CFR 146.82(a)(3)(iii)]

Injection Zone Details

The TCCSP injection zones ([redacted]) are deep, porous, and permeable rock formations able to safely store commercial quantities of CO_2 injectate. These formations provide adequate capacity to safely sequester commercial injectate volumes, are permeable enough to enable efficient CO_2 movement into and within the formation and feature mechanical properties capable of withstanding simulated changes in pressure in response to CO_2 injection. The CCS development potential of the TCCSP site was demonstrated by the TCCSP_OBS-1 well, which features a comprehensive suite of subsurface data including mud cuttings, recovered sediment cores and core analysis data, advanced wireline log data, formation test data, and in-situ fluid analysis data. The following subsections provide a detailed assessment of TCCSP_OBS-1 subsurface data per each reservoir and seal interval (confining zones and intermediate seals) along with a review of petrophysical modelling techniques used to model the TCCSP_OBS-1 and regional offset wells, which facilitated creation of the TCCSP static earth model and subsequent dynamic computational modeling detailed in the **Area of Review and Corrective Action Plan**. The large suite of core analysis and wireline well log data referenced throughout this section for reservoirs can be found in **Figure 1-18** through **Figure 1-28** and **Table 1-7** to **Table 1-8**. Please note that most of the figures and tables, apart from zone-specific well log profiles, are found at the end of the injection zone details subsection.

[redacted]

As mapped, the [redacted] includes the [redacted] At the TCCSP_OBS-1 well, the [redacted], and mud log descriptions indicate it consists of [redacted]. [redacted] were observed to feature [redacted] The zone is also noted to feature [redacted]. While notably [redacted]. Depositional analysis of recovered sediment cores from [redacted].

Characteristic log signatures across the [redacted] observed at TCCSP_OBS-1 are depicted in **Figure 1-18**. Well log signatures and analysis within the [redacted] corroborate mud log descriptions, indicating the section to be comprised of [redacted]. [redacted] are observed to [redacted]. [redacted] within the zone are shown to feature a [redacted]. This apparent [redacted]. The core-calibrated NMR permeability log shows the [redacted]. The [redacted] has a net reservoir thickness of [redacted] and a cumulative permeability thickness of [redacted].

Saturation modeling indicates the [redacted] the primary TCCSP confining zone. Further details on the [redacted] are discussed in confining zone subsection below.

Analysis of cores recovered from the [redacted], support geologic and petrophysical profiles observed in well log and drill cuttings. Mineralogically, the [redacted] (**Figure 1-24.**) with some [redacted] Routine Core Analysis (RCA) demonstrates porosity ranges between [redacted] (**Table 1-7**). Mercury injection capillary pressure (MICP) experimentation (**Figure 1-27)** of sampled [redacted] NMR core data further supports reservoir quality, indicating effective porosities (PhiE) values ranging from [redacted]

Based on mud cuttings, well log, and core analysis profiles, the [redacted], compartmentalized by [redacted]).

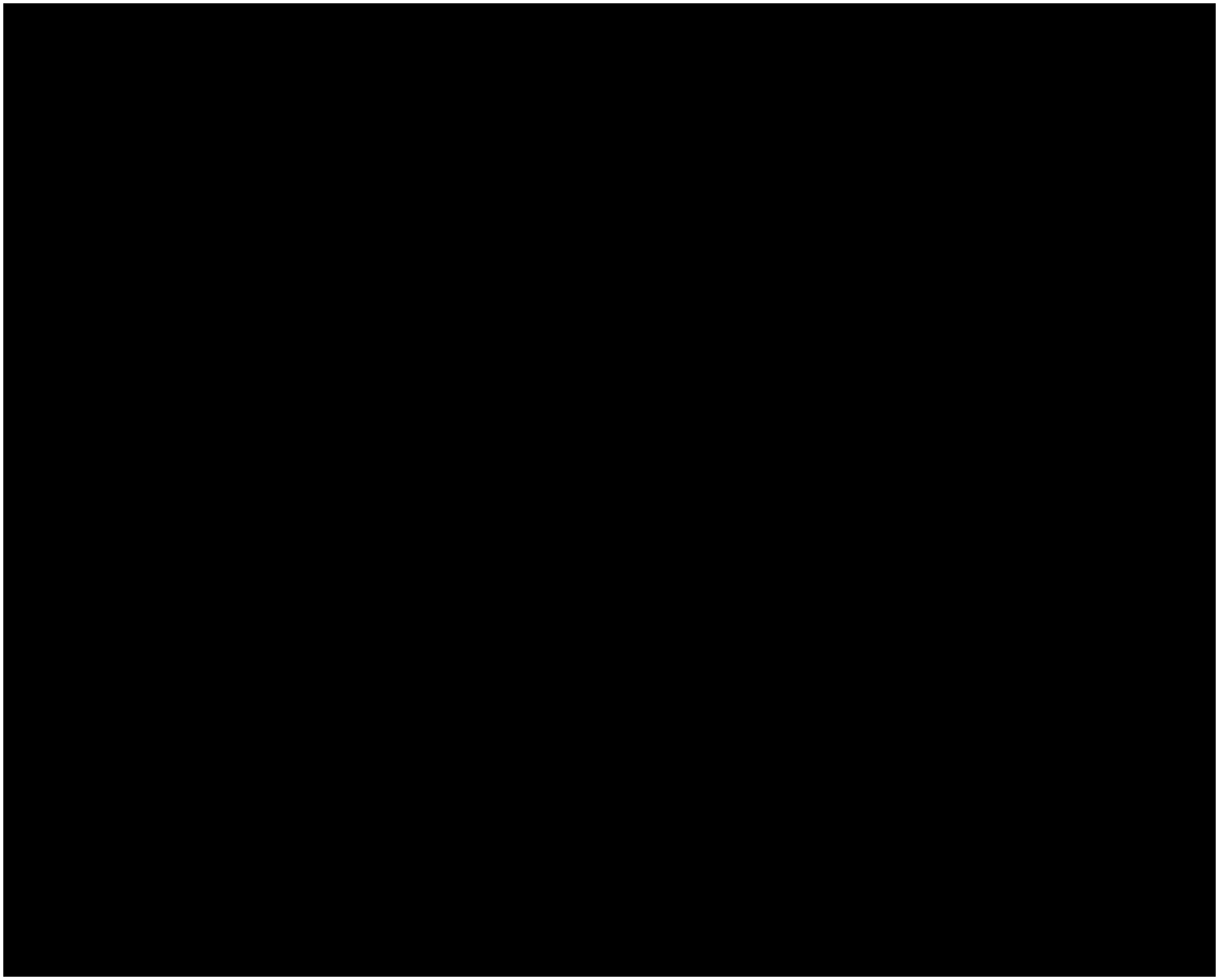

Figure 1-18. Summary well log plot illustrating the subsurface character of the

[redacted]

At TCCSP_OBS-1, the [redacted] is [redacted] thick and was observed in mud cutting descriptions to be comprised of [redacted]. [redacted] are described as being [redacted]. Mud gas chromatograph analysis suggests the [redacted]. A statistical summary of mud gas chromatograph data is available in the section below. Depositional analysis of recovered cores indicates the zone to be comprised of [redacted].

Characteristic log signatures within the [redacted] are depicted in **Figure 1-19**. The unit is observed to be comprised of an [redacted]. [redacted] are observed to [redacted]. NMR analysis suggests [redacted]. Core-calibrated NMR permeability modeling suggests [redacted]. [redacted] are also interpreted to feature [redacted]. The [redacted] is corroborated by the [redacted], where [redacted], indicating [redacted], a relative [redacted]. [redacted] within [redacted] show a good amount of [redacted].

At TCCSP_OBS-1, the [redacted] is a promising reservoir with a net thickness of [redacted] and a permeability thickness value of [redacted]; this, and other values are tabulated later in Tables **Table 1-15** and **Table 1-16**. Mineralogical analyses show that [redacted]. Whole rock mineralogy shows a [redacted] (**Figure 1-24.**). RCA results indicate porosity between [redacted] permeability ranging from [redacted], and grain densities between [redacted]. MICP indicates the unit to feature [redacted] with porosities between [redacted] and permeability ranging from [redacted] NMR measurements supports these findings, irreducible water value range from [redacted] but are [redacted] for [redacted], while [redacted] Laser particle size analysis shows that [redacted] (**Figure 1-25**). The mercury injection data for the [redacted] suggest that it is a better reservoir than the [redacted] as the [redacted] as compared to the [redacted] (**Figure 1-27**).

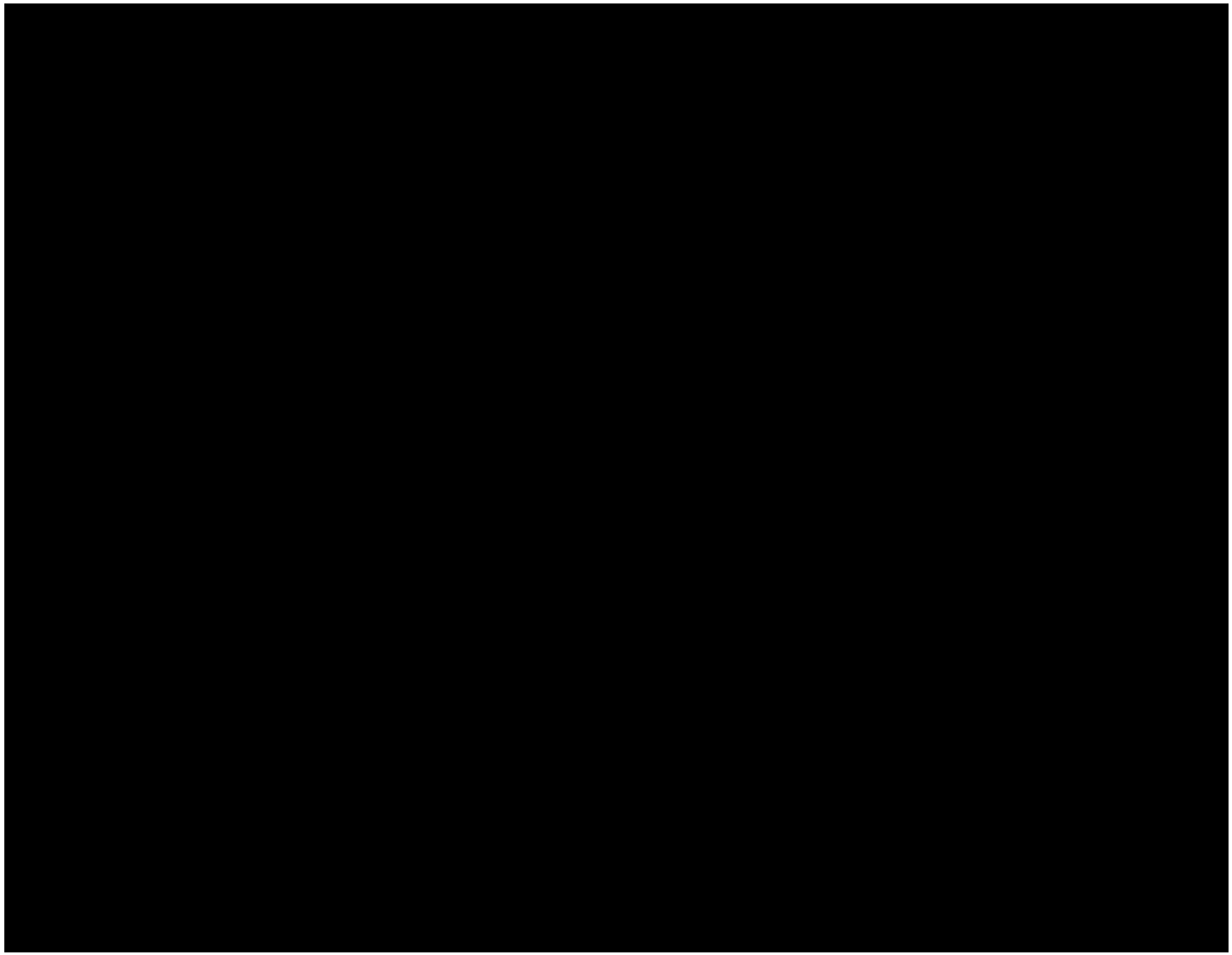

Figure 1-19. Summary well log plot illustrating the subsurface character of the [redacted]

[redacted]

The [redacted], as mapped within the TCCSP project study area, is comprised of the [redacted] At TCCSP_OBS-1, mud log describes the zone to be comprised of [redacted]. [redacted] were noted to feature [redacted]. [redacted] ambient CO_2 and methane were observed within the [redacted]. Depositional analysis of sediment cores recovered from TCCSP_OBS-1 indicated the [redacted].

Characteristic well log profiles of the [redacted] are depicted in **Figure 1-20**. The [redacted] is observed to be comprised of [redacted]. [redacted], whereas [redacted], consistent with [redacted] Petrophysical modeling indicates the [redacted], with effective porosities averaging around [redacted] and core-calibrated NMR permeability estimates ranging from [redacted] These estimates of permeability are [redacted]. Saturation modeling indicates the [redacted] features [redacted].

The [redacted] features excellent petrophysical attributes, with a net reservoir thickness of [redacted] and permeability thickness value of [redacted] Mineralogically, the unit is [redacted] and is comparable to the [redacted], though slightly more [redacted] Whole rock mineralogy shows [redacted] (**Figure 1-24.**). RCA data indicate porosity between [redacted] and permeability values between [redacted] with grain densities ranging from [redacted]. SCAL tests identify both unimodal and bimodal pore-throat distributions, with porosity values between [redacted] and permeability in the range of [redacted]. NMR results indicate irreducible water volume to be range from [redacted] (**Table 1-8)**. Laser particle size analysis shows particle size dominated by [redacted] (**Figure 1-25**). The mercury injection data in **Figure 1-27** show that the reservoir quality of the [redacted] is like the [redacted]. The [redacted] is interpreted to have excellent reservoir quality; however, [redacted].

.

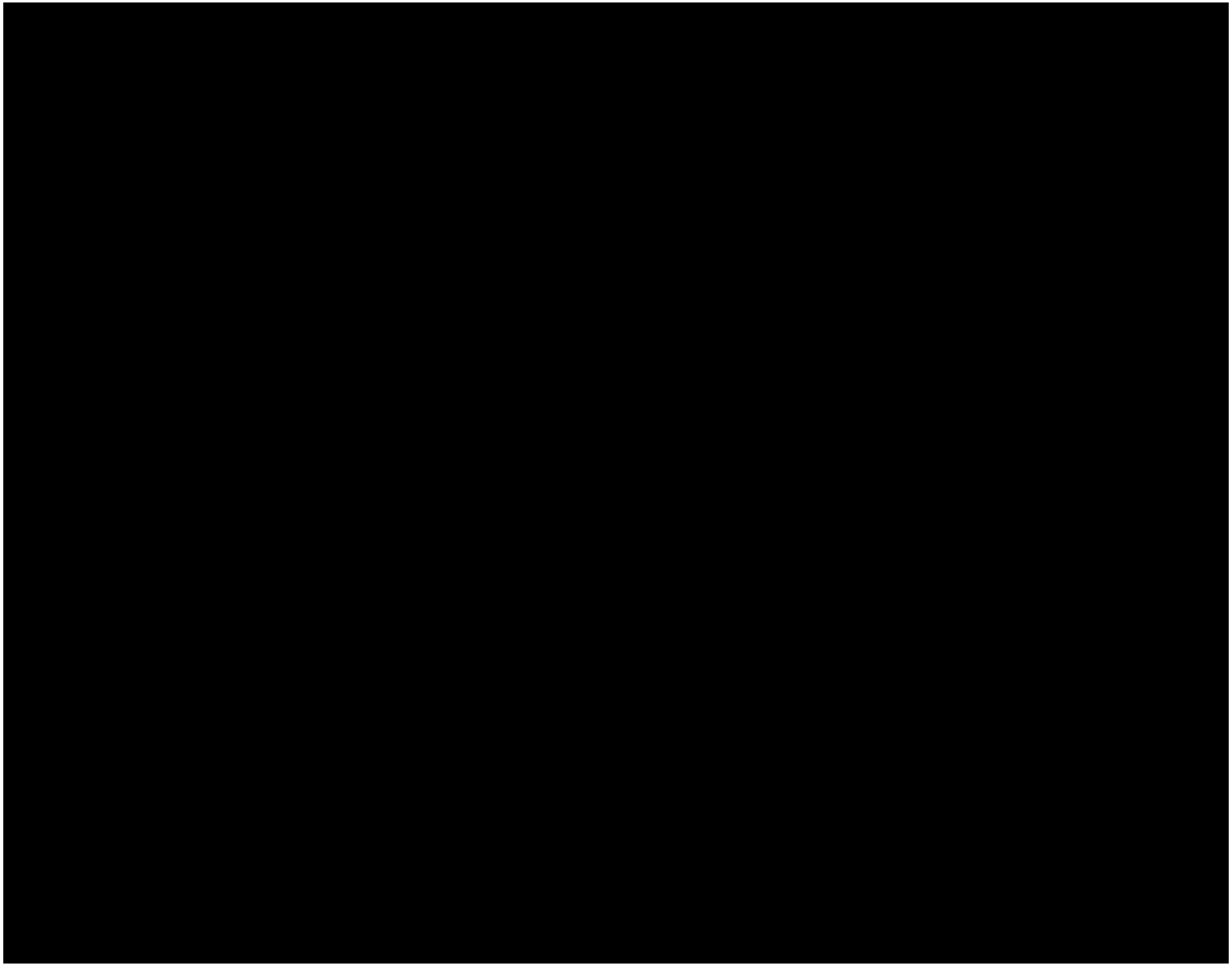

Figure 1-20. Well log profiles of the [redacted]

[redacted]

At TCCSP_OBS-1, the [redacted] was described in mud cuttings as a [redacted]. Gas chromatograph data indicate the zone features [redacted] of CO_2 and methane. Depositional analysis of sediment cores recovered from the [redacted].

Characteristic well log profiles of the [redacted] are depicted in **Figure 1-21**. The [redacted] is observed to be comprised of [redacted]. The lowermost [redacted] The [redacted] is estimated to feature a [redacted] permeability profile with estimated NMR permeability values ranging from [redacted]). The overlying [redacted]. The core-calibrated NMR permeability model estimates this zone to be [redacted], with values reaching [redacted]. Water saturation modeling indicates the [redacted].

The [redacted] is comparatively [redacted], with a net reservoir thickness of [redacted] and a permeability thickness of [redacted] The formation is dominated by [redacted] and is noted to include [redacted] that could act as [redacted]. Whole rock mineralogy shows that the [redacted] (**Figure 1-24.**). RCA results indicate porosity ranges between [redacted] permeability values from [redacted], and grain densities of [redacted]. Laser particle size analysis shows [redacted] throughout the [redacted] (**Figure 1-25**).The [redacted] is interpreted as having [redacted], making it suitable for commercial CO_2 injection.

Figure 1-21. Well log profiles of the [redacted].

[redacted]

The [redacted] is comprised of several units, including the [redacted]. The upper portion of the zone ([redacted]) was observed in mud cuttings to be comprised of [redacted] which persist throughout the formation. The remaining portion of the zone [redacted]) was observed to be comprised of [redacted]. Mud gas chromatograph analysis indicates the [redacted]. Depositional analysis of recovered sediment cores suggests the [redacted] at TCCSP_OBS-1, and consisted of [redacted]

Characteristic well log signatures of the [redacted] are depicted in **Figure 1-22**. The unit is observed to be [redacted] and comprises [redacted]. [redacted] from [redacted]. The [redacted] is interpreted to occur from [redacted] and exhibits a [redacted] The [redacted] is interpreted to occur from [redacted], was cored during [redacted] and is characterized by a [redacted]. The remainder of the [redacted] is [redacted]. [redacted], as indicated by the amount of [redacted] ([redacted]), compared to less than [redacted]. Petrophysical modeling indicates the [redacted]. The unit also features pockets of [redacted] Borehole image log analysis found [redacted], and its moderately [redacted] are more desirable to limit the size of CO_2 and pressure plume than some of [redacted]

The [redacted] has a net reservoir thickness of [redacted] and a permeability thickness of [redacted]. Mineralogically, it is [redacted]. The lithology in [redacted] is also observed to be dominated by [redacted] as observed from whole rock mineralogy (**Figure 1-24.**). RCA indicates porosity between [redacted], permeability ranging from [redacted], and grain density values of [redacted] SCAL results show both [redacted], with porosity values of [redacted] and permeability in the range [redacted] mD (**Figure 1-24.**). NMR analyses yielded effective porosity values[redacted]n 14-25% and irreducible water volume valu[redacted]een 15-44%. Laser particle size anal[redacted]nd lithology (**Figure 1-25**). Core sa[redacted] artinez z[redacted]ure pr[redacted]th varying behaviors observed in the[redacted]-Martinez is interpreted t[redacted]ir quality for CCS development.

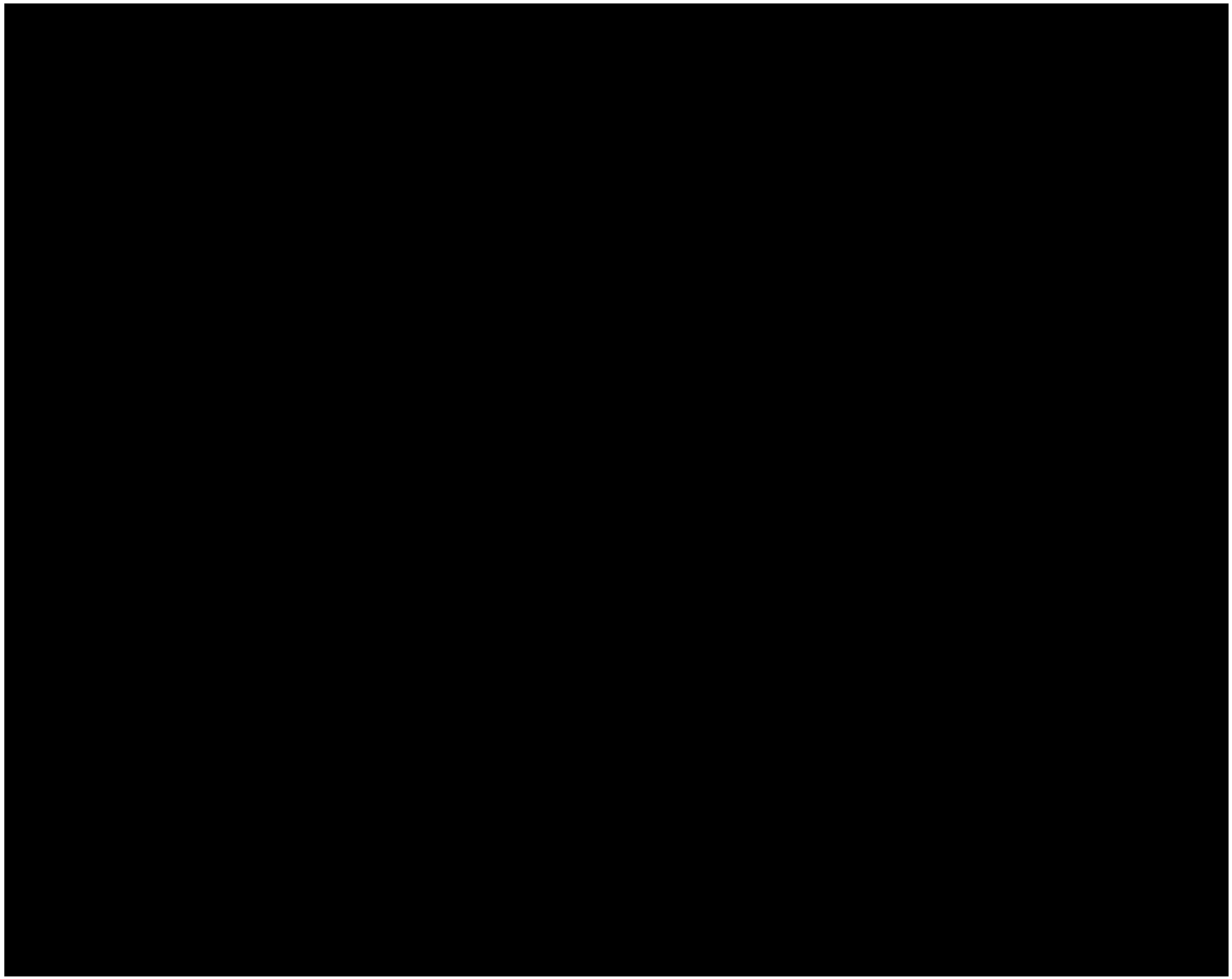

Figure 1-22. Well log profiles of the [redacted]

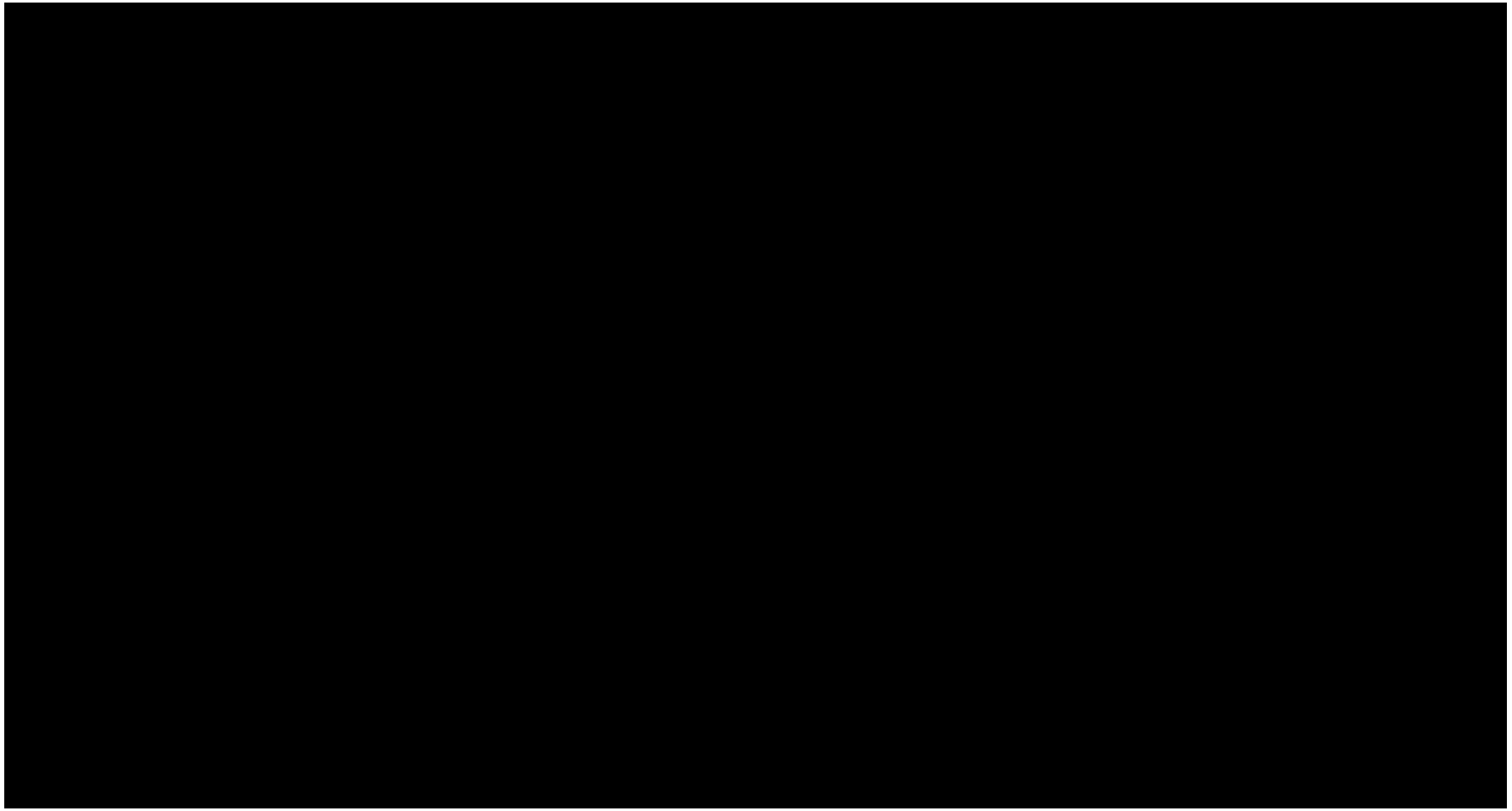

Figure 1-23. Thin-section analyses of representative sections for the injection zones.

Figure 1-24. Whole-rock mineralogy for TCCSP_OBS-1 reservoir units. Left: Sample ID. Center: Whole-rock mineralogy with [redacted] percentage values (in white) and [redacted] (in black). Right: Normalized [redacted] abundance with percentage values of [redacted] (in white) and [redacted] (in black).

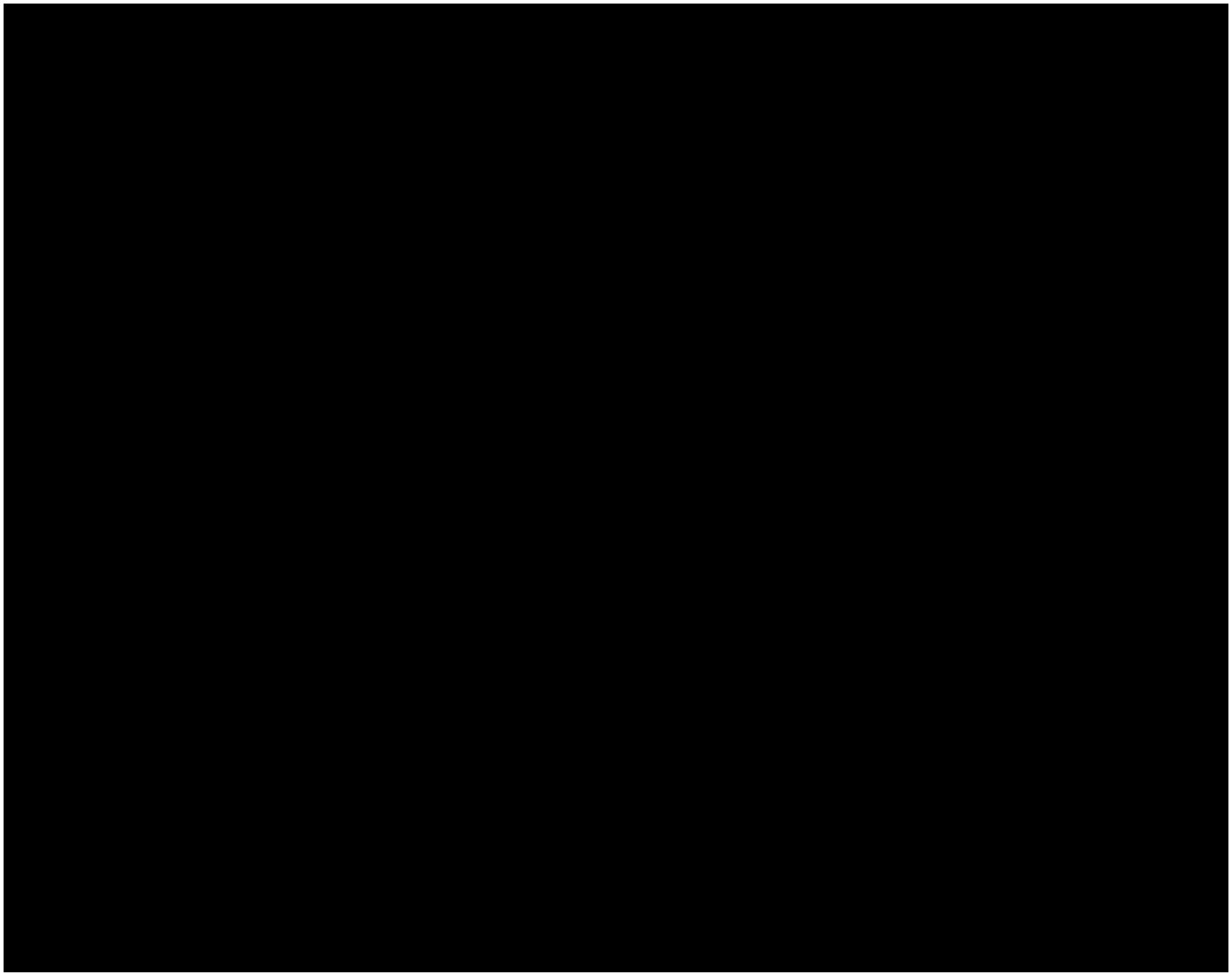

Figure 1-25. Laser Particle Size Analysis for the injection zones.

Figure 1-26. Porosity vs permeability for TCCSP_OBS-1 characterized according to core type.

Table 1-7. Descriptive Statistics for Rotary Sidewall Core Analysis and Whole Core Analysis (Reservoir Zones).

Zone	P10	P50	P90	Standard Deviation

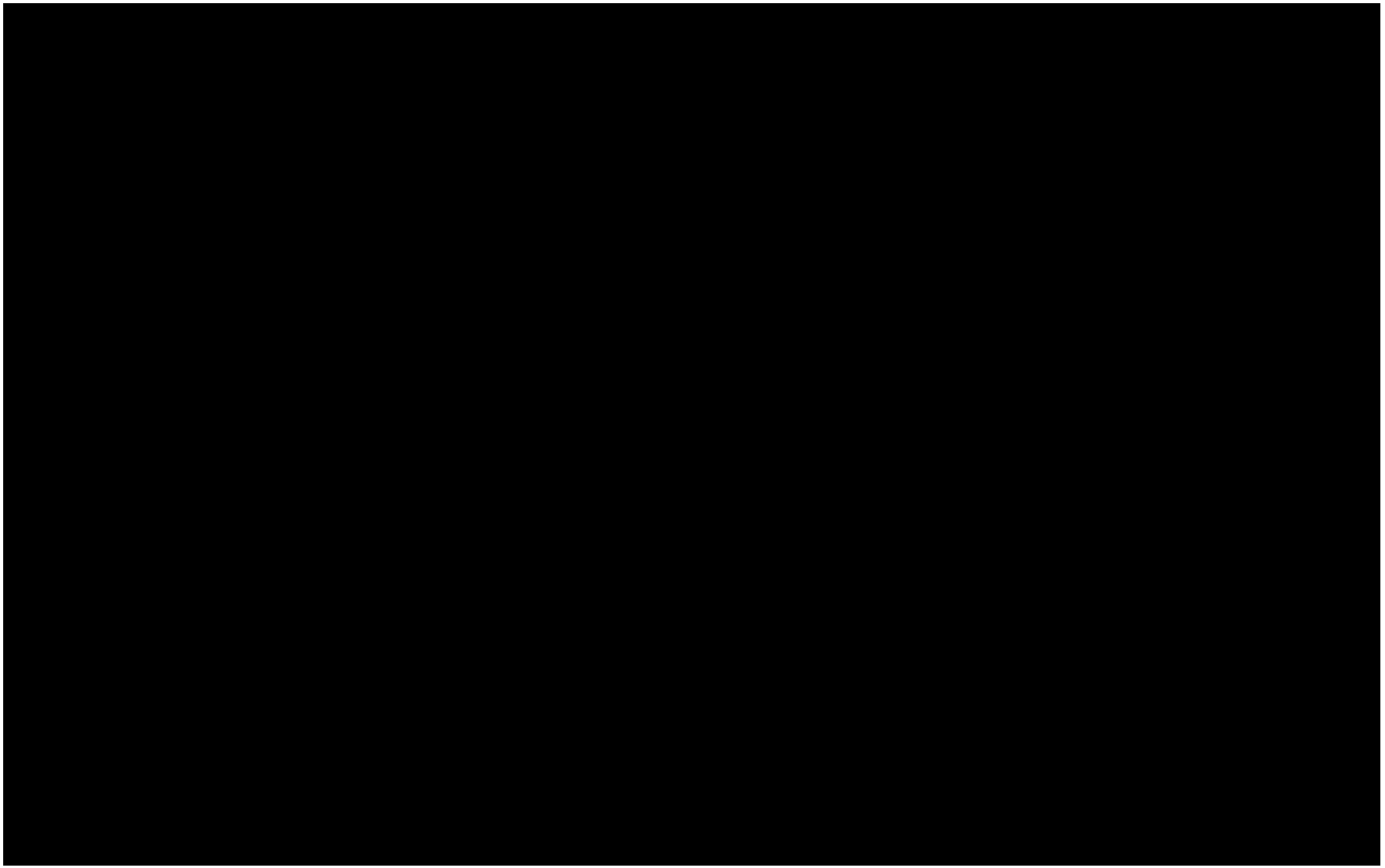

Figure 1-27. MICP plots for ■ samples across all TCCSP reservoirs illustrating injection pressure to CO_2 saturation, with annotations of general capillary pressure classes. This data was converted from a Hg-air system to a CO_2-brine system.

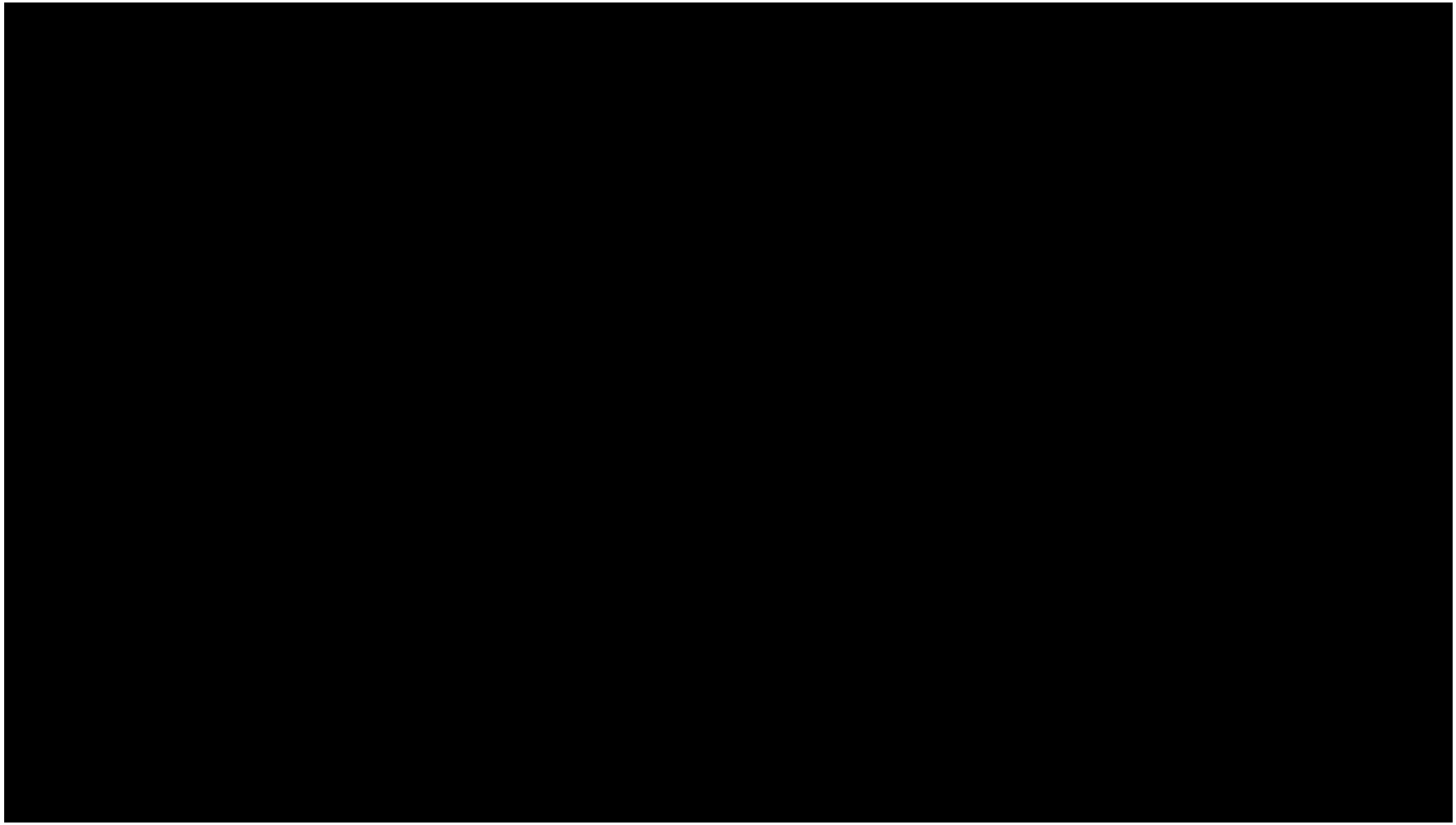

Figure 1-28. Pore throat radius distribution at TCCSP_OBS-1.

Table 1-8. Core test data from TCCSP_OBS-1 reservoir zones, including RCA, NMR, and MICSP tests.

Sample ID	Depth (ft)	Geologic Unit	Routine Properties		NMR Data			MICP Data				
			Porosity (%)	Klink. Permeability (md)	Total Porosity (%)	Effective Porosity (%)	Swi (%)	Pore throat distribution type and class dominance	Entry pressure (psia)		Swi-CO_2 brine (%)	MICP Swanson K (mD)
									A-Hg	CO2-W		
[redacted]												

Confining Zone Details

TCCSP confining zones ( ) and intermediate seals (are capable of vertically sealing commercial quantities of CO_2, under simulated pressure changes without fracturing or meeting threshold entry pressure. The confining potential of TCCSP confining zones and intermediate seals was demonstrated at TCCSP_OBS-1 leveraging mud cuttings, recovered sediment cores and core analysis data, advanced wireline log data. Subsections below describe subsurface data and related interpretations which evaluate the quality, capacity and safety of TCCSP confining zones and intermediate seals.

The is comprised of the , and at TCCSP_OBS-1, was observed to be , collectively. The was observed in mud cuttings to be comprised of . At , a was observed, marking the transition of . The was comprised of . Mud log chromatograph analysis indicates the zone to feature the in the well.

Well log profiles within the are split between the approximate . The was due to , within the intermediate section of the wellbore that extends just after the . Well log signatures captured within the are depicted in **Figure 1-29**. Log signatures for the are limited due to being acquired The is observed to feature an . This is interpreted to indicate the unit is comprised of .

The was logged, featuring a full suite of basic and advanced logging, from Type log signatures for the are depicted in **Figure 1-29**. This interval is interpreted to be comprised of . Neutron-density cross-over suggests the presence of ; however, this is interpreted as a false indication likely stemming from the presence of , coupled with , resulting in the of .

Core analyses confirm that [redacted] is negligible, with measured permeabilities of [redacted]. The predominance of [redacted] indicate that this interval functions as an effective primary confining unit, capable of providing vertical seal to the underlying reservoirs. MICP data from TCCSP_OBS-1 core samples from the [redacted] are shown in **Table 1-9**. [redacted] CO_2 column height measurements indicate that these confining rocks are more than adequate for confining CO_2.

The [redacted] is dominated by [redacted], ranging from [redacted] of the bulk mineralogy. Framework minerals such as [redacted] but the [redacted], along with additional [redacted]. The whole rock mineralogy also suggests that [redacted] is most dominant in the [redacted], **Figure 1-29**. The MICP data indicate the [redacted] caprock where CO_2 is observed to be reaching [redacted] **Table 1-9**.

Figure 1-29. Summary well log plot illustrating subsurface profile of the [redacted]. Open-hole well logs are not available above [redacted] because the intermediate logging program was discontinued at [redacted]. The decision was based on operational difficulties caused by a thick interval of [redacted], which exhibited [redacted] during the intermediate logging attempt.

[redacted]

The [redacted] was observed in mud cuttings to be comprised of [redacted]. Some [redacted] were identified to be [redacted] Gas chromatograph analysis of mud gas indicates the [redacted]. A statistical summary of mud gas chromatograph data per zone is available in the section below.

Characteristic log signatures for the [redacted] are shown in **Figure 1-21**. The unit is observed to be a [redacted]

[redacted] The unit features [redacted] of N/D CBW cross-over, which is interpreted to stem from [redacted]. Borehole image log analysis revealed [redacted] to be present within the [redacted]. The [redacted] is interpreted to be a [redacted].

Despite attempts, [redacted] were suitable for various core analysis experiments.

XRD analyses of the [redacted].

[redacted]

The [redacted] observed within sediment cores obtained from the [redacted]. The facies immediately caps the [redacted]. Wireline logs indicate an effective porosity of [redacted]. The [redacted] permeability was estimated using the [redacted] The [redacted] represents [redacted]. The [redacted] make this unit an effective seal for TCCSP.

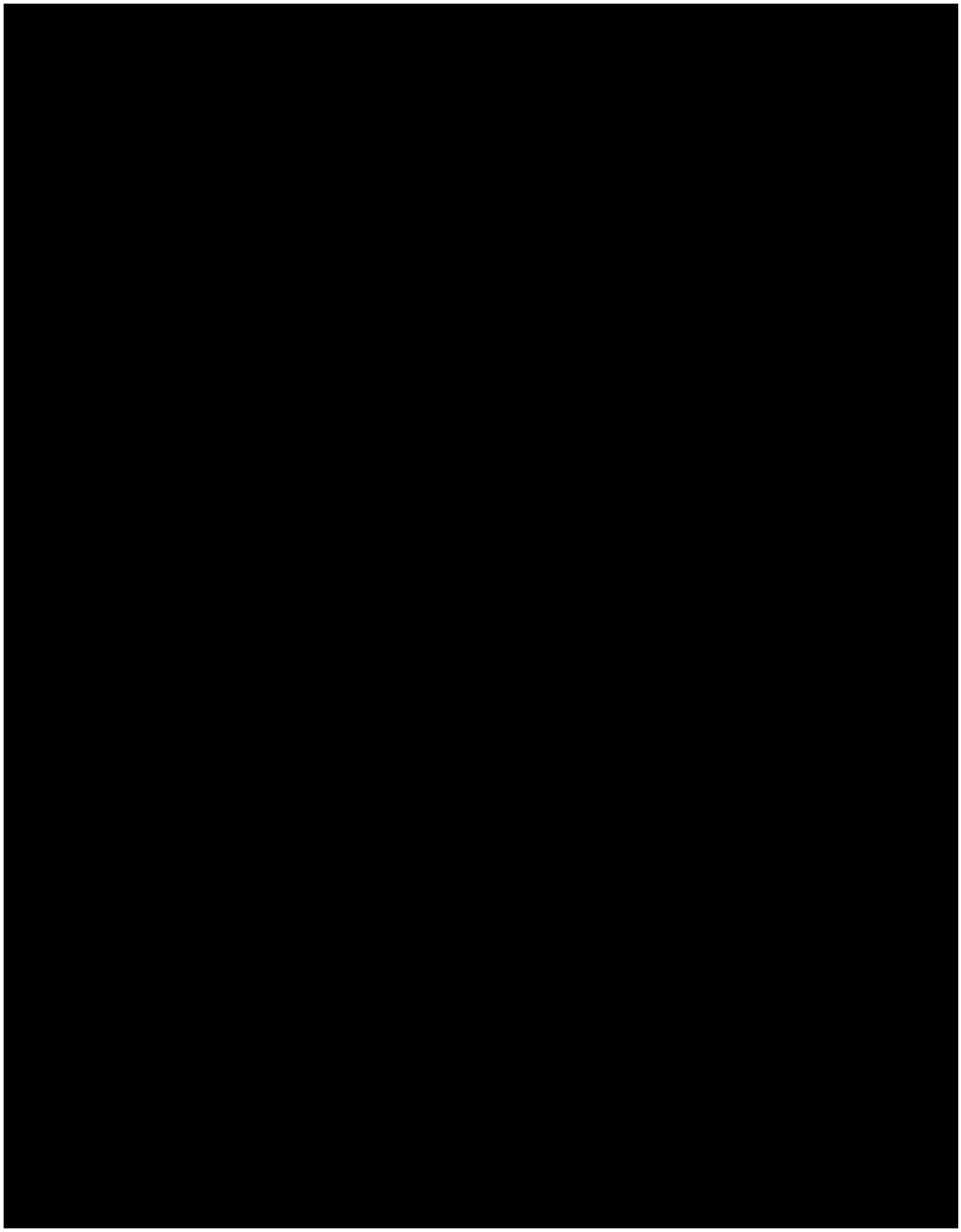

Figure 1-30. Example thin-sections from the [redacted]. The fractures in the [redacted] are [redacted].

Figure 1-31. Rock mineralogy abundance from the TCCSP_OBS-1 sealing units. Left: Sample ID. Center: Whole-rock mineralogy with [redacted] percentage values (in white) and [redacted] (in black). Right: Normalized [redacted] abundance with percentage values of [redacted] (in white) and [redacted] (in black).

Table 1-9. MICP data from TCCSP_OBS-1 core samples from the [redacted]

Formation	Sample ID	Depth (ft)	MICP Capillary Pressure Classes	MICP Swirr	Entry pressure to Hg-Air (psia)	Entry pressure to CO_2-Brine (psia)	Qv (meq/ml)	CO_2 Column Height (ft)
[redacted]								

Figure 1-32. Threshold Entry Pressure experiment results for the caprock sample.

Figure 1-33. Caprock MICP curve with textures.

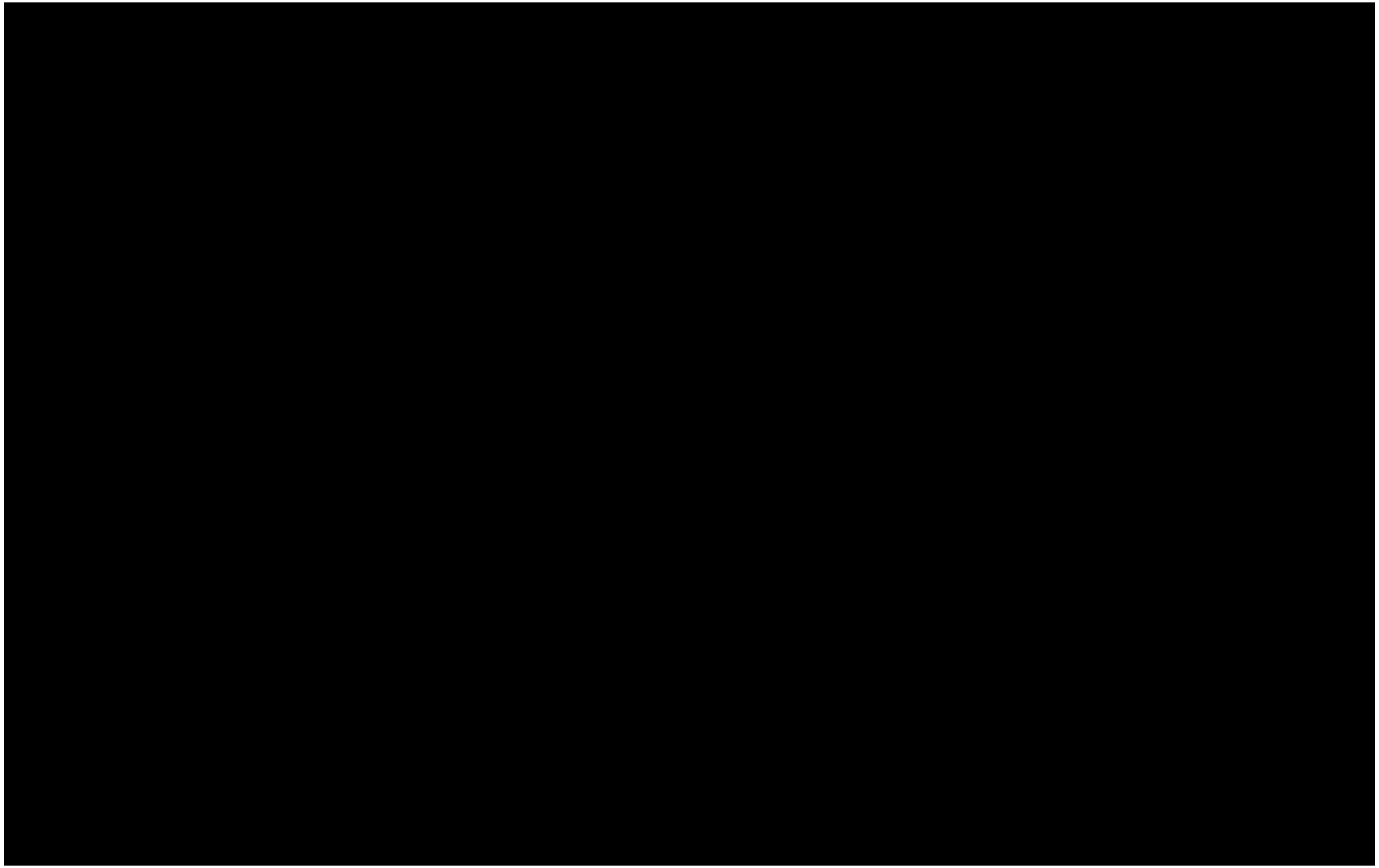

Figure 1-34. Fluid Inclusion Study (FIS) summary for TCCSP_OBS-1. The log plot shows the gas concentrations for [redacted] throughout the well. The annotated depths indicate probable [redacted]

TCCSP Petrophysical Modeling

Petrophysical modeling of TCCSP reservoir and caprock units was conducted to create derivative logs of estimated properties (porosity, permeability, water saturation, salinity) for use in the 3D SEM and dynamic reservoir simulations. Petrophysical modeling was conducted in two parts involving: [redacted] Petrophysical analysis was conducted using [redacted]

TCCSP_OBS-1 Type Well Analysis

NMR Log Calibration and Interpretation

Type well analysis of the TCCSP_OBS-1 well leveraged advanced well log and core analysis data to build a detailed petrophysical model and develop permeability prediction algorithms capable of being applied to offset wells with less advanced data sets. TCCSP_OBS-1 type well analysis consisted of: [redacted]

The NMR data collected at the TCCSP_OBS-1 well were a foundational element of the type well petrophysical model, which, once corrected and calibrated, served as a guide and comparative example in subsequent petrophysical modeling. The nuclear magnetic resonance log is an excellent technique for obtaining matrix-independent estimates of porosity, permeability, and clay-bound water, especially once calibrated to core T2 cutoff measurements.

With their shallow depth of penetration [redacted] NMR log measurements may be [redacted]. [redacted] through the wellbore, likely originating from the [redacted]. The TCCSP_OBS-1 NMR log was first corrected for [redacted] where needed, using the [redacted] Once corrected, routine core analysis and NMR-plug analysis results were used to calibrate porosity, permeability, and NMR T_2 cutoff values. The NMR permeability log was optimized by varying the permeability function types ([redacted]) and regressing permeability coefficients zone-by-zone to yield results that best match core data. An overview of the final NMR petrophysical model compared to core data is summarized in **Figure 1-35** through **Figure 1-37.**

Figure 1-35. Core-calibrated NMR profiles from select cored intervals within the [redacted].

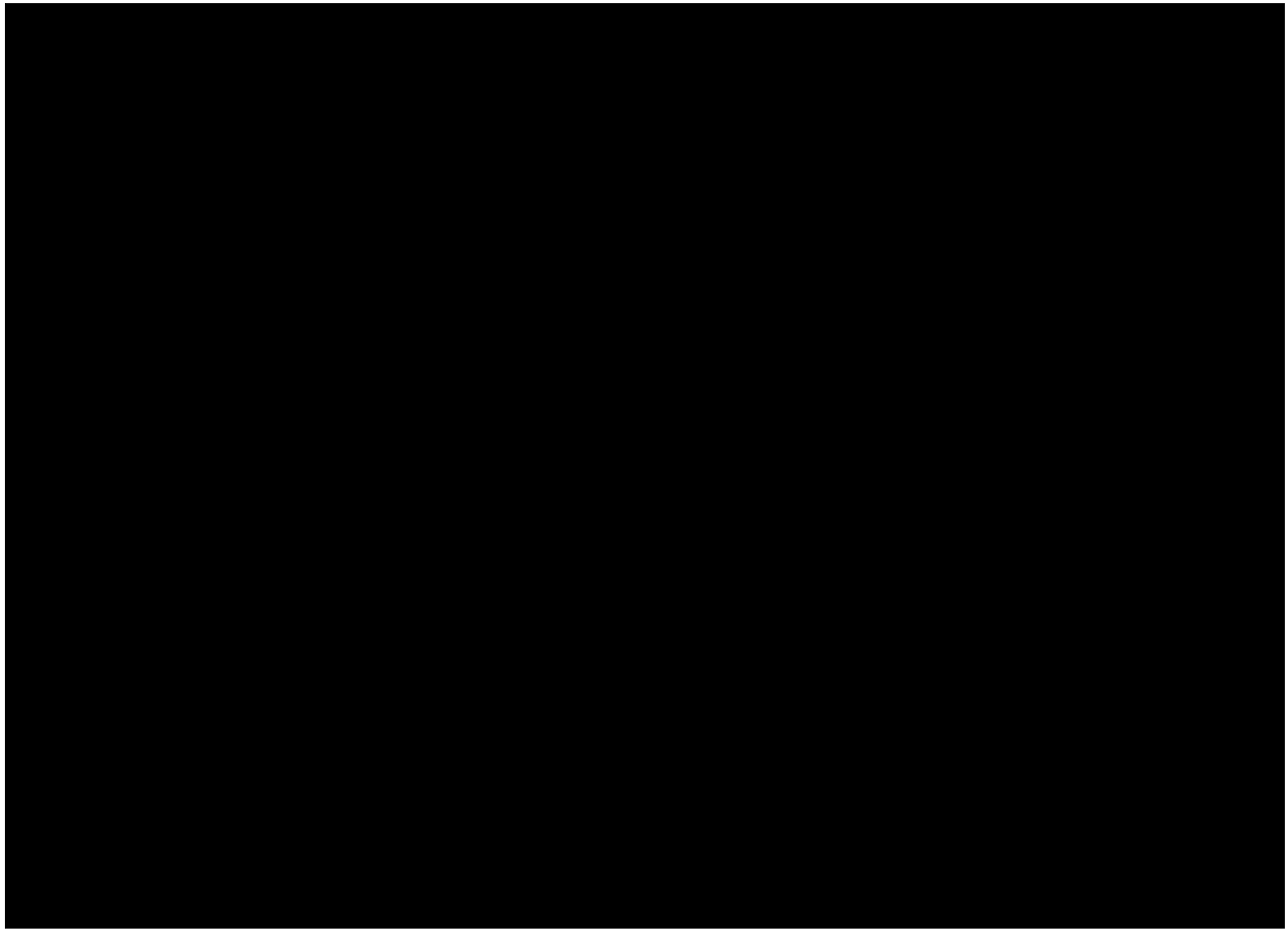

Figure 1-36. Core-calibrated NMR profiles for select cored intervals within the [redacted].

Figure 1-37. NMR profiles of cored sections of the [redacted].

Table 1-10. Summary statistics of calibrated NMR porosity log model

Formation	NMR Total Porosity (%)			NMR Effective Porosity (%)			NMR Clay-Bound Water (CBW) (%)			NMR Capillary Bound Water (Swirr) (%)			*NMR Permeability (mD)		
	P10	P50	P90	P10	P50	P90	P10	P50	P90	P10	P50	P90	P10	P50	P90
[redacted]															

Clay and Shale Volume Modeling

Clay volume (VCL) and shale volume (VSH) models were generated to facilitate calculations of effective porosity, net reservoir/caprock, and support permeability and facies modeling. Due to the availability of advanced data (NMR, XRD) at the type well, both shale volume and clay volume-based approaches were used at TCCSP_OBS-1; however, [redacted] for the TCCSP_OBS-1 well specifically. An excellent overview of the differences in theory and interpretation between clay and shale volume modeling is summarized by Spooner (2014) [45].

The type-well VCL model was generated using a combination of the [redacted]. Due to the presence of [redacted]. Separate VCL curves were generated for each input curve, and a composite VCL curve was created by taking the minimum value between the models on a depth-by-depth basis or by manual selection, zone-by zone. The [redacted] The shale-based model is interpreted to offer a better method of comparison to offset wells, as the TCCSP SEM is [redacted]. A [redacted]. Statistical summaries of TCCSP_OBS-1 Vsh and Vcl volumes are available in **Table 1-11.**

During the construction of the VSH/VCL models within confining units, a [redacted]. Generally, [redacted]. During subsequent porosity modeling, these [redacted]. The contrasting depicts are interpreted to be related to [redacted]. The SP log is governed by the ability of [redacted] and therefore offer the most optimistic case in confining zones. It was decided to [redacted]

Table 1-11. Descriptive statistics of the TCCSP_OBS-1 clay and shale volume models. P10, P50, and P90 values show the percentile statistics for clay volume and shale volume

Formation	Clay Volume (%)			Shale volume		
	P10	P50	P9	P10	P50	P90
[redacted]						

Porosity and Water Saturation Modeling

Deterministic porosity and water saturation modeling methods were used to derive accurate estimates of porosity (total and effective) and water saturation at the TCCSP_OBS-1 type well. The porosity and water saturation analysis performed in [redacted] utilized an integrated analysis logic, drawing from multiple best-practice petrophysical principals and workflows. A flow-chart of the analysis logic used in the porosity-water saturation model of the TCCSP_OBS-1 well, also available in [redacted] is provided in **Figure 1-38**. [redacted] were recognized and addressed using a [redacted]). If [redacted] were met, [redacted]) were used in the total and effective porosity calculation.

Due to the [redacted] of the TCCSP well section, a [redacted] was used to solve for total and effective porosity values at the TCCSP_OBS-1 well, where [redacted]. The use of [redacted] is limited to [redacted], assuming the [redacted] is used. The deterministic [redacted] is limited to solving for [redacted] minerals; however, core analysis found [redacted] to be present within each zone which significantly impact log signatures and subsequent petrophysical models [redacted]) in addition to principal framework grains of [redacted]. Due to the presence of these [redacted]

[redacted]. The proportions of [redacted]. TCCSP porosity values are corrected for [redacted]. Porosity modeling results are depicted in **Table 1-12** and **Figure 1-39** below. The porosity model is observed to be [redacted]

Water saturation modeling was conducted within the TCCSP_OBS-1 well to (1) obtain relative water/gas saturation values, (2) estimate salinity and determine the lowermost USDW, and (3) identify and correct zones where gas effects may be skewing porosity model values. An [redacted]l was used within [redacted], while a [redacted]. Gas chromatography performed on mud gas circulated to surface found [redacted] of CO_2 and methane along with [redacted] of other hydrocarbon gases. Deterministic water saturation models can quantify one fluid in addition to brine but generally cannot split out specific volumes of more than one "non-brine" fluid. Therefore, the TCCSP_OBS-1 water saturation model was s[redacted]
Gas dominance was determined by taking the ratio of [redacted]. The TCCSP_OBS-1 saturation model is thought to be fairly accurate; however, specific volumes of [redacted]. A more detailed summary of the Picket plot analysis used in modeling salinity is available in section **1.2.9 Hydrologic and Hydrogeologic Information** [40 CFR 146.82(a)(3)(vi), 146.82(a)(5)] below.

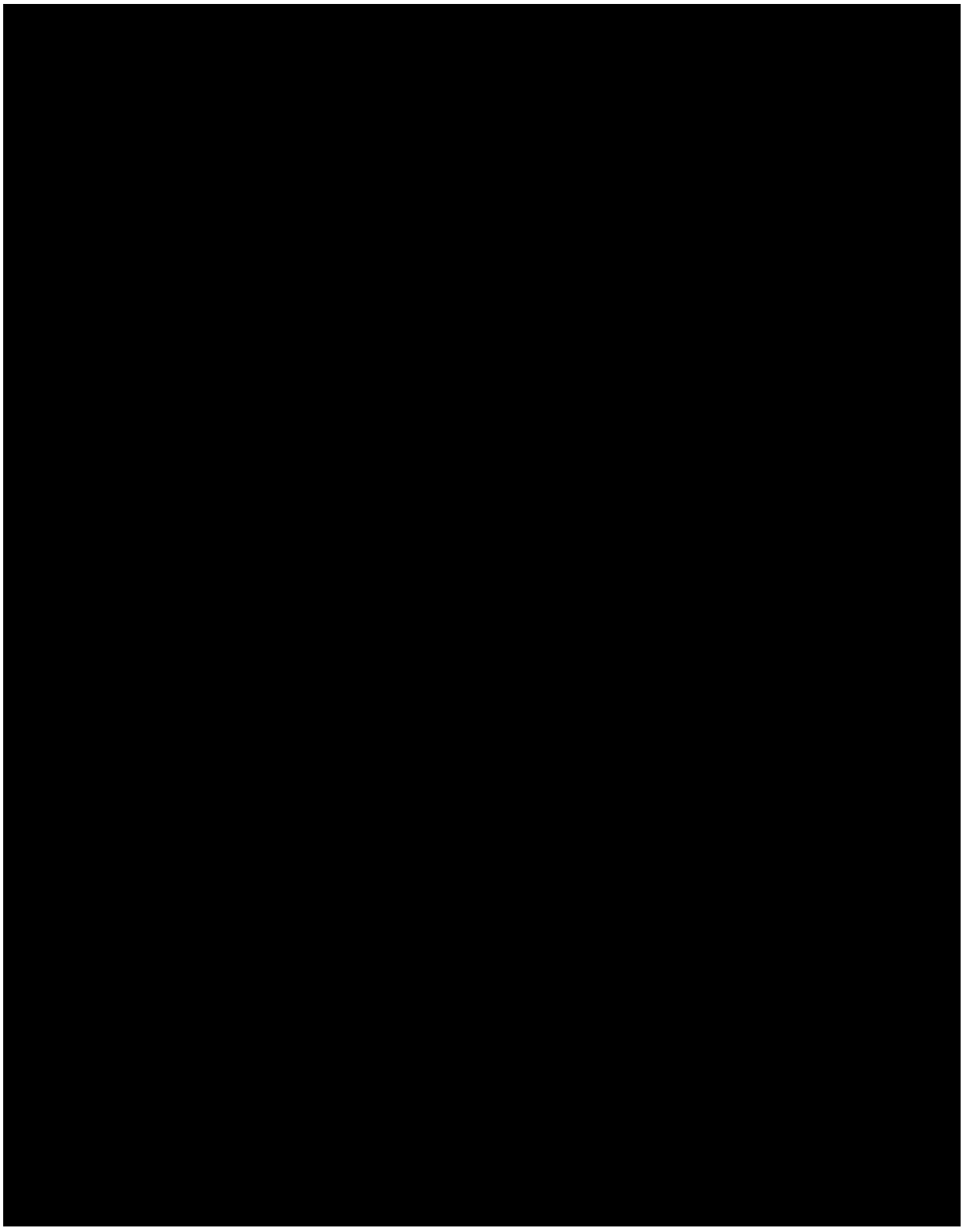

Figure 1-38. Deterministic porosity and water saturation analysis logic used by [redacted].

Table 1-12. Summary statistics of the TCCSP_OBS-1 deterministic multimineral porosity model.

Formation/Zone	Porosity Model Type	Porosity Model Statistics for [redacted] (VCL<0.3)					
		Total Porosity (PHIT)			Effective Porosity (PHIE)		
		P10 (%)	P50 (%)	P90 (%)	P10 (%)	P50 (%)	P90 (%)
[redacted]							

Figure 1-39. Overview of the porosity and water saturation model within the cored interval of the [redacted]

Type Well Permeability Modeling

While the permeability model developed from the NMR log at the TCCSP_OBS-1 successfully addressed reservoir heterogeneity observed from core analysis, petrophysical transforms were needed to generate permeability estimates from offset wells without NMR data. Core analysis results indicated that at least [redacted] petrophysical rock types (PRTs) exist within the reservoirs, however a method of differentiating between rock types and calling representative algorithms could not be identified during this iteration (such as a log-based facies scheme).

To address issue, [redacted] to evaluate potential correlations between log properties and permeability so that algorithms can be generated for application to offset wells. [redacted] from one another (**Figure 1-40**) and **Table 1-13**. T2LM is the log-mean of the T2 distribution, which in water-saturated rocks correlated to the log-mean of pore-body size (Kennedy, 2015). Many [redacted] exhibit a correlation between pore-body size and pore-throat size; this relationship serves as a foundational assumption in many wireline-based permeability prediction functions. These [redacted] based on T2LM were hypothesized as an effective way to [redacted]. Polynomial regression within the defined trend areas reveals [redacted] where the correlation is observed to [redacted] with a lower T2LGM. This [redacted] is interpreted to correspond to [redacted]. If T2LM permeability algorithms are to be used, T2LGM must be predicted in offset wells. [redacted]. An example VSH-T2LGM trend for the [redacted] is available in **Figure 1-42** and the defined VSH-T2LGM functions are summarized in **Table 1-14.**

A series of zone-specific T2LM curves were then calculated from VSH and spliced together using numeric IDs per zone into a composite T2LM curve. T2LGM types ([redacted]), represented as various colors on **Figure 1-41** were then [redacted] from the composite T2LM curve, serving as the mechanism to call respective trend-specific T2LM-Permeability prediction algorithms (detailed in **Table 1-13**). Permeability was bounded to [redacted].

Overall, this permeability algorithm was observed to [redacted] (see **Figure 1-43**, [redacted]). Additional work on developing more accurate permeability models for offset well analysis in the absence of NMR is needed.

Table 1-13. Summary table depicting zone-specific T2 log mean permeability prediction algorithms, where Φ = PHIT.

T2LM Trend	NMR T2LM trend value range	R2 value	T2LM Permeability (k) Prediction Algorithm
[redacted]			

Table 1-14. Summary of the zone-specific functions used to predict T2 log mean (T2LM) values in offset wells.

Zone	T2LGM (g) Prediction algorithm
[redacted]	

Figure 1-40. Cross-plot of multimineral total porosity and core-calibrated nuclear magnetic resonance (NMR) permeability values at the TCCSP_OBS-1 well colored by NMR T2 log mean. Approximately [redacted] colored clusters were used to generate [redacted] porosity-permeability transforms, based on the range of T2LM values.

Figure 1-41. NMR permeability-to-total porosity trends with annotated T2LGM trend area and fitted polynomial regressions.

Figure 1-42. Example cross-plot of shale volume to nuclear magnetic resonance (NMR) T_2 log mean (T2LM) from [redacted] showing the predictive relationship used to create pseudo-NMR logs for offset well permeability prediction.

Figure 1-43. Well log image depicting predicted T2LM-permeability (purple) to NMR permeability (blue).

TCCSP_OBS-1 Net Reservoir Cutoff and Summation Results

Type well petrophysical model properties (porosity, permeability, shale volume) were used to calculate net-to-gross thickness and attributes of both reservoir and caprock units to support the feasibility assessment of the TCCSP site. Net reservoir and caprock results are summarized in **Table 1-15** and **Table 1-16.**

Table 1-15. TCCSP net reservoir cutoff and summation results. MD = Measured Depth, mD= millidarcies, dec = decimal fraction.

Zone Name	Top (ft) MD	Bottom (ft) MD	Gross (ft)	Net (ft)	N/G	Average Phie (dec)	Average VSH (dec)	Average NMR Perm (mD)	NMR Permeability Height (mD*ft)
[redacted]									

Table 1-16. Summary table of net caprock cutoff and summation results. MD = Measured Depth, dec = decimal fraction.

Zone Name	Top (ft) MD	Bottom (ft) MD	Gross (ft)	Net (ft)	N/G	Average Phie (dec)	Average VSH (dec)
[redacted]							

Offset Well Petrophysical Modeling

Petrophysical modeling was conducted on eligible offset wells within the TCCSP study area (**Figure 1-44**). To be eligible for petrophysical modeling, offset wells needed to feature well logs capable of modeling shale volume (SP or GR), porosity (neutron, bulk density, compressional sonic) and water saturation (deep resistivity). A [redacted] was used for offset wells due to the regional scale of the SEM, the [redacted] hold across the [redacted], and the limited data availability of offset wells. [redacted]. Offset well porosity models preferably used [redacted] Water saturation modeling was not conducted [redacted]; otherwise, water saturation was assumed to be [redacted]. Due to the [redacted] to estimate permeability. As discussed in the section above, this permeability model fits reasonably within low and medium-permeability facies; however, it underperforms within the facies with the highest permeability.

Figure 1-44. Overview of the TCCSP SEM boundary showing wells used in SEM structural modeling and petrophysics labeled with a unique well ID (see Appendix Table 1-2), faults, existing oil and gas wells, and populated areas.

TCCSP Petrophysical Modeling Data Gaps and Recommendations for Future Work

To address current knowledge gaps and guide future field development, petrophysical investigations at the TCCSP should prioritize:

Furthermore, in addressing data gaps, planned investigations will generate datasets to refine the depth, thickness, porosity, permeability, mineralogy, and geochemistry of the [redacted]. Building on lessons from the TCCSP_OBS-1 well, the **Pre-Operational Testing Program** will focus on:

- [redacted]

Baseline data will also be collected from the [redacted] and the [redacted] to establish geologic, geochemical, and groundwater quality conditions above the storage complex. These above-zone datasets, supported by monitoring wells, will enable early detection of containment loss and help protect underground sources of drinking water (USDW) throughout CO_2 injection.

Storage Resource Estimates

CO_2 exists in a supercritical state when reservoir temperature exceeds [redacted] and pressure exceeds [redacted] - the critical point. Subsurface conditions within the TCCSP area satisfy these criteria, primarily due to target reservoir depths exceeding [redacted] across the SEM project footprint.

MDT data from the TCCSP_OBS-1 well confirm that both temperature and pressure within the target formations meet or exceed supercritical thresholds, validating their suitability for CO_2 storage in the supercritical phase.

To estimate CO_2 density under in-situ conditions, the following linear depth-based gradients were used to calculate pressure and temperature across the 3D geologic model:

- [redacted]

Using these gradients, 3D models of P and T were constructed in [redacted]. Based on the NETL CO2-SCREEN tool (Goodman et al., 2016) [46], a CO_2 density lookup surface was prepared where the [redacted]. **Figure 1-45** shows the CO_2 density lookup surface along with the pressure, temperature, and CO_2 density models.

As expected, [redacted]. Based on the 3D modeling, the range of reservoir conditions and resulting CO_2 densities for the target reservoir intervals ([redacted]) are depicted in the histograms shown in **Figure 1-45.**

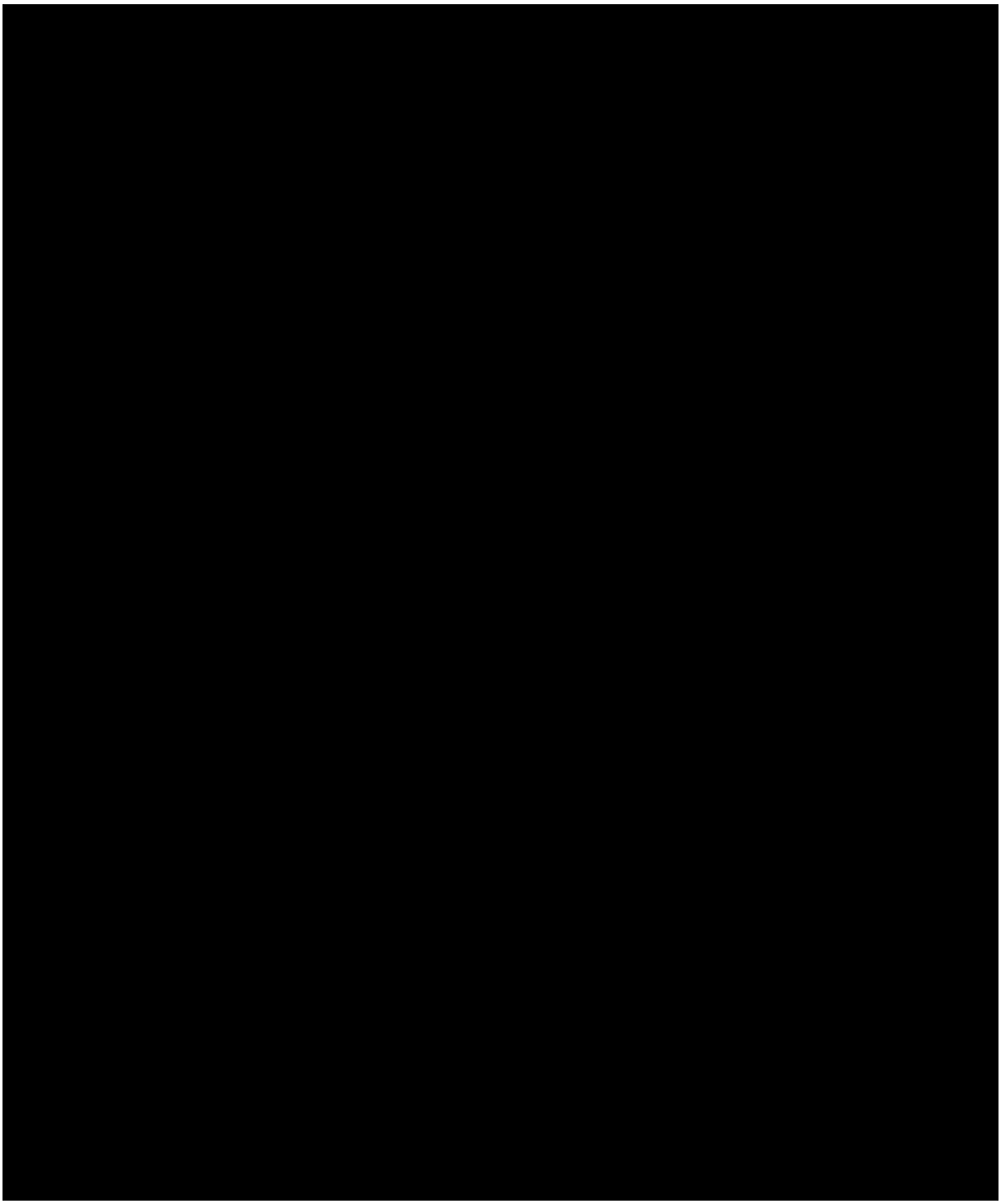

Figure 1-45. Pressure, temperature, and CO_2 density models for the TCCSP, from the [redacted], based on DST data. (a) Pressure models: pressure gradient function, modeled pressure range, and 3D pressure distribution. (b) Temperature models: temperature gradient function, modeled temperature range, and 3D temperature distribution. (c) CO_2 density models: CO_2 density look-up surface, modeled CO_2 density range, and 3D CO_2 density distribution.

A common "mass-based" method for calculating CO_2 storage potential in saline formations is given by the following equation from Peck et al. (2014) [48] and is also described in Goodman et al. (2011) [47]:

[redacted] **Equation 1**

Where:

[redacted]

Equation 1 was adapted for use in a 3D geocellular model such that estimates of CO_2 storage mass can be computed directly on individual cells and added together to produce CO_2 storage mass estimates (**Equation 2**). Furthermore, because [redacted] And thus, the storage efficiency factor is reduced to just the displacement terms: [redacted]

[redacted] **Equation 2**

Where:

[redacted]

A storage resource was not reported for [redacted]

With reservoir cells defined and using an effective porosity model, we are left with generating randomized E_{saline} efficiency factor models based on parameters from the NETLCO2-SCREEN [46] for a [redacted] and this was computed for the following three confidence levels: P10, P50, and P90 (**Table 1-17**)**.** The resulting $E_{saline} = (E_v * E_d)$ models had mean values of [redacted] for the P10, P50, and P90 confidence levels, respectively.

Thus, M_{CO2} could be computed and reported by model zone while [redacted], (**Figure 1-46**)**.**

Finally, the CO_2 storage resource estimate for the storage complex was computed using the 3D SEM which included models for bulk volume (Vc), effective porosity (ϕ_e), Pressure (P), Temperature (T), CO_2 Density (ρ_{CO2}(P, T)), and a storage efficiency factor models Esaline at the P10, P50, and P90 levels, **Figure 1-46.** CO_2 mass estimates are computed for all sand facies cells and for all three confidence levels. Results are tabulated and summarized in **Table 1-17** based on the area of [redacted] (the entire SEM footprint) and for a local area of [redacted] near the injection wells. The calculation assumed that all units are [redacted]. The P10 levels result in the smallest estimates with the greatest confidence; conversely, the P90 level reports the largest resource estimate but with the least confidence. The P50 level is between these two endmembers.

Resource Estimate Summary

Using a 3D SEM covering a [redacted] CO_2 storage resource estimates were calculated for reservoir zones from the [redacted], excluding the [redacted]. The resource estimates were computed on a "cellular level," meaning that each model cell had a corresponding volume, depth, pressure, temperature, facies, effective porosity, CO_2 density, storage efficiency factors, and resulting CO_2 mass. The CO_2 mass could then be computed (summed) for each reservoir zone based on [redacted].

The resource estimates reported for the [redacted] SEM area range from [redacted] of storage and depend on the confidence levels. Moreover, these estimates do not explicitly handle the [redacted]. Thus, a smaller "localized region" of [redacted] near the injection wells was used to produce a resource estimate that is [redacted] and would be more representative of the local geology. This assessment resulted in a local [redacted] for the P10 and P90 levels, respectively.

Figure 1-46. CO_2 resource estimate determination. a) Oblique 3D view of the facies model. Estimates are based on [redacted]. b) Oblique 3D view of the effective porosity model. [redacted] are omitted. c) Oblique 3D view of the Esaline efficiency factor model at the P50 level for a [redacted]. d) Histogram of the Esaline efficiency factor model at the P50 level for [redacted]. e) Oblique 3D view of the computed CO_2 mass per cell given effective porosity for [redacted] and the Esaline model. f) Zoomed-in portion of the P50 CO_2 mass model featuring a [redacted] near the proposed storage site. Resource estimates can be determined by model zone by adding up the CO_2 mass that has been computed for each cell.

Table 1-17. CO_2 storage resource estimates based on a lithostratigraphic static earth model and storage efficiency factors for a [redacted]. [redacted]. na = not applicable; these zones are not targeted for CO_2 injection.

Reservoir Unit	P10 Million Metric Tonnes	P50 Million Metric Tonnes	P90 Million Metric Tonnes
[redacted]			

1.2.7 Geomechanical Information [40 CFR 146.82(a)(3)(iv)]

A geomechanics characterization study was conducted on TCCSP reservoirs and caprock to evaluate their geomechanical profiles and assess their suitability for CO_2 confinement and injection. This analysis was conducted principally by [redacted], with most core analysis experimentation being conducted by [redacted]. The geomechanical study comprised three components, including (1) core-based testing and analysis of TCCSP_OBS-1 core; (2) well-log based geomechanical property modeling (mechanical earth model) and incorporation into a dynamic reservoir model; (3) fault slip potential analysis.

The geomechanical core analysis plan was designed to characterize various geomechanical properties of the units within the storage system, including their static and dynamic elastic properties (Young's modulus, Poisson's ratio, Bulk Moduli etc.) via triaxial and ultrasonic compressive testing, uniaxial pore volume compressibility, tensile strength (Brazilian indirect tensile strength), and mechanical creep behavior. Note that due to the limited available whole core within the [redacted]

[redacted] where possible. By geologic zone, a list of geomechanical tests are summarized in **Table 1-18**.

Table 1-18. Geomechanical tests by geologic zone and corresponding sample IDs.

Geologic Unit or Zone	Test Type	Sample Depths	Sample ID
[redacted]			

A well-log based mechanical earth model (MEM) was then created at TCCSP_OBS-1, well using [redacted]. The constructed MEM included continuous log-derived estimates of dynamic mechanical properties which were subsequently used to calculate [redacted] resulting in construction of a log-based mechanical earth model. Once the MEM was constructed at TCCSP_OBS-1, a [redacted] to facilitate MEM development in offset wells, where only [redacted] were available. The MEM model properties were then upscaled into the TCCSP SEM and exported for geomechanically-tied dynamic reservoir simulation. More information on the geomechanical SEM and dynamic reservoir simulations can be found in the **Area of Review and Corrective Action Plan**.

A probabilistic fault slip potential analysis study was then conducted on all resolvable faults within or around the TCCSP AoR and the region to assess reactivation pressure and induced seismicity risk in the context of simulated dynamic pressure buildup and net stress changes in response to CO_2 injection. The following subsections describe the results and interpretations from each stage of characterization.

Core-Based Analysis

Mechanical Creep Study Analysis

Core-based triaxial creep experiments were performed on three samples of [redacted] as summarized in **Table 1-19**. Mechanical creep tests are conducted to assess the time-dependent deformation of rock samples under constant stress. This helps to determine the rock strength (both reservoir and caprock) for long-term storage of CO_2.

The test [redacted]. Confining pressures ranged [redacted] (**Figure 1-47**). Compliance constant [redacted]. All samples showed [redacted]. [redacted] Compared to conventional [redacted] **Table 1-19**.

Table 1-19. TCCSP samples from caprock in the [redacted].

Formation	Sample Name	Depth (ft)	Confining Pressure (MPa)	Compliance Constant (MPa)	Creep Exponent
[redacted]					

Figure 1-47. Modified triaxial creep experiment design for sample

Triaxial Compressive and Ultrasonic Testing

Triaxial and ultrasonic compressive testing were performed on whole and routine sidewall core collected from the TCCSP_OBS-1 well, to obtain a variety of mechanical properties from TCCSP confining zones and caprocks. vertical plugs from whole core samples were subject to static and dynamic triaxial compressive strength testing. The plug samples from the whole core consisted of . additional sidewall core samples from the were subjected to static and dynamic (ultrasonic) triaxial compressive testing. Triaxial experimental analysis results are summarized in **Table 1-20** and **Table 1-21**, below.

Static and dynamic triaxial strength values

The sediment cores were . In the , static Young's moduli values (i.e., ranging between) and Poisson's ratios (i.e., below were , which would yield an
The yellow cells in **Table 1-20** highlight static Poisson's ratio values

values, ranging between [redacted] compared to typical values of [redacted], whereas red cells with no values indicate much lower [redacted] or higher [redacted]. As a result, these much [redacted] were omitted and should be used with caution. Due to the nature of the core, ultrasonic velocities could only be measured in the [redacted]

Table 1-20. Summary of static data, including the triaxial static Young's modulus, Poisson's ratio, and compressive strength measured from TCCSP_OBS-1 sediment cores.

Sample ID	Depth	Formation	Static Properties					
			As-Tested Bulk Density	Confining Pressure	Pore Pressure	Compressive Strength	Young's Modulus	Poisson's Ratio
[-]	[ft]	[-]	[g/cm^3]	[psi]	[psi]	[psi]	[Mpsi]	[-]
[redacted]								

Table 1-21. Summary table of ultrasonic triaxial properties.

Sample Number	Depth	Confining Pressure	Differential Stress	Axial Stress	Bulk Density	Acoustic Velocity[(1)]				Dynamic Bulk Modulus	Dynamic Young's Modulus	Dynamic Shear Modulus	Dynamic Poisson's Ratio	Vp/Vs
						Compressional		Shear						
[-]	[ft]	[psi]	[psi]	[psi]	[g/cm^3]	[ft/sec]	[us/ft]	[ft/sec]	[us/ft]	[Mpsi]	[Mpsi]	[Mpsi]	[-]	[-]
[redacted]														

(1) For all samples, [redacted]

#N/A: unreliable readings / readings not available

Brazilian Tensile Strength Testing and Core-based Fracture Pressure Estimates

[redacted] samples [redacted]) were subjected to Brazilian tensile strength tests to obtain indirect estimates of tensile strength. Tensile strength values were much higher in the [redacted]. As described in the TCCSP_OBS-1 mud log, the [redacted] was observed to be [redacted] than the remainder of the underlying formations, which likely made it more suitable for geomechanical analysis.

As summarized in **Table 1-22**, tensile strength in the [redacted] RSWC [redacted] samples was found to be between [redacted], versus the [redacted], and range [redacted]. The higher values from the [redacted] indicate more tensile strength, and therefore, a larger load is required for them to break. The low values from the [redacted] samples indicate that it does not take much load for them to break; however, this is likely due to the presence of a [redacted].

Table 1-22. Summary table of Brazilian Indirect Tensile Strength Testing Results.

Sample Number	Depth (ft)	Formation	Plug Orientation	Sample Length (in)	Sample Diameter (in)	L:D Ratio	As-Tested Bulk Density (g/cm^3)	Max. Axial Load (lbf)	Tensile Strength (psi)
[redacted]									

Uniaxial Pore Volume Compressibility

Uniaxial Pore Volume Compressibility test measures the change in the pore volume under uniaxial strain conditions. This is critical to analyze the storage capacity of reservoirs with increasing pressure as the CO_2 is injected into the formation. [redacted] samples from the [redacted] were subjected to uniaxial pore volume compressibility (UPVC) tests to determine pore volume changes as a function of changing net stress conditions which may result from CO_2 injection.

The UPVC test results for [redacted] show that the [redacted] (**Figure 1-48**, **Figure 1-49**, and **Figure 1-50**).

The [redacted] showed that [redacted] of [redacted] (**Figure 1-48**). However, in the [redacted], [redacted] after the pressure drop (**Figure 1-49** and **Figure 1-50**). It was observed that the tensile strength in the [redacted] RSWC samples was [redacted] when compared to the samples from the [redacted]. The low tensile strength of the [redacted] from the [redacted] may be partly due to the [redacted].

Figure 1-48. UPVC test results from [redacted]. Cbp refers to the bulk compressiblity , Cpp refers to the pore compressibility.

Figure 1-49. UPVC test results from [redacted]. Cbp refers to the bulk compressibility, Cpp refers to the pore compressibility.

Figure 1-50. UPVC test results from the [redacted]. Cbp refers to the bulk compressibility, Cpp refers to the pore compressibility.

Geomechanical Earth Modeling

A mechanical earth model (MEM) was constructed from well-log data from TCCSP_OBS-1 and eligible offset wells to estimate geomechanical properties of TCCSP reservoir and caprock units and be ultimately included as properties within the TCCSP SEM to feed into subsequent geomechanically-tied dynamic reservoir simulations of CO_2 injection. The TCCSP MEM included elastic properties (i.e., Young's modulus, and Poisson's ratio) and principal stress components (vertical stress [overburden], pore pressure gradient, minimum horizontal stress [fracture pressure/gradient], and maximum horizontal stress [tectonic compressive stress]).

Dynamic geomechanical data was intended to be used to calibrate the TCCSP MEM however, due to a [redacted], the MEM model was currently based entirely off of [redacted]

Elastic properties were calculated starting from [redacted] given that there were [redacted] available. Elastic properties such as compressional and shear velocities, Poisson's ratio, and Young's modulus were calculated. Sonic velocities were calculated by inverting travel time data:

[redacted]

Equation 3

Equation 4

Equation 5

[redacted]

Sonic velocities and densities were then used to calculate Young's modulus with the following equation where [redacted]

[redacted]

Equation 6

Additionally, sonic velocities were used to calculate Poisson's ratio using the following equation where [redacted], respectively:

[redacted]

Equation 7

Some elastic properties from static and dynamic laboratory tests were calculated on samples from the pilot well. The site is located in a region that is [redacted], which signifies that the [redacted]. The ratio of the principal stresses is given by the magnitude of A_{Φ}, which is [redacted] and calculated using the following equation:

[redacted]

Equation 8

Where [redacted] using the equation:

[redacted]

Equation 9

Where [redacted]

[redacted]

Equation 10

[redacted] **Equation 11**

Where [redacted], and has a range of [redacted], which gives a value of [redacted]. Earthquake focal mechanism inversion on earthquakes from an area [redacted] around the site was used to compute the magnitudes of the [redacted] principal stresses. Based on the values of [redacted] was estimated. For the pore pressure, a value of [redacted]

The variations of S_{hmin} with depth can be related to the variations in Young's modulus through an effective medium model, where [redacted]

[redacted] **Equation 12**

Equation 13

Equation 14

Where [redacted]. Based on the mineral assemblage of the [redacted] samples, [redacted]. While relatively stiff rocks are able to support differential stresses through geological time, more compliant lithologies relax differential stress over geological time through inelastic deformation. Elastic properties derived from both well logs and static/dynamic laboratory data on cores were used to estimate the variations of differential stress (difference between the maximum and minimum stress components) with depth.

[redacted] **Equation 15**

Where [redacted]. The well log data were put through a median filter to remove any spikes and outliers.

Figure 1-51. Elastic property and stress profiles for TCCS_OBS-1. (a) Sonic velocities. Curves represent log data and points represent static and dynamic lab data. (b) Poisson's ratio (c) Young's modulus (d) Stress and pore pressure.

Table 1-23. Statistical populations for Young's Modulus and Poisson's Ratio.

Formation	Depth Range	Young's Modulus			Poisson's Ratio		
		STD	Mean	Range	STD	Mean	Range
[redacted]							

Table 1-24. Statistical populations for Shmin, Sv and SHmax.

		Shmin (psi)			Sv (psi)			SHmax (psi)		
Formation	**Depth Range**	**Mean**	**Range**	**STD**	**Mean**	**Range**	**STD**	**Mean**	**Range**	**STD**
[redacted]										

Table 1-25. Statistical populations for Pore Pressure and Fracture Gradient.

Formation	Depth Range	Pore Pressure (psi)				
		Mean	Range	STD	PP gradient (psi/ft)	Fracture gradient (psi/ft)
[redacted]						

Once elastic properties and stress profiles were estimated for the TCCSP_OBS-1 type well, the properties and stress components were calculated for nearby offset wells. In wells with [redacted]. Stress profiles were then calculated for all offset wells with [redacted]. Once the elastic and stress profiles were calculated for offset wells, Young's modulus, Poisson's ratio, and other profiles were distributed between wells throughout the mechanical earth model in [redacted]

Table 1-26. Type wells for TCCSP used to calculate 3D elastic and stress profiles are denoted by an asterisk.

A geomechanical model was constructed and executed to analyze the impact of planned injection rates on storage formation and caprock integrity. The inputs for the model were based on the TCCSP_OBS-1 well core and log data, including the nearby wells. A one-way coupling and a single grid were used for flow and geomechanical modeling. The reservoir modeling results indicate that [redacted]. For the [redacted]. However, the maximum modeled pressure buildup is only [redacted] – demonstrating a substantial safety margin even at the weakest point. For the other storage zones, which have higher permeability and greater depth, the [redacted]. Consequently, the geomechanics results indicate that a [redacted]

Fault Slip Potential

To evaluate the risk of induced seismicity from potential fault slippage in response to CO_2 injection, a fault slip potential study was conducted using known mapped faults and theoretical faults based on historic seismicity data. Seismic data indicates the presence of a [redacted]. In addition, a total of [redacted] were identified from the catalog of earthquake occurrences (**Figure 1-52**). Beyond these directly mapped faults, additional potential fault planes were inferred by analyzing the spatial distribution of earthquake events in the vicinity of TCCSP_OBS-1. Each seismic event was interpreted as evidence for a fault at depth, even though its precise geometry, including orientation, length, and vertical extent, could not be fully resolved. Event magnitudes were used to place approximate limits on possible fault dimensions, following the approach of Walters et al. (2015) [49]. Within the SEM boundary, these data led to the interpretation of [redacted] in the TCCSP_OBS-1 area. These faults were assumed to be [redacted]. They were further assumed to [redacted]. To account for uncertainty, fault strikes were permitted to [redacted] of the [redacted]. **Figure 1-52** displays the combined fault map.

Fault Slip Potential (FSP) analysis with probabilistic [redacted]) showed [redacted] at expected injection pressures (**Figure 1-53**). Pressure buildup from [redacted] remains [redacted] required to elevate slip risk.

Figure 1-52. Mohr-Coulomb analysis, faults are colored by the change in pore pressure to induce slip. (left) Fault map with mapped faults from seismic imaging and interpreted faults from earthquake hypocenters. (right) Mohr-Coulomb diagram showing the initial stress state of fault populations around TCCSP_OBS-1.

Figure 1-53. Histograms of realizations of geomechanical parameters used in probabilistic fault slip analysis for

Figure 1-54 shows the results of the geomechanical parameter study. It is inferred that the probability of fault slip is [redacted]. This is because the faults are [redacted]. This is why the area has a low background seismicity. There is almost [redacted]. **Figure 1-54** shows that [redacted]

Figure 1-54. Probabilistic fault slip analysis. (a) Probability of fault slip as a function of change in pore pressure. (b) Variability of geomechanical parameters. (c) Sensitivity of fault slip probability to geomechanical parameters for [redacted]

The probabilistic fault analysis results are combined with those of the dynamic reservoir model to estimate the change in the probability of fault slip with time. **Figure 1-55 (a)** shows the change in pore pressure after [redacted]. This layer is chosen to assess the change in fault slip potential as it consists of the greatest perturbation of pore pressure. **Figure 1-55 (b)** shows the change in pore pressure at the [redacted]. The pressure change values range from [redacted] Comparing this to the probability of fault slip curves, [redacted] after CO_2 injection.

Figure 1-55. Dynamic reservoir model results [redacted]. (a) Pore pressure change due to CO_2 injection. (b) Pressure change at fault midpoints.

TCCSP Geomechanical Investigation Conclusions

The caprock at the TCCSP site is [redacted], with Young's modulus values ranging from [redacted] and Poisson's ratio between [redacted]. Laboratory creep experiments show a [redacted] and a [redacted] indicating [redacted] behavior. The in-situ stress regime is [redacted], [redacted], and [redacted]. Fault slip potential analysis suggests that the probability of slip on mapped and interpreted faults is [redacted]. Taken together, these findings imply that the caprock provides favorable conditions for long-term CO_2 storage, with [redacted]

1.2.8 Seismic History [40 CFR 146.82(a)(3)(v)]

The TCCSP site lies within a region of [redacted] earthquake hazard based on the Long-term National Seismic Hazard Model Map [20] from the USGS (**Figure 1-56**). This represents a regionally moderate level of damaging earthquake shaking, equivalent to Modified Mercalli Intensity VI and higher in 100 years, from the 2023 50-state National Seismic Hazard Model [20]. However, the AoR and associated SEM boundary are located in a region with [redacted] within the Central Valley compared to the rest of the state of California.

The closest identified active fault to the AoR is the [redacted]. As displayed by the USGS Quaternary faults [21] catalogue, this is a [redacted]-trending fault, dipping to the [redacted] at roughly [redacted]. The active section of the fault [redacted] from the AoR) is shown to demonstrate [redacted] [22], with identified earthquake epicenters of no greater than [redacted] that are local to this fault [23].

The [redacted] situated [redacted] of the AoR, similarly, is a [redacted] that is associated with a compressional regime initiated by strike-slip movement from the [redacted]. Major earthquakes [redacted] associated with the [redacted] have been focused within the [redacted] [24], over [redacted]. The closest major fault system to the AoR is the [redacted]. The fault is predominantly active within its [redacted] sections, especially as the center experiences aseismic creep. The greatest earthquake associated within the [redacted] was the magnitude [redacted] of the AoR.

The United States Geological Survey Earthquake Catalogue was screened for all earthquakes within a [redacted] radius of the AoR and was used to generate a historical earthquake magnitude and location map from 1800 to 2024 (**Figure 1-57)** [24]. Within [redacted] of the AoR, [redacted] earthquakes with a magnitude [redacted] have occurred from [redacted] (see **Attachment A**). All of these earthquakes are [redacted] The largest earthquake within a [redacted] radius around the AoR occurred on [redacted]. This earthquake occurred [redacted] of the AoR. The earthquake nearest to the AoR, located [redacted], occurred on [redacted] (see **Attachment A**). Most of the earthquakes, [redacted] earthquakes since [redacted], are below a magnitude [redacted]. It is for this reason that Tulare County has been designated a [redacted] seismicity shake risk, further indicated by the California Integrated Seismic Network (CISN) [23], [25].

Given the historically low-magnitude earthquakes recorded within [redacted] of the AoR and the [redacted] within the AoR and storage complex, seismic activity is not expected to disrupt the confining unit, the storage reservoirs, or the containment of CO_2 within the storage zone. The [redacted] within the AoR and storage complex indicates that [redacted], which could offset the confining unit of the storage zone and lead to CO_2 leakage. In addition, the storage reservoirs are [redacted]. The more [redacted] within the storage zone suggests that these storage reservoirs would likely [redacted], in response to earthquake stress. These observations indicate that [redacted] with containment in the TCCSP AoR.

Figure 1-56. U.S. National Seismic Hazard 2023 Model (NSHM) earthquake risk map that indicates the chance of any level of damaging earthquake shaking in 100 years [20]. The shaking is equivalent to Modified Mercalli Intensity VI and higher. The TCCSP site is indicated by the black star. Modified from the United States Geological Survey [20].

Figure 1-57. Location map of earthquakes above a magnitude [redacted] since 1800 from the United States Geological Survey Earthquake Catalog [24].

Seismicity Conclusions

The TCCSP "geologic system" has been spatially defined by its AoR and its storage complex, comprised of confining and reservoir zones. Based on nearby 2D seismic lines, this subsurface region appears [redacted] CO_2 containment. Based on borehole image data from the TCCSP_OBS-1 well, [redacted]. Moreover, geomechanical testing from TCCSP_OBS-1 core samples indicates that [redacted]. For these reasons, the site is believed to offer favorable conditions for receiving and containing the proposed volumes of CO_2 for this project. Furthermore, the site is believed to be [redacted] in the AoR.

[redacted] is an integral component of site operations and is being actively developed as part of the **Testing and Monitoring Plan**. Although [redacted], TCCSP recognizes the importance of [redacted]. The monitoring network will be designed to provide reliable coverage of the storage complex and surrounding AoR.

Consistent with permit requirements, the site will be operated and monitored in a manner that limits risk of endangerment to USDWs, including risks associated with induced seismicity. Should an induced seismic event occur, the monitoring system will enable timely detection and response, ensuring that risks are promptly addressed and mitigated. Overall, the site poses a [redacted]

1.2.9 Hydrologic and Hydrogeologic Information [40 CFR 146.82(a)(3)(vi), 146.82(a)(5)]

A hydrologic and hydrogeologic framework of the TCCSP site was created by conducting a multifaceted study involving (1) geospatial assessment and cataloging of publicly available water wells within TCCSP area; (2) hydrogeologic literature review; (3) resistivity-log based hydrosalinity modeling; and (4) analysis of live MDT fluid samples from TCCSP reservoirs. The subsections below describe the results of these studies.

Geospatial Assessment and Cataloging of Local Groundwater Wells

The California Department of Water Resources (DWR) Sustainable Groundwater Management Act (SGMA) Data Viewer was consulted to identify water wells in the AoR [30]. Groundwater well locations and completion reports were identified and imported into ArcGIS Pro® mapping software to determine the locations of water wells within the AoR. Because the California DWR registers water well completion reports both to their exact locations and to Public Land Survey System (PLSS) section centroids, wells were tabulated within the AoR and [redacted] to account for positional uncertainty. There are [redacted] water well completion records within the AoR and the [redacted] [30] (**Figure 1-58**). The water well type, completion depth, perforation depths, and latitude/longitude coordinates are shown in **Appendix Table 1-1**. The well completion depths range from [redacted] feet and are primarily [redacted] [30]. The perforation and completion depths indicate that these water supply wells source groundwater from the undifferentiated [redacted] and the underlying [redacted]. [redacted] of the water wells penetrate the storage zone reservoirs or confining units and are separated by nearly [redacted] of overburden from the top of the primary confining unit ([redacted]).

Figure 1-58. Location map of shallow groundwater wells within the AoR. Water well locations are taken from the California Department of Water Resources and tabulated for the AoR [30].

Hydrogeologic Literature Review

The TCCSP site contains a single aquifer system called the [redacted]. The [redacted] is comprised of near-surface alluvium and the [redacted] that consists of [redacted] deposited along a [redacted] [26]. The [redacted] and is considered the deepest USDW in the project area. The base of the [redacted] is encountered at approximately [redacted] measured depth, whereas the base of the USDW is estimated at [redacted] MD, indicating that the USDW lies within the [redacted]

A groundwater study conducted near the town of [redacted], by Luhdorff and Scalmanini (2017) using primarily shallow electric logs indicated that the [redacted] at depth are saturated with [redacted] and are not an Underground Source of Drinking Water [26]. In addition, the overlying [redacted] may be [redacted]. The [redacted] based on their electric logging responses (**Figure 1-60).** Moreover, a statewide groundwater study by Kang et al. (2020) estimated that the

base of freshwater within the region was at a depth range of [redacted] (**Figure 1-61)** [27]. A historic groundwater flow map is provided in **Figure 1-62**, indicating that the regional groundwater flow direction is [redacted] the TCCSP site. A site-specific hydrogeologic assessment will be conducted in future characterization efforts once site-specific hydrogeologic data is available after construction of the [redacted] and [redacted].

Figure 1-59. Location map of the H-H' hydrogeologic cross-section line [redacted] of the TCCSP project area (yellow star). Modified from Luhdorff and Scalmanini, 2017 [26]. AMEC stands for AMEC Foster Wheeler Environment & Infrastructure, Inc., formerly Associated Mining and Engineering Consultants.

Figure 1-60. Hydrogeologic cross-section showing interpreted hydrogeologic units near the AoR. Modified from Luhdorff and Scalmanini, 2017 [26].

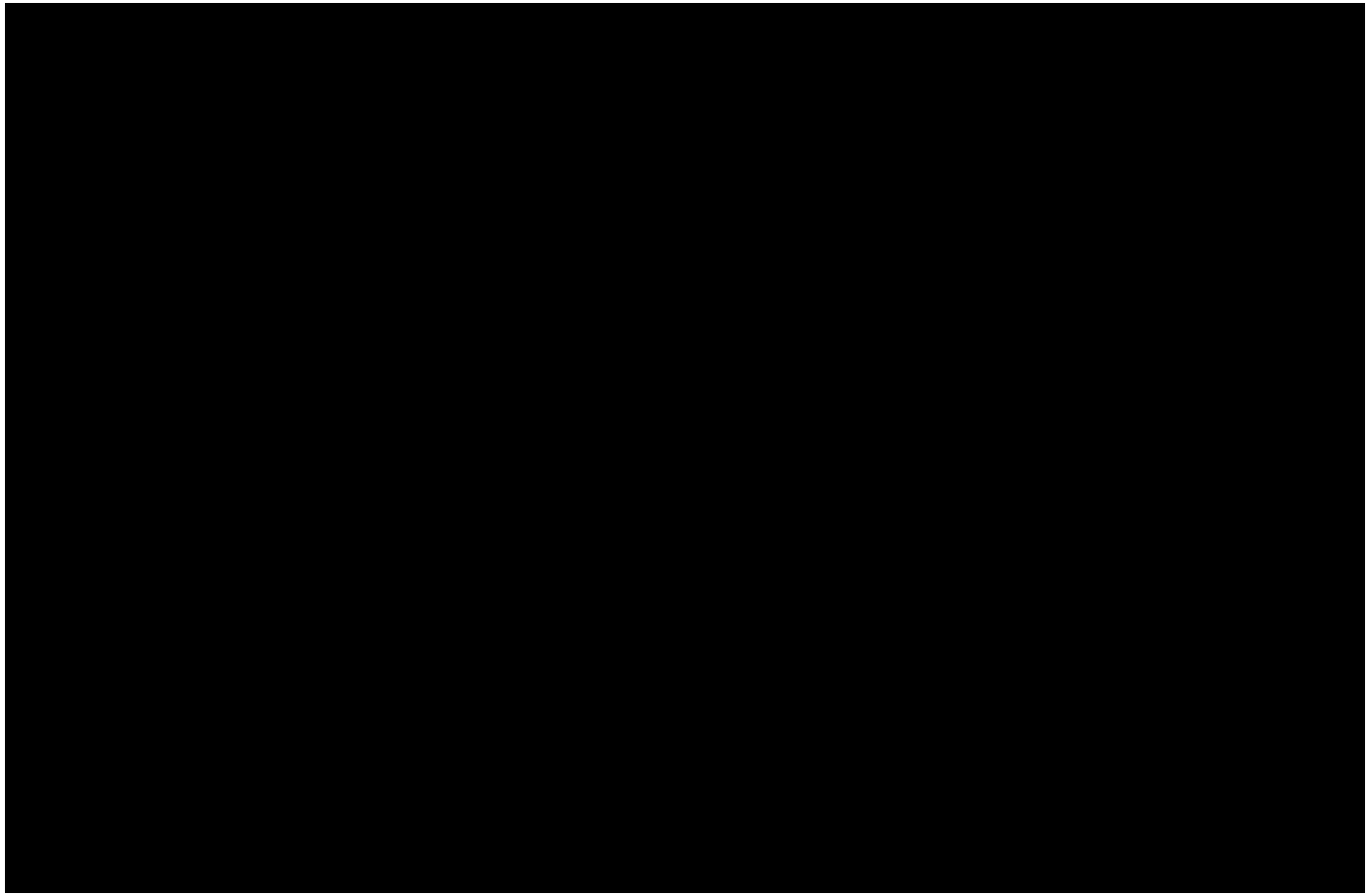

Figure 1-61. Elevation (meters below land surface) of the base of freshwater [redacted]); [A] overview map of larger base of freshwater map with reference to the approximate TCCSP project location, denoted by gold star. [B] site specific map of base of freshwater zoomed in within the TCCSP study area with injection wells. Modified from Kang et al., (2020) [27]. The AoR is indicated by the blue circle within the SEM (dashed line) boundary). The AoR falls within the [redacted].

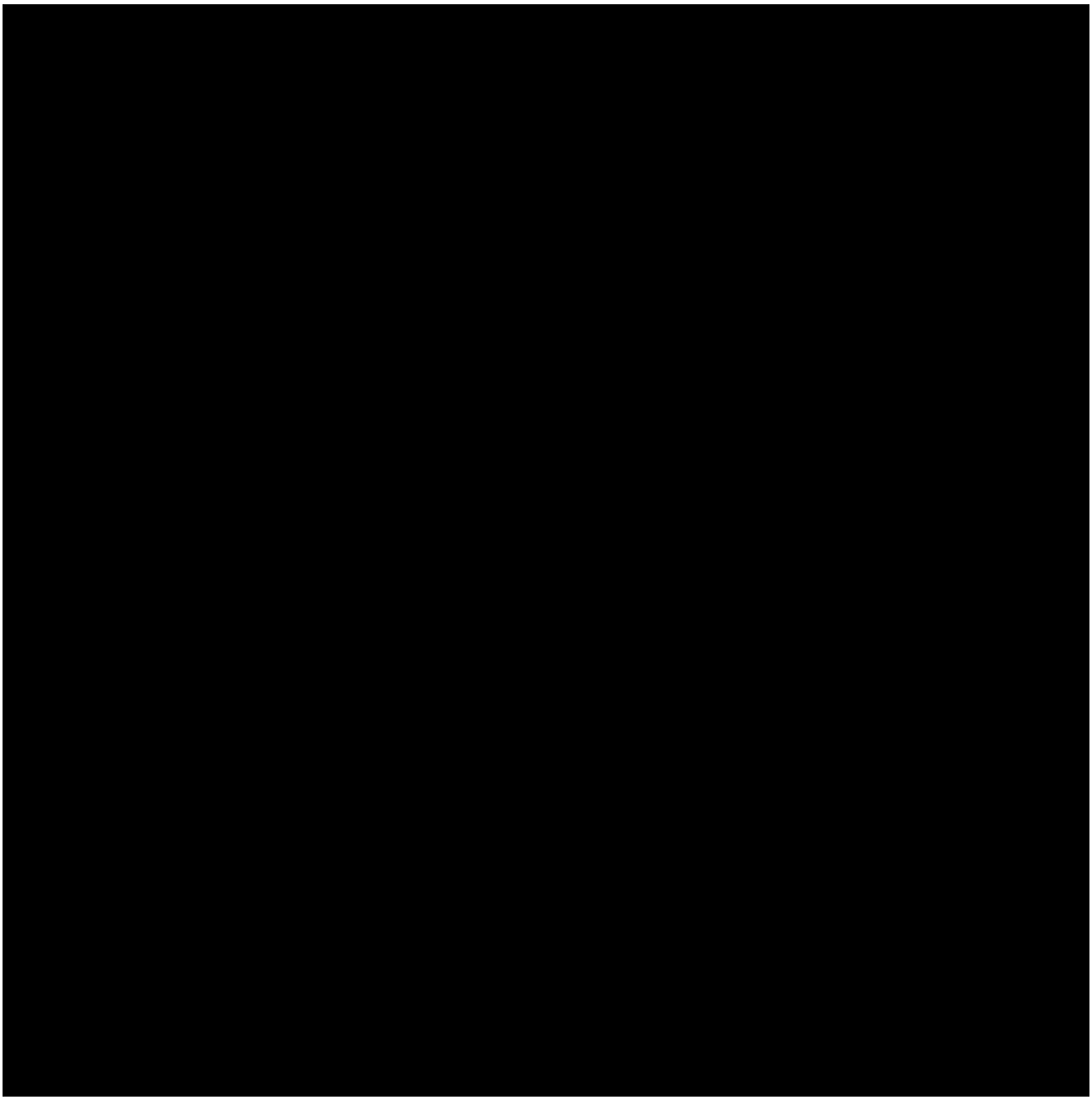

Figure 1-62. Regional groundwater flow map showing the relative position of the TCCSP study area (yellow box; not georeferenced) and the groundwater modeling study area (purple box), modified from Quin (2008).

Well-Log Based Hydrosalinity Modeling and Fluid Sample Analysis

The depth of the lowermost USDW and reservoir salinity values were estimated using [redacted] to estimate the resistivity of water (Rw), and subsequently the concentration of total dissolved solids (TDS) using [redacted] each geologic unit present at the site. [redacted] was conducted by [redacted]. **Table 1-27** summarizes the values of Rw, *m*, and *n* for each zone, and example interpreted [redacted] for the [redacted] are depicted in **Figure 1-63** and **Figure 1-64.** TCCSP reservoirs feature a range of estimated salinity values from [redacted], and the lowermost USDW contact is estimated to be located at the [redacted]. This [redacted] is interpreted to serve as an [redacted] targeted for injection by TCCSP. These results support Luhdorff and Scalmanini (2017), who identified the [redacted] [27].

TDS values of MDT-derived direct live fluid samples are summarized in **Table 1-27**, below which suggest TCCSP reservoirs TDS values to range between [redacted]. These direct fluid samples verify the [redacted], despite them likely being [redacted]. Further details on TCCSP reservoir fluid chemistry and MDT fluid samples are found in section **1.2.10** Geochemistry [40 CFR 146.82(a)(6)]. To refine characterization of reservoir salinity and TDS in the TCCSP, [redacted] will be collected in accordance with the **Pre-Operational Testing Program**.

Table 1-27. Interpreted Resistivity of Water (Rw) Values of TCCSP Aquifers

Zone	[1] *m* exponent	*n* exponent	[1] Rw @ [redacted]	Rw Salinity (kppm)
[redacted]				

Figure 1-63. [redacted] interpretation for the cleanest [redacted] Values of Rw, m, n, a and salinity are shown at the bottom of the image.

Figure 1-64. [redacted] interpretation for the cleanest [redacted]. Values of Rw, m, n, a and salinity are shown at the bottom of the image.

Table 1-28. TDS values of direct MDT fluid samples from TCCSP reservoirs.

Analyte	[redacted]	[redacted]
	Concentration (mg/L)	Concentration (mg/L)
[redacted]		

1.2.10 Geochemistry [40 CFR 146.82(a)(6)]

Fluid Phase Geochemistry

The fluid phase geochemistry of TCCSP reservoirs was characterized by analyzing direct in-situ (live) fluid samples collected using an MDT tool, and these results are supplemented with a review of publicly available data from the regional USGS Produced Water Database [32]. The subsections below summarize results from both analysis types.

Geochemical Analysis of TCCSP Direct Fluid Samples

A total of [redacted] live fluid samples were collected using a [redacted] at TCCSP_OBS-1. Fluid samples were analyzed via [redacted] to determine the baseline ionic (cation and anion) and trace metal concentrations, isotopic and physiochemical profile (such as pH, temperature, salinity, and resistivity of water). A summary of analytical results depicting these geochemical profiles of the TCCSP reservoirs are available in **Table 1-29**, **Table 1-30**, **Table 1-31**, and **Table 1-32.**

Both MDT samples are suspected to be likely be [redacted]. It is thought that the TCCSP_OBS-1 well likely features a [redacted], given the [redacted] Questions regarding how representative the fluid chemistry values are for the TCCSP site will be addressed as additional [redacted] are obtained as described in the **Pre-Operational Testing Program** and **Testing and Monitoring Plan**.

Table 1-29. Summary of the physiochemical properties of the TCCSP reservoirs.

Analyte	[redacted]	[redacted]
	Concentration	Concentration
[redacted]		

Table 1-30. Summary of the ionic concentrations detected within the TCCSP reservoirs.

Parameter	Symbol	[redacted]	[redacted]
		Concentration (mg/L)	Concentration (mg/L)
[redacted]			

Parameter	Symbol	[redacted]	[redacted]
		Concentration (mg/L)	Concentration (mg/L)
[redacted]			

Table 1-31. Summary table of trace elements composition (metals/metalloids) detected within TCCSP Reservoirs

Analyte	[redacted]	[redacted]
	Concentration (mg/L)	Concentration (mg/L)
[redacted]		

Table 1-32. Summary table of stable and radiogenic isotope concentrations measured in TCCSP_OBS-1 reservoirs.

Analyte	[redacted] Concentration (mg/L)	[redacted] Concentration (mg/L)
[redacted]		

Review of Regional USGS Produced Water Database

The USGS Produced Waters Database [32] was screened for available pore-fluid water quality data throughout the San Joaquin basin to determine the baseline fluid-phase geochemistry in the project AoR and SEM. The closest well locations with available produced water quality data for the storage zone geology reservoirs ([redacted]) occur over [redacted], California, **Table 1-33** and **Figure 1-65**. Average TDS for these reservoirs are [redacted]. Fluid-phase geochemistry values for the nearby wells are reported in **Table 1-33**.

Additional fluid-phase geochemical data will be collected as a part of the **Pre-Operational Testing Program** and [redacted] will be collected from the storage zone reservoirs and hydrogeologic units. The fluid-phase geochemical data indicates that the storage reservoirs are [redacted]

Table 1-33. Water quality data of produced waters from the USGS Produced Waters Database [32].

Figure 1-65. Accompanying map to Table 1-33 showing the locations of wells used to sample pore-fluids.

Solid Phase Geochemistry

Solid-phase mineralogy of the [redacted] are discussed in more detail in section **1.2.6 Injection and Confining Zone Details** [40 CFR 146.82(a)(3)(iii)] of the **Project Narrative**. Additional mineralogical and geochemical data for the storage zone reservoirs will be acquired through [redacted] which is further discussed in the **Pre-Operational Testing Program**.

Geochemical Modeling

The current dynamic computational model includes the dissolution of CO_2 into formation brine throughout the project's lifespan. Modeling results indicate that approximately [redacted] Approximately [redacted]. The mineralization, which, on the project's life span, is expected to be [redacted] [41] is not accounted for at this stage. But a literature review of [redacted] [42,43]. The geochemical analysis of storage formation rock fabric is in progress. If warranted, this information will be incorporated into the future iterations

of the model, but [redacted] are expected for TCCSP storage formations. The current simulation model possesses the ability to couple advanced geochemical processes in case it is needed.

Geochemical reactivity between reservoir brine, solid phase minerals and TCCSP CO_2 injectate remains a data gap. Geochemical modeling will be conducted in subsequent investigations as the fluid and mineral profiles are further delineated, as described in the **Pre-Operational Testing Program.** Depending on geochemical modeling results, [redacted] to determine if there are any porosity and permeability impacts that could affect the reservoir properties and resultant AoR. Based on the evidence from these tests, if required, the reservoir model will be promptly updated and re-ran to assess updates to the project AoR. If applicable, the model will also be geochemically coupled to fully understand the impact of any in-situ geochemical reactions on the solid reservoir matrix. Findings from this assessment will be provided to the U.S. EPA Region 09 UIC Program Director promptly.

1.2.11 Other Information (Including Surface Air and/or Soil Gas Data, if Applicable)

No surface air and/or soil gas data are available or were used for the Tulare County Carbon Storage Project.

1.3 Site Suitability [40 CFR 146.83]

Site characterization results indicate TCCSP's subsurface strata provide excellent properties for safe, long-term storage of commercial quantities of CO_2 at the [redacted] scale, as demonstrated by the TCCSP_OBS-1 well data.

The TCCSP storage complex leverages a [redacted]), and the [redacted]. TCCSP reservoir [redacted]

Well-log and 2D seismic-based regional mapping of TCCSP reservoir [redacted] and confining zones indicate the complex features excellent geologic attributes. All TCCSP reservoirs were observed to be comprised of [redacted] AoR and greater region. At TCCSP_OBS-1, reservoirs are generally observed to be [redacted] The [redacted] units are [redacted]. Both units are observed to occur within supercritical depth ranges across the study region, [redacted]. At TCCSP_OBS-1, the [redacted] composed of [redacted]

[redacted]. The [redacted] is observed to be [redacted] and be comprised of [redacted]

Findings from depositional analysis of TCCSP_OBS-1 sediment cores and review of regional geologic literature indicate TCCSP reservoirs, confining units, and intermediate seals feature favorable depositional settings for commercial storage. The site's [redacted] from the project AoR. Some [redacted]; these likely represent [redacted] in and around the site. Intermediate seals within [redacted] generally coincide with [redacted]. The primary confining zone ([redacted]) and secondary confining zone ([redacted]) both represent similar [redacted].

Many historical demonstrations of the suitability and regional sealing capacity of the TCCSP confining zones and intermediate seals can be found at oil and gas fields across the San Joaquin Basin. As summarized by Hewlett et al. (2014) [4], the sealing performance of the [redacted]). Demonstrations of [redacted].

The TCCSP AoR and surrounding region was evaluated using well-log, seismic and literature-review based techniques, which found the site to feature a low amount of structural complexity. Review of regional literature [1] and historic seismicity data indicate the TCCSP AoR and surrounding area to be in a [redacted] portion of the basin. Evaluation of historic 2D seismic around the site found [redacted] the TCCSP storage complex (confining zone or reservoirs) within or near the project AoR. [redacted] faults were observed within the [redacted] of TCCSP_OBS-1, however they are [redacted]). These [redacted]

Resistivity-based borehole image log (RBIL) analysis was conducted at TCCSP_OBS-1 to evaluate the presence of unmapped/sub-seismic faults and natural fractures in reservoirs and confining zones. RBIL analysis found [redacted]. The [redacted] at TCCSP_OBS-1.

Core analysis results (RCA, MICP, NMR) from the TCCSP reservoirs indicate the complex possesses [redacted]. Petrophysical modeling and core analysis data indicate the TCCSP reservoirs are [redacted] and feature [redacted] permeability [redacted] occur throughout the reservoir section, most commonly within the [redacted]. Net reservoir attributes for the TCCSP_OBS-1 reservoirs are [redacted] which is estimated to have [redacted]. Using core-calibrated petrophysical modeling values, static CO_2 storage capacity resources estimate within the AoR estimate the TCCSP site to be capable of storing between [redacted]

Petrophysical properties of the TCCSP confining zones ([redacted]) and intermediate seals were characterized by core and, to a lesser degree, conventional petrophysical analysis techniques. Porosity and permeability values measured using [redacted]. XRD and MICP analysis found these same cored samples to be [redacted]. MICP-based CO_2 column height modeling conducted on [redacted]. Furthermore, a threshold entry pressure experiment conducted on an [redacted] would be required to allow for entry into the pore throats of the sealing facies, which is far [redacted] for TCCSP reservoirs generated during dynamic simulations. Although no core analysis data exists for the [redacted], the NMR log indicates the zones to be [redacted]. Collectively, these properties demonstrate the ability of sealing facies of the [redacted] to safely and effectively confine commercial quantities of CO_2 for permanent storage.

Geomechanical modeling and core analysis found the TCCSP site to feature [redacted]. A mechanical creep study conducted on [redacted]

[redacted]. These results indicate that [redacted]. Variations in estimated Sh_{min} (fracture pressure) values between seal and reservoir units indicate Sh_{min} [redacted] than reservoirs indicating good conditions for CO_2 storage. Additionally, simulated pressure build ups during computational modeling were found to be well below [redacted] fracture pressure of TCCSP reservoirs. Probabilistic fault slip analysis found that [redacted]. The increase in simulated pressure buildup from [redacted], and therefore the TCCSP site exhibits [redacted] as a response to CO_2 injection. More information on computational modeling can be found in the **Computational Modeling Details** document.

The dynamic storage capacity for the TCCSP storage formations is based on the results of the reservoir simulation. A total of [redacted] is planned to be injected over the time frame of [redacted] Due to the good permeability of the storage formations, the pressure buildup is not a limiting factor. The maximum well bottomhole pressure of injection wells remains much lower than the [redacted] limit of the fracture pressure. Therefore, the storage capacity is based on the CO_2 lateral plume extent at the end of the [redacted]. The reservoir simulation inherently accounts for all types of flow-related efficiency factor. The dynamic storage capacity is then estimated by dividing the total mass injected (MMt) by the area of the CO_2 plume ($mile^2$) at the end of [redacted] of the post-injection phase. The modeling results indicate an approximate value of [redacted] for dynamic storage capacity.

1.4 AoR and Corrective Action [40 CFR 146.84]

AoR and Corrective Action GSDT Submissions

GSDT Module: AoR and Corrective Action
Tab(s): All applicable tabs

Please use the checkbox(es) to verify the following information was submitted to the GSDT:
☐ Tabulation of all wells within AoR that penetrate confining zone ***[40 CFR 146.82(a)(4)]***
☐ AoR and Corrective Action Plan ***[40 CFR 146.82(a)(13) and 146.84(b)]***
☐ Computational modeling details ***[40 CFR 146.84(c)]***

The information and files submitted in the **AoR and Corrective Action Plan** satisfy the requirements of 40 CFR 146.84(b). This plan addresses the details of computational modeling to delineate AoR, corrective action in the AoR, and triggers for AoR re-evaluation. The AoR is delineated by the lateral and vertical migration extent of the CO_2 plume, formation fluids and pressure front in the subsurface. A computational model was built to predict the lateral and vertical movement of CO_2 injected into the [redacted] at TCCSP. The computational model incorporates physical flow, geochemical reactions and trapping processes associated with CO_2 injection into subsurface reservoirs.

Computer Modeling Group's General Equation of State Model, widely known as GEM, was used as the simulator. A multi-component and multi-phase fluid flow process was employed to assess the development of the CO_2 plume, the pressure front, and the long-term fate of the injection.

Two injection wells, TCCSP_INJ-1 and TCCSP_INJ-2, will be used to inject a total of [redacted] over a period of [redacted]. Constant injection rates of [redacted] and [redacted] were assigned to the TCCSP_INJ-1 and TCCSP_INJ-2, respectively. TCCSP_INJ-1 injects into the [redacted] injection period. Meanwhile, TCCSP_INJ-2 will target the [redacted] for the [redacted] and the [redacted] for the [redacted].

The AoR is defined as an area encompassing the region surrounding the TCCSP where USDWs may be endangered by injection activity **(Figure 1-66**). This is usually the largest of either the CO_2 plume at [redacted] post-injection period or the elevated pressure front during the injection phase. The CO_2 lateral plume extent at [redacted] for TCCSP formations. Consequently, the CO_2 lateral plume's extent defines the AoR for TCCSP. The geologic model is calibrated to the petrophysical data obtained from the [redacted], which is [redacted] away from the proposed injection site. Updating reservoir architecture and petrophysical properties as necessary upon importing geophysical logs from drilled project wells. Details of the computational modeling, assumptions that are made, and the site characterization data that the model is based on satisfy the requirements of 40 CFR 146.84(c).

Figure 1-66 shows the AoR, project infrastructure, and relevant surface and subsurface features near TCCSP pursuant to 40 CFR 146.82(a)(2). There are [redacted]

Figure 1-66. Map showing injection wells, project AoR, and relevant surface and subsurface features as required by 40 CFR 146.82(a)(2).

1.5 Financial Responsibility

Financial Responsibility GSDT Submissions
GSDT Module: Financial Responsibility Demonstration ***Tab(s):*** Cost Estimate tab and all applicable financial instrument tabs Please use the checkbox(es) to verify the following information was submitted to the GSDT: ☐ Demonstration of financial responsibility ***[40 CFR 146.82(a)(14) and 146.85]***

The **Financial Responsibility** document demonstrates the financial responsibility for corrective action, injection well plugging/conversion, post-injection site care (PISC) and site closure, and emergency and remedial response according to 40 CFR 146.85. Injection well plugging and costs are estimated according to the **Injection Well Plugging Plan** and PISC and site closure costs are presented to reflect a [redacted] period. The Emergency and Remedial Response costs cover one (1) unmitigated leakage event throughout the life of the project. TCCSP, LLC. will work with a [redacted] to fulfill all financial responsibility obligations noted in this permit

application. For more details, refer directly to the **Financial Responsibility** document, where the financial instrument(s) are outlined, and costs are presented in more detail.

1.6 Injection Well Construction

The construction details for TCCSP_INJ-1 and TCCSP_INJ-2 of the Tulare County Carbon Storage Project (TCCSP) are described in the following sections. The injection wells have been designed to accommodate the maximum instantaneous mass rate of [redacted] per well of CO_2 that could be delivered to site in the case that one injection well is shut-in for workover operations. Target average injection rates for each well are listed in **Table 1-34**. Key characteristics of the [redacted] which are the storage reservoirs, were considered in the design of these wells. This attachment illustrates the comprehensive analysis performed to meet U.S. EPA UIC Class VI well design requirements for casing, cement, and wellhead under 40 CFR 146.86(a).

TCCSP_INJ-1 is proposed to be drilled to a total drilled depth (TD) of [redacted] from surface and will be completed in the [redacted] with injection taking place for the [redacted] TCCSP_INJ-2 is proposed to be drilled to [redacted]. TCCSP_INJ-2 will be first completed in the [redacted] of injection and subsequently plugged and recompleted into the [redacted] for the remaining [redacted]. This well construction plan has been designed around this completion strategy to utilize the [redacted] while managing the lateral extent of the free phase CO_2 and elevated pressure plume.

1.6.1 Wellhead Injection Pressure

[redacted] software was used to conduct a nodal analysis to determine the feasibility of injection of the target rate for TCCSP_INJ-1 and TCCSP_INJ-2 through [redacted]. The analysis assumed an estimated wellhead pressure of approximately [redacted]. The nodal analysis was designed with a long-string of [redacted] premium thread long-string set through the injection zone. See **Table 1-37** for long-string casing depths. The injection tubing strings in both injection wells used are planned to be [redacted]. The composition of the CO_2 stream used in the modeling is available in **section 6.3 Specifications of CO_2 Stream** of the **Injection Well Operations Plan.** Modeling results are shown for the two injection wells TCCSP_INJ-1 and TCCSP_INJ-2. Design parameters from the geologic model and target injection rates are shown in **Table 1-34.** The schematics for the tubular design used in nodal analysis are shown in **Figure 1-67**.

Table 1-34. [redacted] Reservoir Data Inputs.

Well	Formation	Average Flow Rate (MMtpa)	Top (ft)	Bottom (ft)	Mid-Point (ft)	Net Thickness (ft)	Pressure at Mid-Point (psi)	Average Permeability (md)	Reservoir Temperature at Mid-Point (F)
[redacted]									

[1] The [redacted] references the [redacted] including the [redacted].

Figure 1-67. Nodal Analysis Schematics.

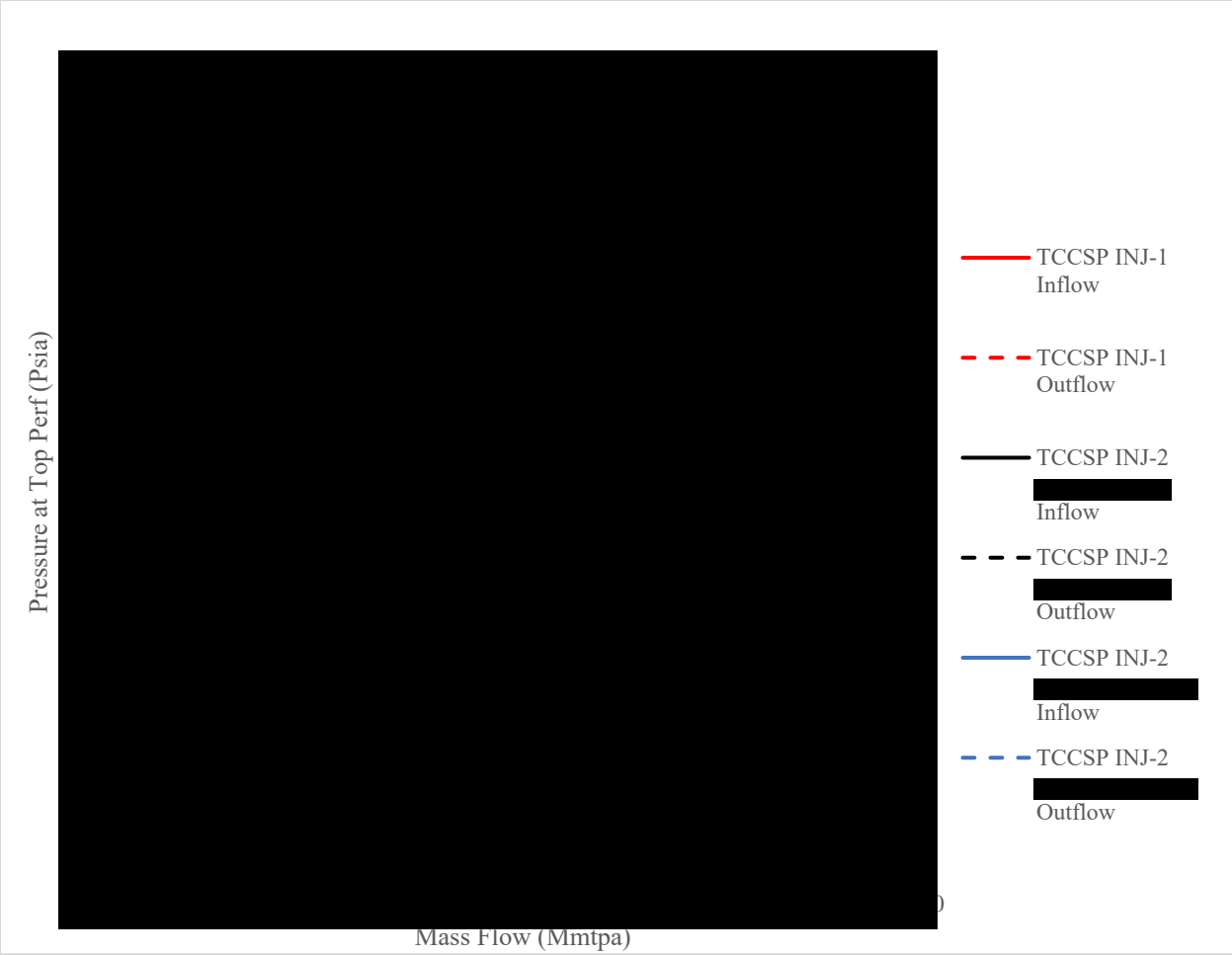

Figure 1-68. [redacted] Tubing Nodal Analysis Results.

The nodal analysis results in **Figure 1-68.** indicate that at the estimated wellhead pressure of [redacted] tubing will be able to deliver the average flowrates listed in **Table 1-34** to the reservoir. All injection wells were modeled to achieve injection rates above the maximum expected instantaneous rate of [redacted] without violating the [redacted] fracture pressure constraint. A [redacted] tubing pipe in each injection well was determined to be adequate to support injection at TCCSP.

[redacted] was also used to determine normal operating ranges for the wellhead pressures for injection wells at modeled injection rates.

Table 1-35 summarizes the expected operating wellhead pressures at the average respective rates and maximum expected instantaneous rates. The maximum instantaneous injection rate was determined based on the possibility of one of the injection wells going offline for maintenance or workovers, therefore routing all the CO_2 to a single injection well. For all modeled cases, the wellhead pressures were found to remain below the maximum allowable wellhead pressure as noted in **section 1.6.2** of this plan.

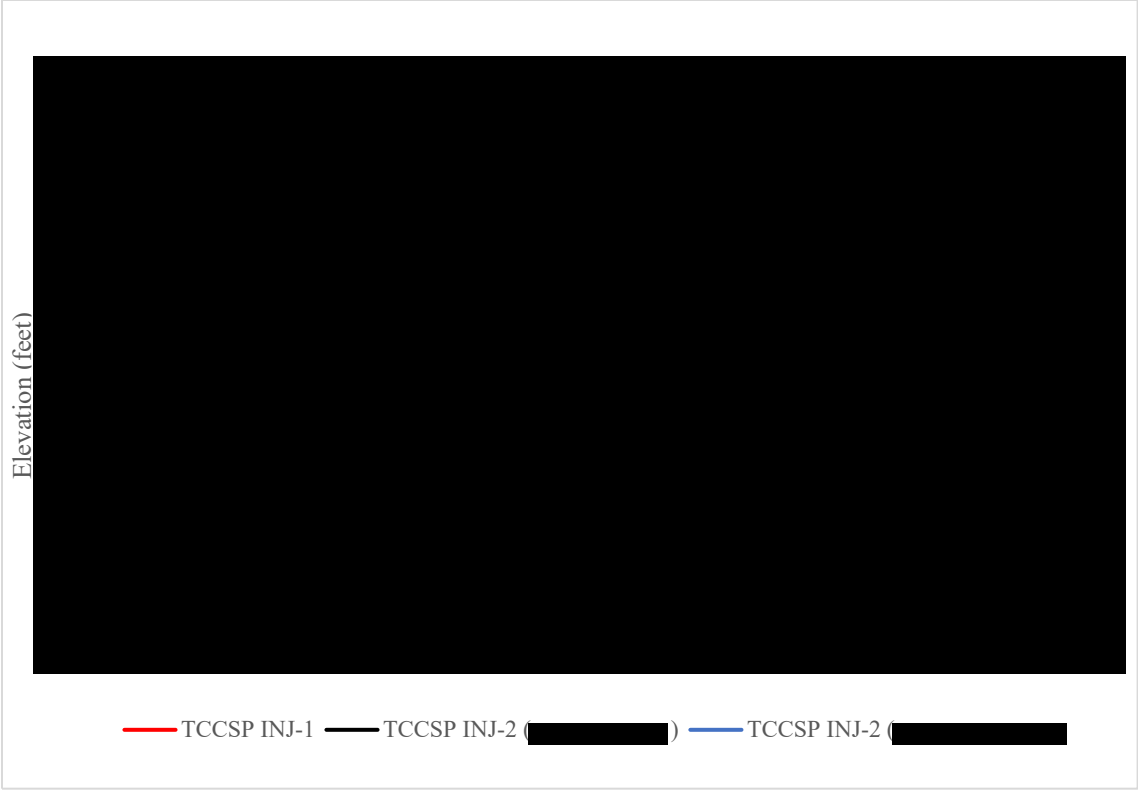

Figure 1-69. Pressure Profile at Average Injection Rates.

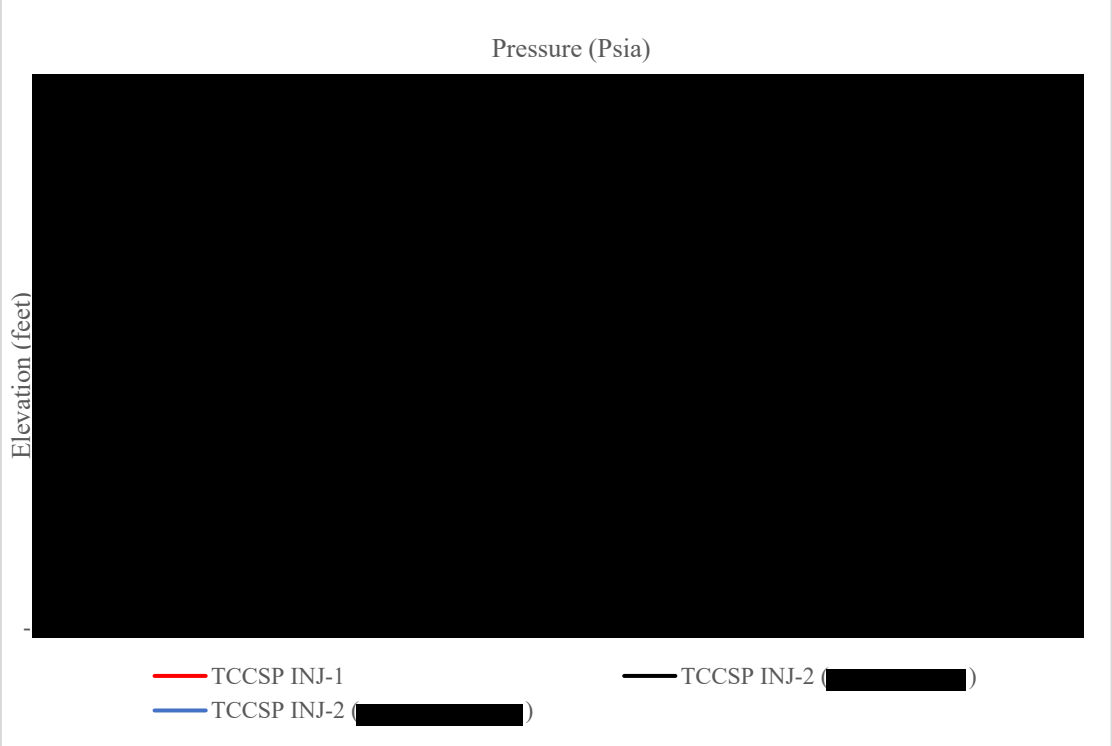

Figure 1-70. Pressure Profile at Maximum Rate Injection Rate ( ).

Table 1-35. Expected Wellhead Operating Pressures.

Well	Average Operating Injection Rate (MMtpa)	Expected Operating Wellhead Pressure (psia)	Expected Operating Wellhead Pressure at [redacted] (psia)
TCCSP_INJ-1	[redacted]		
TCCSP_INJ-2 [redacted])			
TCCSP_INJ-2 ([redacted])			

1.6.2 Maximum Allowable Wellhead Injection Pressure

[redacted] modeling was completed to determine the maximum allowable wellhead pressure. This was done by determining the required wellhead pressure at the maximum instantaneous rate that corresponded to [redacted] of the fracture pressure of the topmost perforation in each well. **Figure 1-71.** shows the pressure profile for each well at the [redacted] fracture pressure. **Table 1-36** shows each wells individual, top perforation depth, [redacted] fracture pressure, corresponding wellhead pressure, and the maximum proposed wellhead pressure.

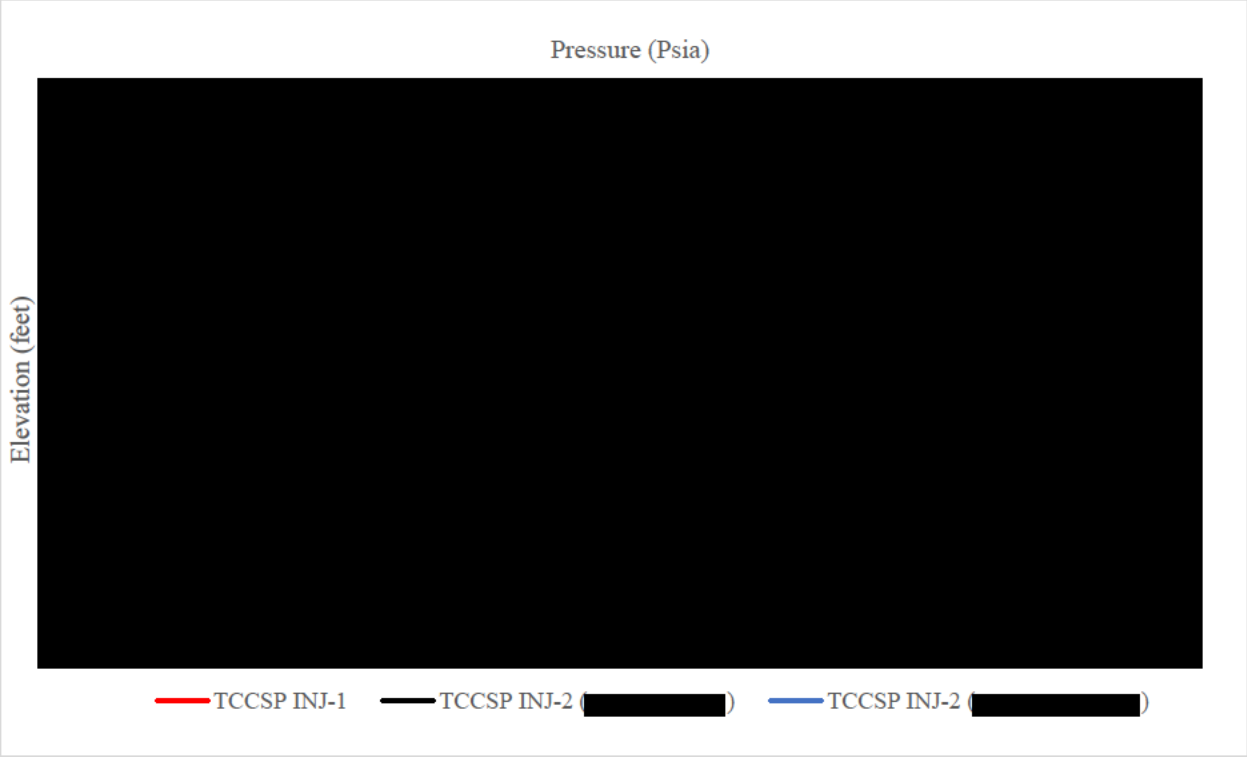

Figure 1-71. Pressure Profile for Maximum Allowable Wellhead Pressure.

Table 1-36. Top Perforation Depth, [redacted] Fracture Pressure, and Associated Maximum Allowable Wellhead Pressures.

Well	Top Perforation Depth (ft)	[redacted] Fracture Pressure (Psia)	Pressure at Top Perforation Depth (Psia)	Associated Wellhead Pressure (Psia)	Maximum Proposed Wellhead Pressure (psia)
TCCSP_INJ-1	[redacted]				
TCCSP_INJ-2 ([redacted])					
TCCSP_INJ-2 ([redacted])					

1.6.3 Casing Program

The injection wells have been sized and designed based on results of the nodal analysis to accommodate [redacted] injection tubing. The wells were designed with concentric casing sizes to isolate the injection zone and protect the USDWs. Carbon dioxide in the presence of water creates carbonic acid, which is mildly acidic and can cause increased corrosion to metal components with which it comes into contact. The water content in the injectate stream will be reduced as much as possible, as shown in **Table 7-3** of **section 7.3.3** of the **Testing and Monitoring Plan.** As the CO_2 stream enters the reservoir, it encounters brine and forms carbonic acid which can create a corrosive environment that mild steel may not withstand. Though formation fluid is not expected to enter the wellbore, the metallurgy for each casing string was selected to be compatible with the fluids and stresses encountered in bottomhole conditions as modeled and to meet API TR 5C3. Casing strings that will come into contact with CO_2 or CO_2-saturated brine will include a minimum of [redacted] similar metallurgy to be resistant to corrosion from carbonic acid or wet CO_2. Results from corrosion testing and modeling under comparable downhole conditions indicate that in a high-temperature CO_2 and steam environment, the corrosion rate of [redacted] steel was less than [redacted] mm/year [1]. The steel also passed the localized corrosion requirements, with no pitting observed and a potential difference between the passivation potential and the corrosion potential greater than [redacted]. Together, these results demonstrate that [redacted] steel provides sufficient resistance to metallurgical corrosion should moisture or formation fluid come into contact with the CO_2. The selection of [redacted] is therefore a conservative measure that exceeds the corrosion resistance offered by [redacted]. The entire injection tubing string will be comprised of [redacted] or higher grade material. The [redacted] long-string casing will be constructed of [redacted] or similar material through the injection zone to approximately [redacted] above the confining zone. In areas where the risk of CO_2 corrosion is not of concern, such as above the caprock where injected CO_2 is not expected, mild steel or similar material will be used. The lithology of the storage reservoir's injection and confining zones are discussed in **section 1.2.6** and reservoir fluid characteristics are discussed in **section 1.2.9**. CO_2 stream characteristics are discussed in **section 1.8.2**. Constructing the wells with [redacted] or a higher grade steel components meets U.S. EPA's requirements and exceeds the corrosion resistance standards established by Guoqing [1].

1.6.4 Casing Summary

Injection well tubulars were designed and analyzed for the TCCSP_INJ-1 location given the geologic formations and target depths at this location were [redacted] compared to TCCSP_INJ-2 albeit the differences being minor since the two wells are [redacted]. However, TCCSP_INJ-1 is estimated to experience [redacted] bottomhole stresses compared to TCCSP_INJ-2. The hydro-static pressure determined from the regional data indicated a pressure gradient of [redacted] as outlined in **section 1.2.6.** This yielded a maximum down hole pressure of [redacted]. Similar design principles from TCCSP_INJ-1 will be adopted in TCCSP_INJ-2. The wells will consist of: a[redacted]. All casing strings will be cemented to the surface using staged cement jobs as needed. The borehole diameters are considered conventional sizes for the sizes of casing that will be used and should allow ample clearance between the outside of the casing and the borehole wall. This will ensure that a continuous cement seal can be emplaced along the entire length of the casing string. **Table 1-37** summarizes the casing program for the injection well. **Table 1-38** summarizes the properties of each casing material. Each section of the well is discussed in a separate section below. Strength calculations for the selected casing strings are provided in **section 1.6.5**.

[2] The [redacted] references the [redacted] including the [redacted].

Table 1-37. Expected Open Hole and Casing Setting Depths.

Well	Conductor Open Hole / Casing Setting Depth (ft)	Surface Open Hole / Casing Setting Depth Setting Depth (ft)	Intermediate Open Hole / Casing Setting Depth Setting Depth (ft)	Long-String Open Hole / Casing Setting Depth Setting Depth (ft)
TCCSP_INJ-1	[redacted]			
TCCSP_INJ-2				

Table 1-38. Borehole and Casing Program for All Injection Wells.

Casing String	Borehole Diameter (in)	Casing Outside Diameter (in)	Casing Material (weight/grade/ connection)	Coupling Outside Diameter (in)
Conductor	[redacted]			
Surface				
Intermediate				
Long-String				

*Premium connection type to be determined based on availability. [redacted] was used for strength calculations.

Table 1-39. Tubular Materials and Strength Properties.

Casing String	Material (weight / grade / connection)	Outside Diameter (in.)	Inside Diameter (in.)	Wall Thickness (in.)	Drift Diameter (in.)	Burst (psia) Plain End	Collapse (psia)	Joint Tensile Strength (psia)
Conductor								
Surface								
Intermediate								
Long-String								
Tubing								

1.6.4.1 Conductor Casing

The conductor casing consists of [redacted] and provides the stable base required for drilling activities in unconsolidated sediment. The conductor will be drilled and cemented into place. A final determination of depth will be made after site preparation. This section of casing is also cemented in place.

1.6.4.2 Surface Casing

The surface casing is a [redacted] with buttress thread couplings (BTCs). The metallurgy of this casing string is carbon steel. Surface casing is to be cemented to surface, isolating the shallow drinking water and the lowermost USDWs. Following the cement setting, a [redacted] will be run to verify cement bond.

1.6.4.3 Intermediate Casing

The intermediate casing is [redacted] with buttress thread couplings (BTCs). The metallurgy of this casing string is carbon steel. The intermediate will be cemented to surface in one or more stages to isolate [redacted] and other drilling hazards. It will be set into the first competent zone identified within the [redacted]. Following the cement setting, a [redacted] will be run to ensure cement bond.

1.6.4.4 Long-String Casing

The long-string casing will be a [redacted]. The long-string casing is designed to extend from the surface to the injection zone per 40 CFR 146.86(b)(3). The uppermost section will be [redacted] or similar with buttress thread couplings (BTCs); the lower section will be a corrosion-resistant alloy [redacted] or a higher grade) having strength properties equivalent to or better than [redacted] with premium connections. The transition will be targeted for approximately [redacted] above the confining zone targeted caprock. A [redacted] will be run outside the casing from surface into the confining unit and cemented in place with the casing.

1.6.4.5 Tubing

The tubing connects the injection zone to the wellhead and provides a pathway for injecting CO_2. This design utilizes [redacted]. A packer will be set to the depths listed in **Table 1-46** to isolate injection zones from the tubing-casing annulus and will be set at approximately [redacted] above the first perforation interval. At the end of the tubing string, a landing nipple, or "no-go" tool will be run. This will allow a plug to be set inside the tubing at this depth and the packer to be released in order to remove the tubing string if needed. [redacted] or equivalent will be hung in the tubing string immediately above the top packer and ported to the tubing. More information on the selected wellbore monitoring technologies is available in **section 7.2** of the **Testing and Monitoring Plan**. Considering the anticipated formation pressure, temperature, and stress, the grade of tubing was selected with the API specifications outlined in **Table 1-39**, which includes the calculated safety factors. These safety factors represent sufficient quality standards to preserve the integrity of the injected fluid, the injection zone, and USDWs. The annulus between the tubing

and long-string casing will be filled with noncorrosive fluid described in **section 1.6.8** in accordance with 40 CFR 146.88(c).

1.6.5 Casing Strength Calculations

Casing stresses and loadings were modeled using [redacted]). To ensure sufficient structural strength and mechanical integrity throughout the life of the project, stresses were analyzed and calculated according to worst-case scenarios and tubular specifications were selected accordingly. Minimum design factors are presented in **Table 1-40** and are based on API TR 5C3 [2]. **Table 1-41** through **Table 1-44** summarize the results of this stress analysis. The burst, collapse, and tensile strength of each tubular was calculated according to the scenarios defined below and was dependent on fracture gradients, mud weight, depths, and minimum safety factors. Modeling was completed at a static temperature gradient of [redacted]. This resulted in a total depth temperature ([redacted]. Due to the nearly identical designs, and the fact that TCCSP_INJ-1 is to be drilled [redacted], only the results for TCCSP_INJ-1 are shown.

The casing and tubing materials were designed to be compatible with the CO_2 stream and formation fluids and the stresses induced throughout the sequestration project. [redacted] design standards were incorporated to develop the casing design load scenarios, and [redacted] group standards were incorporated to develop the tubing design load scenarios. These design standards used to develop the [redacted] software are based on work by Klementich et al. [3] and Prentice [4] and use the API TR 5C3 [2] standard equations for burst, collapse, axial, and triaxial strength calculations.

Table 1-40. Minimum Design Factors.

Load	Casing Design Criteria	Tubing Design Criteria
Burst	[redacted]	
Collapse		
Tension		
Compression		
VME		

The casing installed in any well should be designed to withstand collapse loading based on the following assumptions:

1. The hydrostatic head of the drilling fluid or cement in which the casing is run acts on the exterior of the casing at any given depth.
2. Subject to the casing being at a minimum two-thirds evacuated.
3. The production casing is two-thirds evacuated.
4. The effect of axial stresses on collapse resistance shall be considered; and
5. The effect of temperature derating, and casing wear shall be considered.

Any casing or liner that creates an annular space with the production tubing was treated as a production casing or liner. The casing installed in any well was designed to withstand tensile loading based on the following assumptions:

1. The weight of casing is its weight in air; and
2. The tensile strength of the casing is the yield strength of the casing wall or of the joint, whichever is lesser.

The following additional assumptions were made during the design process for the injection well:

1. A [redacted] casing wear due to bottomhole assembly (BHA) rotation is assumed on all casing design segments with consecutive hole sections.
2. Wall tolerance of [redacted] is assumed as per API standard TR 5C3 [2].
3. Temperature deration is considered on the design of the [redacted] casing string; and
4. The [redacted] casing is being proposed and engineered to comply with a casing designed to pass a two-thirds evacuation loading on collapse.

If the casing as designed is not available, final casing selection would be based on available technical options that are in stock at the time of construction provided they satisfy or exceed the design criteria discussed here.

Table 1-41. Surface Casing Load Scenarios Evaluated the Calculated Design Factors (DF).

Load Case	Pressure Profile; Pressure at Minimum DF		Axial Loading	Temperature Profile	Wear Percentage	Minimum Design Factor				
						Pressure		Axial		Triaxial
	Internal	External				Load	Factor	Load	Factor	Factor
[redacted]										

Table 1-42. Intermediate Casing Load Scenarios Evaluated and the Calculated Design Factors (DF).

Load Case	Pressure Profile; Pressure at Minimum DF		Axial Loading	Temperature Profile	Wear Percentage	Minimum Design Factor				
						Pressure		Axial		Triaxial
	Internal	External				Load	Factor	Load	Factor	Factor
[redacted]										

Table 1-43. Long-String Casing Load Scenarios Evaluated and the Calculated Design Factors (DF).

Load Case	Pressure Profile: Pressure at Minimum DF		Axial Loading	Temperature Profile	Wear Percentage	Minimum Design Factor				
						Pressure		Axial		Triaxial
	Internal	External				Load	Factor	Load	Factor	Factor
[redacted]										

Table 1-44. Tubing Load Scenarios Evaluated and the Calculated Design Factors (DF).

Load Case	Pressure Profile: Pressure at Minimum DF		Axial Loading	Temperature Profile	Wear Percentage	Minimum Design Factor				
						Pressure		Axial		Triaxial
	Internal	External				Load	Factor	Load	Factor	Factor
[redacted]										

1.6.6 Packer Details

The packer system will be equivalent to [redacted] or better, depending on availability, and [redacted]. The packer will be connected to a [redacted] for easy workover operations. Both the packer and locator seal assembly will feature premium couplings matched to the tubing and will be comprised of [redacted] alloy to be compatible with expected reservoir fluids. Please refer to **Table 1-44** for modeled load scenarios for tubing and **Table 1-45** specifications for the packer. The packers will be set per the depths listed in **Table 1-46**. TCCSP_INJ-2 will feature a re-completion after the first [redacted] years of injection, therefore, both set depths are listed. The annulus between the tubing and long-string casing will be filled with noncorrosive fluid described in further detail within the annular fluid program in **section 1.6.8** below.

Table 1-45. Packer Details.

Item	Tensile Strength (1000 lbs.)	Burst Strength (psi)	Collapse Strength (psi)	Material (weight/grade/ connection)
Packer ([redacted] or equivalent)	[redacted]			

Table 1-46. Packer Setting Depths.

Well	Packer Setting Depth (ft)
TCCSP_INJ-1	[redacted]
TCCSP_INJ-2 ([redacted])	
TCCSP_INJ-2[redacted]	

1.6.7 Cementing Program

This section discusses the types and quantities of cement that will be used for each string of casing. Cement selection (composition and volume) and cementing procedure discussed here is anticipated to be applied to both injection wells. The conductor, surface casing, intermediate, and long-string casing will be cemented to surface in accordance with requirements at 40 CFR 146.86(b)(3). The proposed cement types and quantities for each casing string are summarized in **Table 1-47** and **Table 1-48**. The final blends and quantities will be determined through discussions with cement vendors. The final volumes will be determined through caliper logs. These will be provided to the UIC Program Director promptly upon finalizing and well prior to injection well construction.

Casing centralizers will be used on all casing strings to centralize the casing in the hole and ensure that cement completely surrounds the casing along the entire length of pipe. The casing string will be centralized to attempt a minimum of [redacted] standoff. The actual hole trajectory as drilled will be input into the cementing service company's mud removal software to optimize centralizer placement. Centralizers will be placed either over the connections or at mid-joint using stop-rings as appropriate. It is estimated that approximately [redacted] centralizers will be used depending upon the hole trajectory. Additionally, collar guards will be run on every-other collar and blast protectors near target perforation intervals on the long-string to protect the [redacted] during installation and perforation. Except for the conductor casing, a guide shoe or float shoe is to be run on the bottom joint of casing, and a float collar will be run on the top of the bottom joint of casing.

The [redacted] long-string casing will be cemented to the surface using a lead and a tail. The tail used will be CO_2 resistant cement such as [redacted] or any other comparable and proven cement blend. Bartlet-Gouédard et al. [5] showed through lab testing that [redacted] provided significant resistance to degradation in the presence of CO_2 at reservoir conditions ([redacted]), as compared to common [redacted] cement. These testing conditions provide a comparable environment in comparison to the TCCSP injection well's bottom hole condition ([redacted]) and indicate that the application of [redacted] should provide adequate CO_2 protection. Final selection of the type of CO_2 resistant cement will be dependent on market availability and technical properties of the selected cement. The selected cement will at a minimum meet or exceed the resistance of [redacted]. The second stage consists of [redacted] The transition will be targeted at an approximate depth of [redacted] feet above the caprock. [redacted] will be run and analyzed for each casing string.

During the recompletion of TCCSP_INJ-2 the perforations will be squeezed with cement via a cement retainer. The plugging procedure is described in the **Injection Well Plugging Plan**.

Table 1-47. Proposed Cement Program.

Casing String	Casing Depth (ft)	Borehole Diameter (in)	Casing O.D. (in)	Cement Interval (ft)	Cement
Conductor Casing					
Surface Casing					
Intermediate Casing					
Long-String Casing					
*See acronym list for definition of abbreviations used in this table.					

Table 1-48. Proposed Cement Design Expected Volumes

Well	Conductor Volume (Sacks / bbls)	Surface Volume (Sacks / bbls)	Intermediate Lead Volume (Sacks / bbls)	Intermediate Tail Volume (Sacks / bbls)	Long-String Lead Volume (Sacks / bbls)	Long-String Tail Volume (Sacks / bbls)
TCCSP_INJ-1						
TCCSP_INJ-2						

1.6.8 Annular Fluid

The annular space above the packer between the [redacted] long-string casing and the [redacted] injection tubing will be filled with fluid to provide a positive pressure differential to stabilize the injection tubing and inhibit corrosion. Annular fluid pressure at the surface will be controlled to remain between [redacted] during injection operations (see **section 7.4.2** of the **Testing and Monitoring Plan** for a full description of the injection well annulus monitoring system). This

surface pressure, added to the hydrostatic pressure of the fluid column, will ensure that the annular pressure downhole will be greater than injection pressure.

The annular fluid will be fresh water treated with additives and inhibitors including a corrosion inhibitor, biocide (to prevent growth of harmful bacteria), and an oxygen scavenger. The fluid will either be mixed onsite using freshwater and liquid and dry additives, or it will be acquired pre-mixed. The fluid will also be filtered to ensure that solids do not interfere with the packer or other components of the annular protection system. The final choice of the type of fluid will depend on availability.

Example additives and inhibitors are listed below along with approximate mix rates:

- [redacted]
- [redacted]
- [redacted]
- [redacted]

These products were recommended and provided by [redacted]. The actual products will be similar but may vary from those described above.

1.6.9 Wellhead

The wellhead will consist of the following or similar components, from bottom to top:

- [redacted] casing head
- [redacted] casing head
- [redacted] port/access
- [redacted] tubing head
- [redacted] port/access
- [redacted] full-open master control gate valve
- [redacted] automated tubing flow control valve
- [redacted] cross with one (1) [redacted] blind flange
- [redacted] automated tubing flow control valve
- [redacted] automated safety shut down valve.
- [redacted] top flange and pressure gauge.

The wellhead and Christmas tree materials are designed to be compatible with the CO_2 stream. Critical components that come into contact with the CO_2 stream will be made of a corrosion-resistant alloy such as stainless steel. Materials that are not expected to contact the injection fluid will be carbon steel. A preliminary materials specification for the wellhead and Christmas tree assembly is presented in **Table 1-49**. This is based on the material classes as defined in API Specification 6A [6]. A summary of material class definitions is provided in **Table 1-50**. The final wellhead and Christmas tree materials specification may vary from the information given below based on availability and final product selection. An illustration of the preliminary wellhead and Christmas tree design is provided in **Figure 1-72.** The flowline leading to the wellhead and Christmas tree will be equipped with an [redacted] as required in 40 CFR 146.88. Additionally, the wellhead will be equipped with a [redacted] on each tubing and annulus. Each annulus will be equipped with a [redacted]. Please refer to **Table 7A-11** of **section 7A.1.4.7** of the **Quality Assurance and Surveillance Plan (QASP)** attached to the **Testing and Monitoring Plan** for additional details on the wellhead gauges to be installed.

Table 1-49. Materials Specification of Wellhead and Christmas Tree.

Component	Material Class[(a)]
[redacted]	

Table 1-50. Material Classes from API 6A.

API Material Class	Body, Bonnet, End & Outlet Connections	Pressure Controlling Parts, Stems, & Mandrel Hangers
[redacted]		

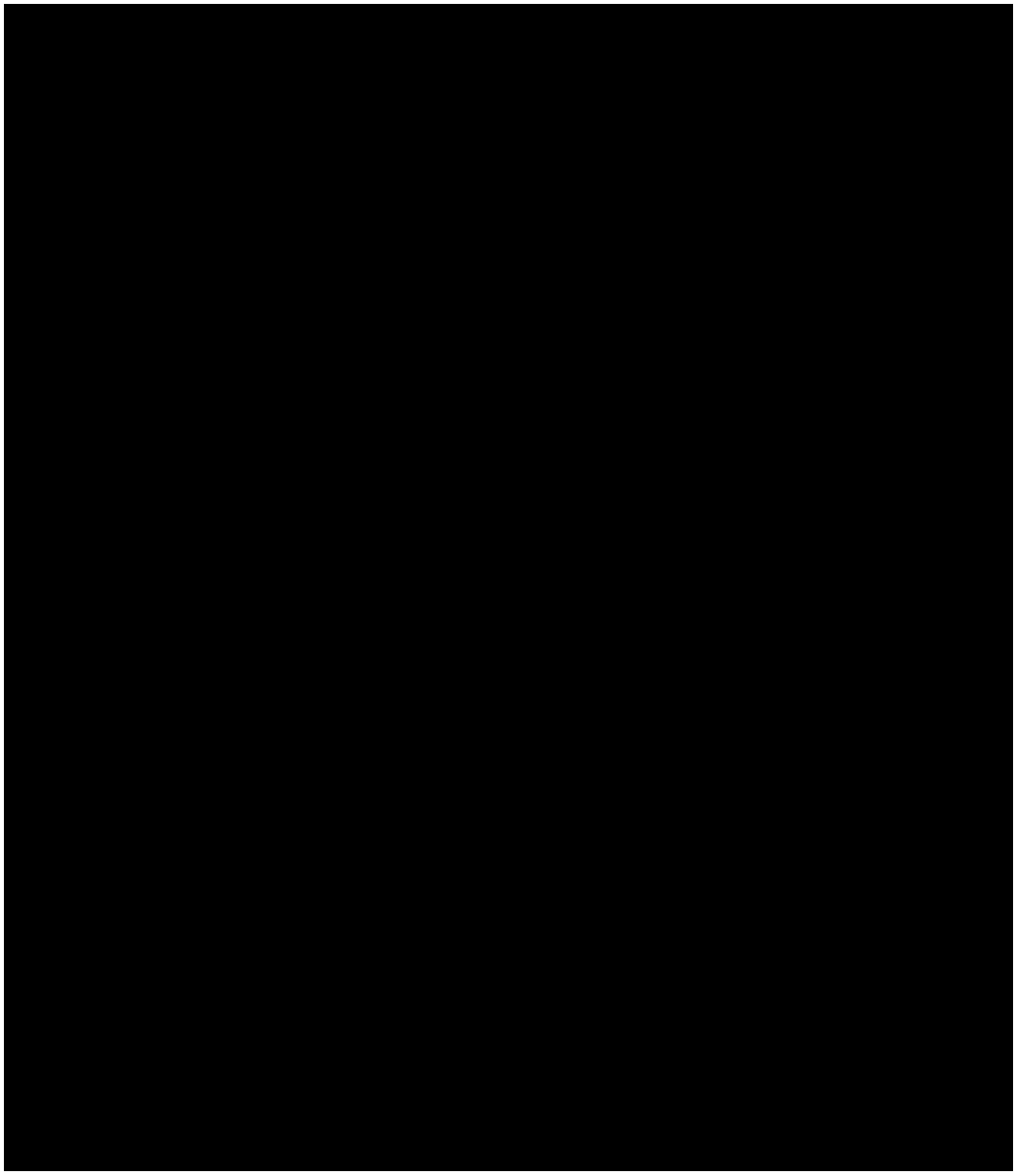

Figure 1-72. Working Wellhead Design Diagram for Injection Wells.

1.6.10 Perforations

The long-string casing will be perforated across the [redacted] with deep-penetrating shaped charges. Due to the installation of [redacted], oriented perforations will be used to avoid damaging the [redacted]. The exact perforation interval will be determined after the well is drilled and characterized with geophysical logging, core analyses, and hydrogeologic testing. The planned perforation intervals will be [redacted] shots per foot. Proposed perforation interval depths are found below in **Table 1-51**. TCCSP_INJ-1 is designed to inject into the perforations in the [redacted] for the entirety of the injection period. TCCSP_INJ-2 is designed to inject into the first set of perforations ([redacted] of injection and subsequently recompleted into the second set of perforations ([redacted]) for [redacted] years of

injection. During the recompletion of TCCSP_INJ-2 the perforations will be squeezed with cement via a cement retainer. The plugging procedure is described in the **Injection Well Plugging Plan**.

Table 1-51. Proposed Perforated Intervals.

Well	Zone	Top (ft)	Mid-Point (ft)	Bottom (ft)
TCCSP_INJ-1	[redacted]			
TCCSP_INJ-2				
TCCSP_INJ-2				

1.6.11 Proposed Stimulation Program

After perforation of all injection wells an acid wash will take place. This will be done with [redacted]. This will be done at low pressures and will not endanger the confining zone or create a leakage pathway while improving the injectivity of the near wellbore and allow for injection of CO_2 to take place at lower startup pressures. No other stimulation is proposed.

1.6.12 Summary of Monitoring Technology

[redacted] will be the primary wellbore technology used to monitor various operational parameters, wellbore mechanical integrity, formation properties, and the movement of CO_2 and the associated pressure front across the project.

Operational parameters such as injection pressure and temperature and annulus pressure will be [redacted] ported to the injection tubing and annulus along with [redacted] ported to the tubing at depth. Internal mechanical integrity will be continuously monitored using [redacted] ported to the injection tubing and annulus whereas external mechanical integrity will be demonstrated [redacted] during injection operations using [redacted]. Formation properties, such as transmissivity (obtained by [redacted]), along with the pressure front associated with the CO_2 plume, will be monitored with [redacted]. [redacted] will be the primary method utilized to track the CO_2 plume across the project; however, [redacted] installed in each injection well may act as an additional method for indirectly tracking the plume. For detailed information on all testing and monitoring activities and technologies including automatic shutoff devices, please refer to **section 7.2** of the **Testing and Monitoring Plan.**

1.6.13 Schematic of the Subsurface Construction Details of the Wells

A schematic of the design for the injection wells is shown in **Figure 1-73**, **Figure 1-74,** and **Figure 1-75.** The injection wells will include the following casing strings: a [redacted] diameter conductor string; a [redacted] diameter surface string; [redacted] diameter intermediate string and a [redacted] diameter long-string. All depths are preliminary and will be adjusted based on additional characterization data obtained while drilling the CO_2 injection wells. All casing strings will be cemented to surface.

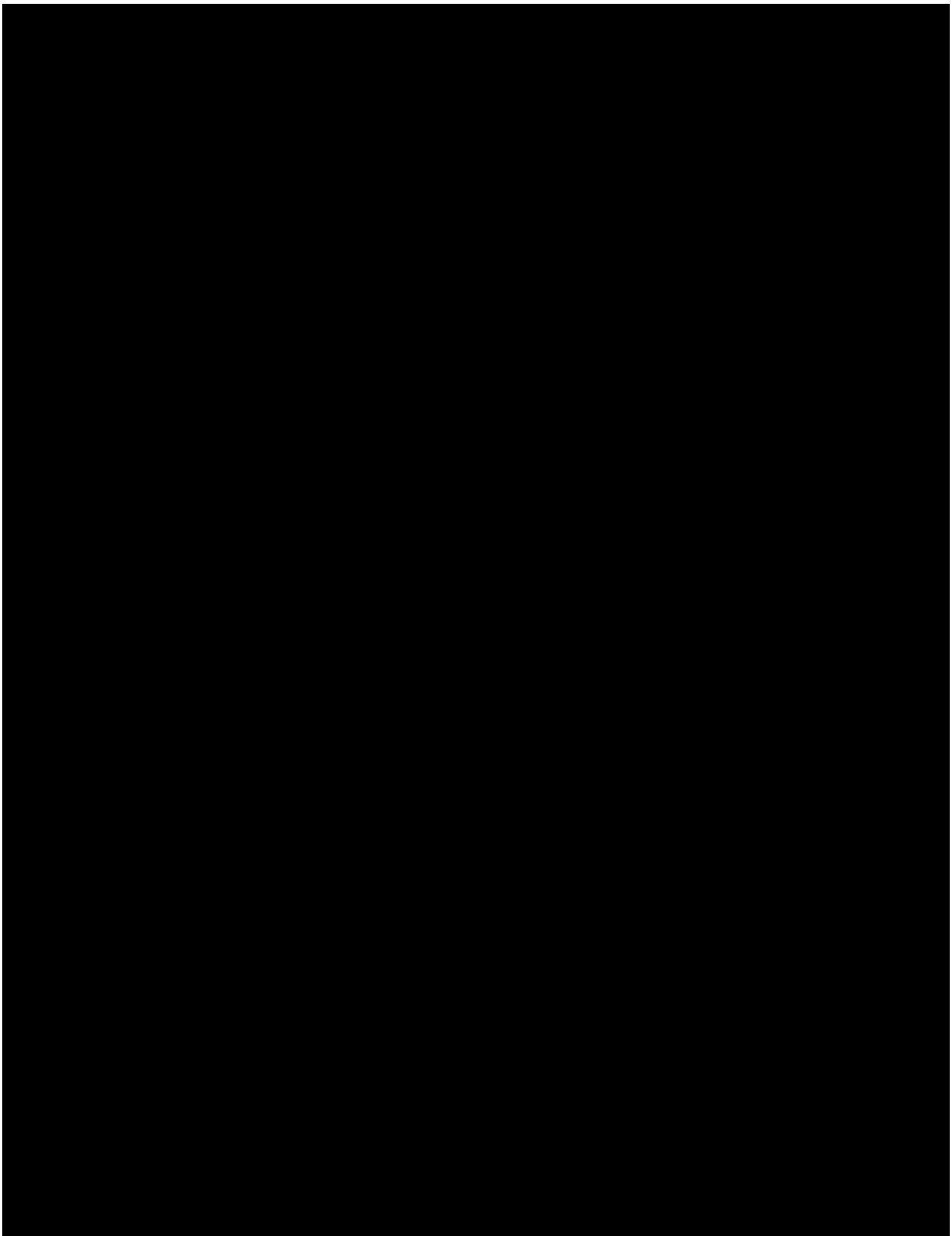

Figure 1-73. Schematic of TCCSP_INJ-1.

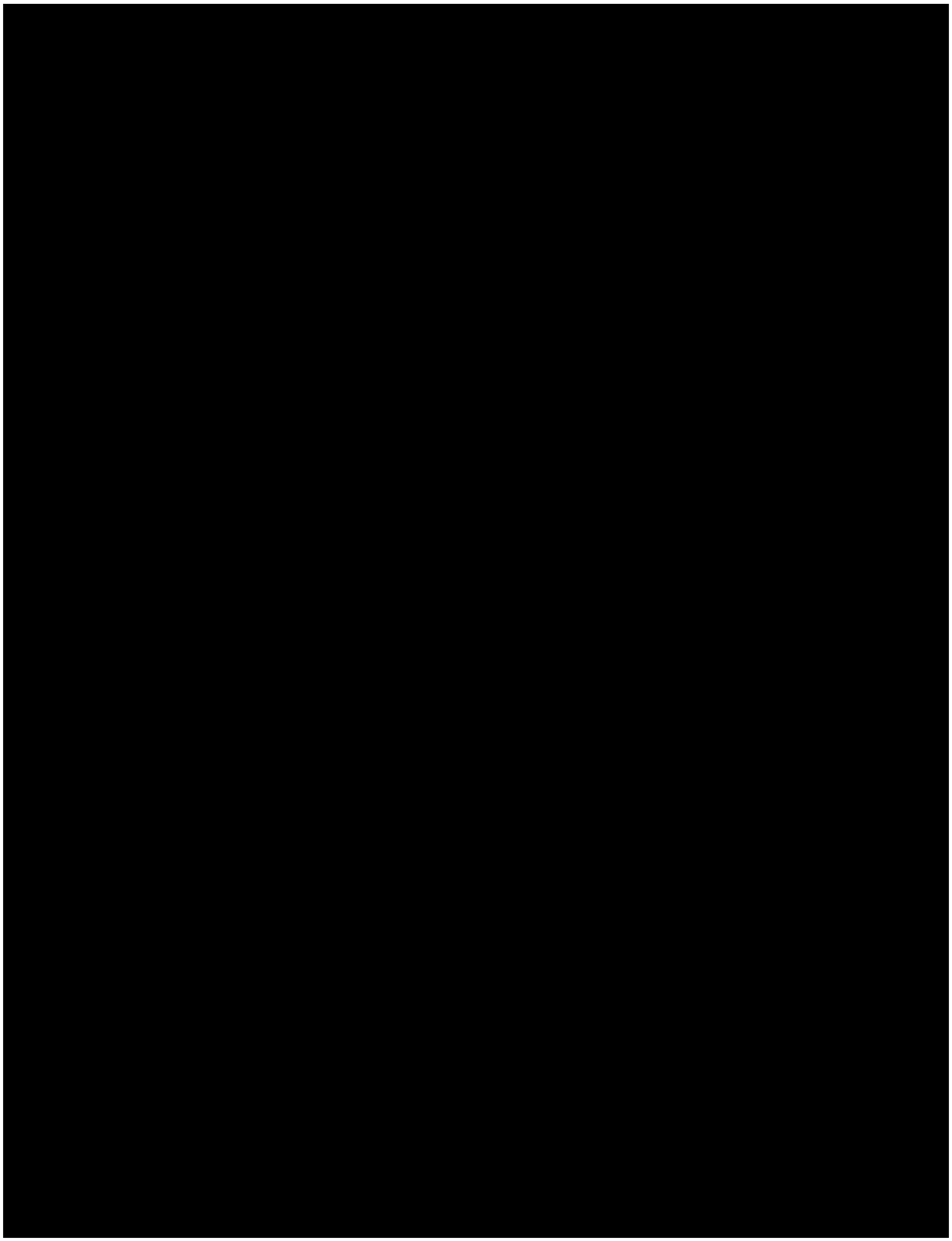

Figure 1-74. Schematic of TCCSP_INJ-2 ( ).

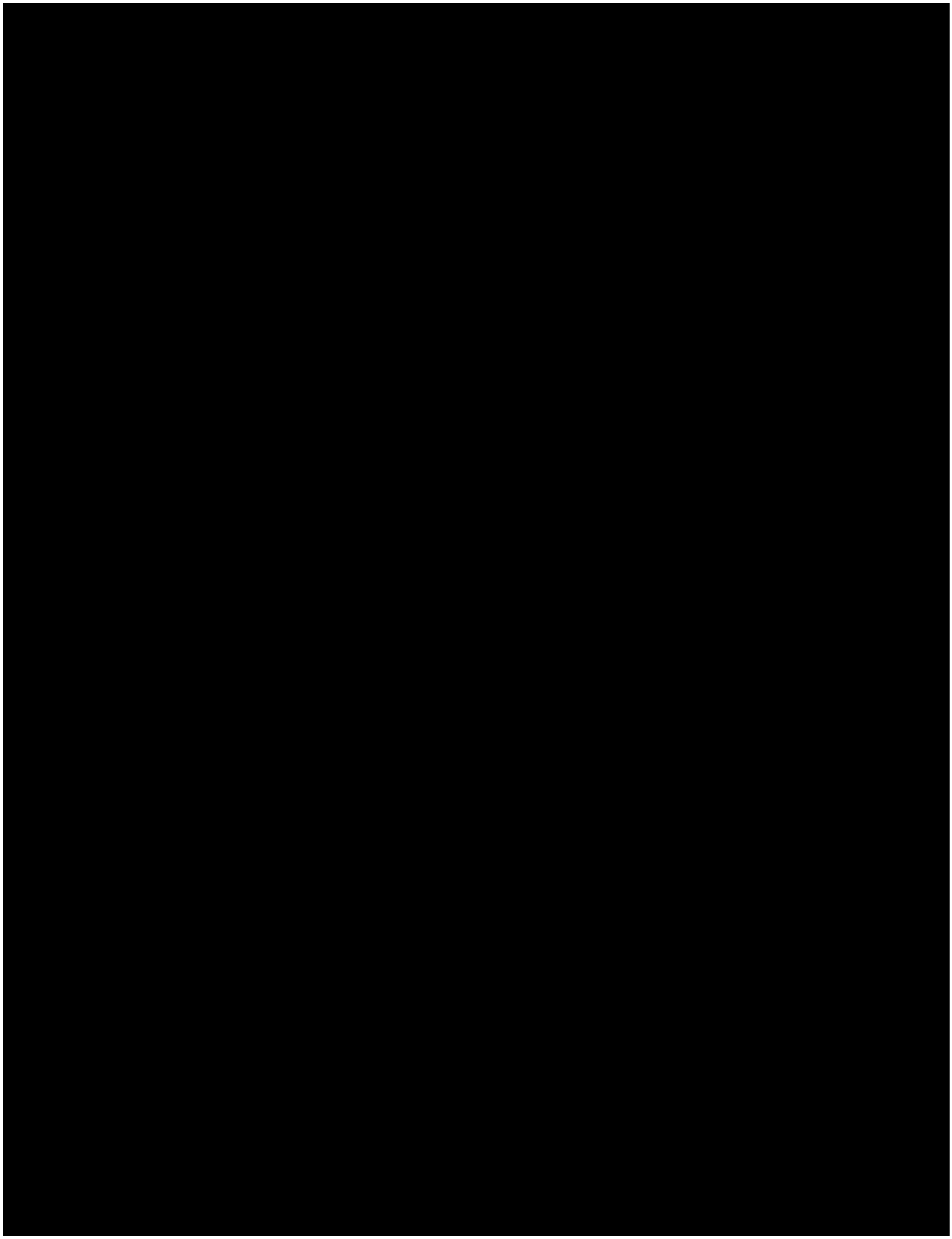

Figure 1-75. Schematic of TCCSP_INJ-2 (Recompleted to the [redacted]).

1.6.14 Schematic of the Subsurface Construction Details of the Monitoring Wells

TCCSP has developed well designs for the [redacted] monitoring wells following the same design standards and basis described for the injection wells. The technology included in the designs is to fulfill the proposed **Testing and Monitoring Plan**. These well designs will be permitted under the jurisdiction of California Geologic Energy Management Division (CalGEM) and are subject to changes required during the state agency's permitting process. Additionally, TCCSP may use new or different technology if it meets or exceeds the requirements proposed in the **Testing and Monitoring Plan**. The location chosen for these wells is discussed in the **Testing and Monitoring Plan** and the coordinates are provided in **Table 1-52**.

TCCSP_OBS-1 is an already drilled well completed as part of TCCSP's site characterization efforts and was equipped with monitoring equipment to satisfy the requirements of the [redacted] proposed in the **Testing and Monitoring Plan**. The as-drilled well schematic is given in **Figure 1-76**. The planned schematics for the remaining deep monitoring wells are provided in **Figure 1-77** through **Figure 1-79.**

Table 1-52. Deep Monitoring Well Locations.

Well	API Number	Latitude	Longitude
[redacted]			

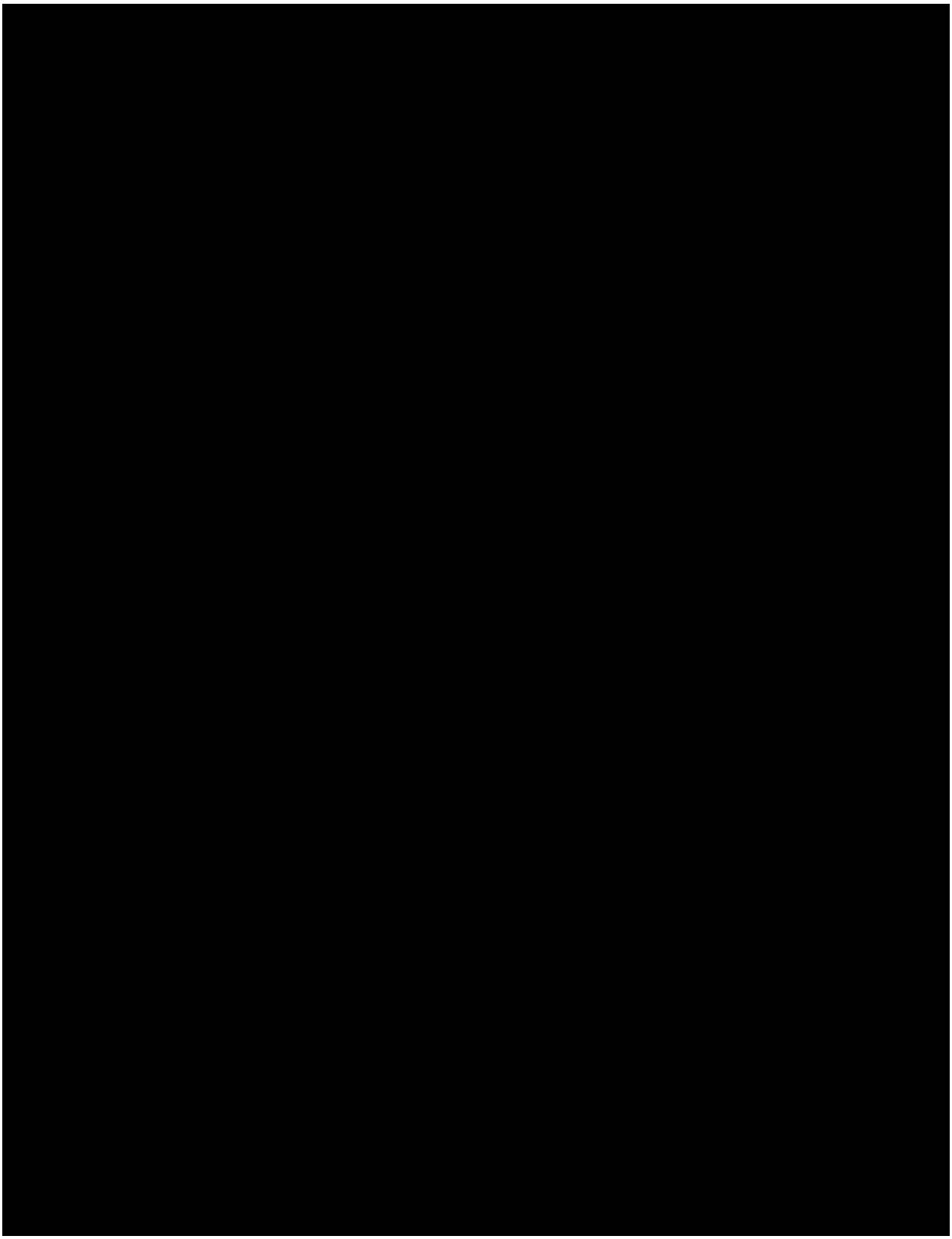

Figure 1-76. TCCSP_OBS-1 As Drilled Well Schematic.

Figure 1-77. [redacted] Well Design.

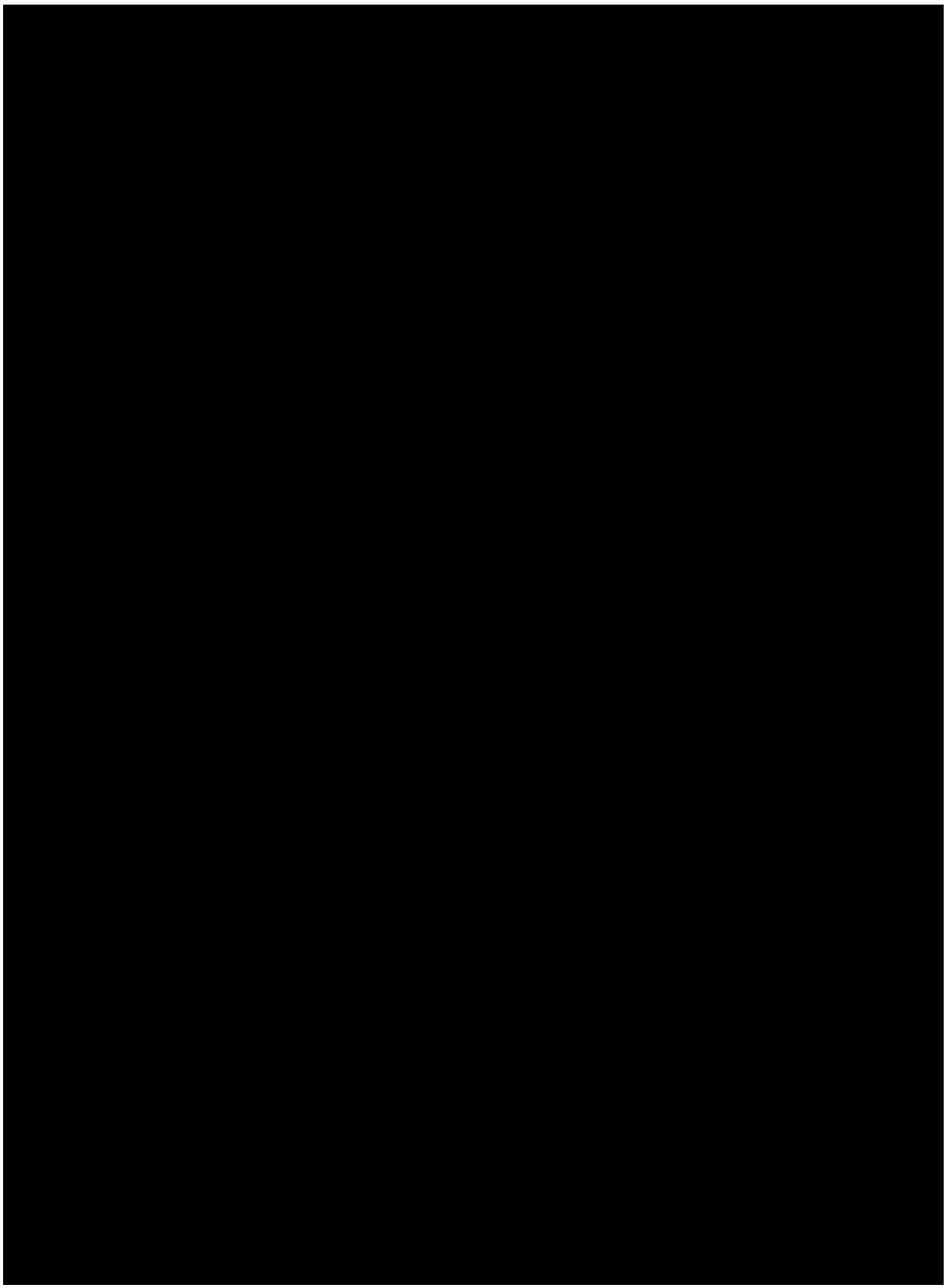

Figure 1-78. [redacted] Well Design.

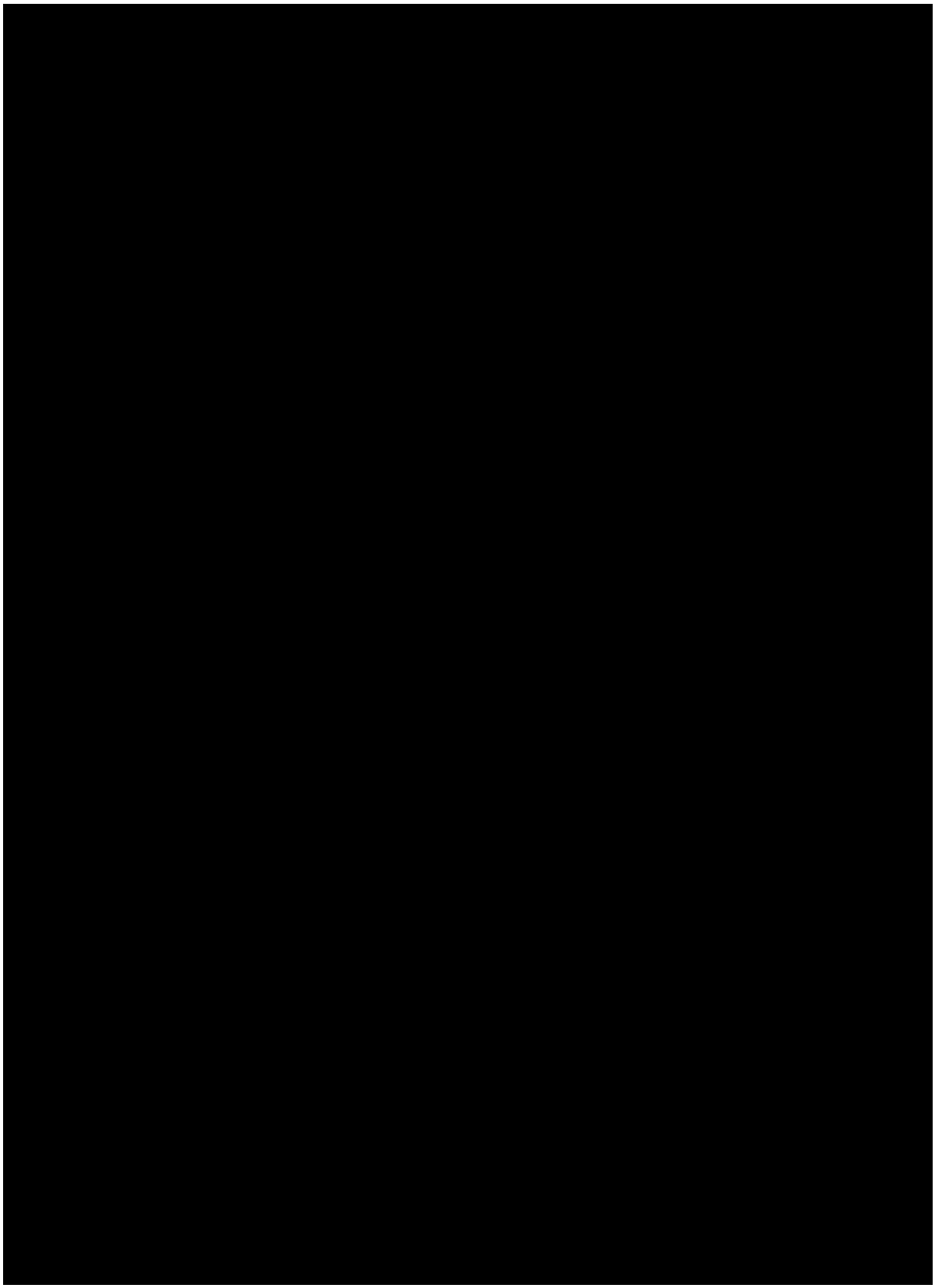

Figure 1-79. [redacted] Well Design.

1.6.15 Corrosion Modeling

Pursuant to 40 CFR 146.86(b)(1), TCCSP, LLC. conducted a comprehensive evaluation of the compatibility of proposed well tubulars with the injectate stream and formation brine. Comprehensive findings and additional details on the corrosion modeling are available in the **Corrosion Modeling Report** attachment. The formation brine properties utilized in this analysis were derived from the [redacted] taken in the TCCSP_OBS-1 well, as well as regional data obtained from the USGS Produced Water Database. The most pessimistic brine composition was selected from regional data since it matched the salinity derivation from the [redacted] in TCCSP_OBS-1, specifically from a well located [redacted]. Using the software [redacted], TCCSP assessed the electrochemical compatibility of various metallurgies under simulated downhole conditions, focusing on both generalized and localized corrosion mechanisms in the TCCSP INJ-1 well. Results were split into 3 categories to evaluate the most suitable metallurgy for the TCCSP INJ-1 well, these categories along with the results are shown below:

- **Generalized Corrosion:** [redacted]
- **Localized Corrosion:** [redacted]
- **Temperature Effects:** [redacted].

Based on the corrosion modeling results, using the TCCSP_OBS-1 data and the closest matching, as well as, most pessimistic formation brine from the USGS produced water database, [redacted] is recommended as the tubular material for the TCCSP INJ-1 well. [redacted]. Higher-grade alloys will be better suited for potential increases in downhole temperature or sustained brine inflow scenarios. The robust corrosion resistance of [redacted] ensures compatibility with the injectate stream and formation brine under the modeled downhole conditions. This assessment underscores the importance of material selection in ensuring the long-term integrity of injection wells under stringent operating conditions.

1.7 Pre-Operational Logging and Testing

The **Pre-Operational Testing Program** describes how TCCSP, LLC. will characterize the TCCSP_INJ-1 and TCCSP_INJ-2 injection wells and all relevant geologic formations at the TCCSP site prior to injection operations pursuant to 40 CFR 146.87. Pre-injection testing will produce data sets that will be used to confirm proper well construction and determine and/or verify the depth, thickness, porosity, permeability, mineralogy, geomechanical, and geochemical profiles of the primary caprock [redacted] and storage reservoirs ([redacted]. Data will also be collected from the [redacted] (first permeable zone above the caprock and lowermost USDW) and the [redacted] (shallow groundwater) to establish a baseline description of the geology, geochemistry, and groundwater quality of the above confining zone formations which will later be compared against data obtained throughout the injection phase. The **Pre-Operational Testing Program** includes:

- Deviation checks (40 CFR 146.87(a)(1))
- Open- and cased-hole well logging (40 CFR 146.87(a)(2) and (a)(3))
- Mechanical integrity testing (40 CFR 146.87(a)(4))
- Rock coring (40 CFR 146.87(b))
- Fluid sampling (40 CFR 146.87(b), (c), and (d)(3))
- Formation and fracture pressure testing (40 CFR 146.87(c) and (d))
- Hydrogeologic testing (40 CFR 146.87(e))
- Baseline above confining zone groundwater quality and geochemistry analysis (40 CFR 146.82(a)(6) and 146.90(d))
- Baseline CO_2 plume and pressure front monitoring (40 CFR 146.90(g))

During the drilling and construction phase of the project, deviation measurements, pursuant to 40 CFR 146.87(a)(1), will be conducted approximately every [redacted] during injection well construction to ensure vertical conduits for fluid movement, such as diverging holes, are not created while drilling. The frequency of deviation checks will be increased as needed based on rock hardness and how formations are drilling to control deviation.

Prior to the installation of the long string casing, caliper, [redacted], and select advanced logs [redacted] will be run within the injection wells. Following open-hole logging and cementing of casing, cased-hole tools, including [redacted], will be run throughout TCCSP_INJ-1 and TCCSP_INJ-2 to provide data that will be used to evaluate injection well construction and critical baseline profiles of geologic units for future comparison.

Internal and external mechanical integrity of the injection wells will be tested to demonstrate the absence of leaks in the wellbore that could result in migration of CO_2 and/or storage reservoir fluids out of the injection zone. Internal mechanical integrity will be demonstrated prior to injection via a [redacted] whereas external mechanical integrity will be demonstrated with temperature measurements obtained via [redacted] installed along the wellbore.

[redacted] will be taken from the confining and injection zones while drilling the injection wells. Analysis of these [redacted] will be coupled with analysis of well logs to demonstrate consistency in subsurface geology, including presence, thickness, porosity, and permeability of the reservoirs across the AoR. Additionally, [redacted] will be collected from the injection zone and analyzed to establish baseline measurements for fluid temperature, pH, conductivity, reservoir pressure, and static fluid level of the injection zones.

Prior to injection operations, formation and fracture pressure will be determined for the injection zones via [redacted] if hole conditions allow. Should [redacted], which minimize damage to the formation, will be performed to determine fracture pressure. Should hole conditions allow, [redacted] will be performed to identify injection zone breakdown pressure. Additionally, upon completion and prior to operations, the hydrogeologic characteristics of the injection zones will be determined via [redacted] within the injection intervals to determine the large-scale transmissivity through the reservoir.

Pursuant to 40 CFR 146.82(a)(6) and 146.90(d), above confining zone samples will be collected to establish baseline conditions for groundwater quality and geochemistry. The [redacted] (shallow groundwater) will be sampled from the [redacted] whereas the [redacted] (first permeable zone above caprock and lowermost USDW) will be sampled from the [redacted] wells. Samples will be collected [redacted] to establish a baseline profile accounting for seasonal variations, threshold values, and the subsequent injection phase sampling suite.

To track CO_2 plume migration throughout subsequent project phases, a [redacted] will be acquired prior to injection which can be compared against subsequent injection phase data to image the CO_2 plume. Baseline profiles from [redacted] will also be collected in all injection, [redacted] wells so that subsequent [redacted] can be performed as needed to verify and quantify fluids if loss of containment is detected via routine testing and monitoring (mechanical integrity testing, injection process monitoring, above confining zone groundwater monitoring, and CO_2 plume and pressure monitoring). Baseline pressure measurements will also be obtained throughout the injection zones and within the above-zone formation ([redacted] to establish baseline conditions which will be used to track the elevated pressure front throughout subsequent phases.

Please refer to the **Pre-Operational Testing Program** for detailed information on the logging, sampling, and testing activities to be performed prior to injection operations.

1.8 Well Operations Plan

Pursuant to the Class VI 40 CFR §146.82, TCCSP, LLC.'s prepared **Injection Well Operations Plan** to describe the planned operation of CO_2 injection wells for the TCCSP. The TCCSP injection wells will be constructed as indicated in the **Injection Well Construction Plan**.

1.8.1 Operational Procedures [40 CFR 146.82(a)(10)]

The CO_2 will come into the site meeting the specifications presented in section **7.3** of the **Testing and Monitoring Plan**. The CO_2 will enter a header and be piped to each injection well. Each well will inject continuously. The CO_2 will be in the supercritical phase as it enters the wellhead and will remain in a supercritical phase within the wellbore. Each injection well will be monitored to ensure safe operations. Safety monitoring includes monitoring the [redacted]
Each system is fully described in section **7.4** of the **Testing and Monitoring Plan.**

Each injection well will have a [redacted], both tied into the injection control system and set to trigger an alarm at the project control room and automatically shut down injection in the well if the maximum allowable surface pressure (MASP) is reached. Injection parameters, including pressure, rate, volume and/or mass, and temperature of the CO_2 stream will be continuously measured and recorded. The pressure and fluid volume of the annulus between the tubing and long-string casing will also be continuously measured by [redacted]. All automatic shutdowns will be investigated before bringing injection activities back online in the well to ensure that no integrity issues were the cause of the shutdown. If an unremedied shutdown is triggered or a loss of mechanical integrity is discovered, TCCSP will immediately investigate and identify as expeditiously as possible the cause of the shutdown. If the investigation determines that the well appears to be lacking mechanical integrity, or if monitoring indicates that the well may be lacking mechanical integrity, TCCSP will:

(1) Immediately cease injection in the affected well and in any other wells that may exacerbate the leakage risk of the affected well

(2) Take all steps reasonably necessary to determine whether there may have been a release of the injected CO_2 stream or formation fluids into any unauthorized zone

(3) Notify the Region 09 UIC Program Director in writing within 24 hours

(4) Restore and demonstrate mechanical integrity prior to resuming injection

(5) Notify the Region 09 UIC Program Director when injection can be expected to resume

The annular space between the tubing and long string casing of each injection well will be pressurized with a non-corrosive fluid. The annulus will be monitored continuously to ensure the integrity of the well. The annulus will be filled with a [redacted]. The annular pressure differential held on the annulus at the wellhead will be [redacted] including times of shut-in. Additional pressure may be required on the annulus; if this is the case, the value will be set in conjunction with U.S. EPA Region 09. The [redacted] will be used to continuously monitor temperature along the length of the casing. Rapid temperature changes or other excursions from a normal operating temperature profile will be investigated to ensure that there has been no breach of wellbore integrity.

TCCSP, LLC. will monitor and maintain the mechanical integrity of each injection well. Well maintenance and workovers will be part of normal operations to keep each injection well in a safe operating condition. Procedures for well maintenance will vary depending on the nature of the procedure, whether that is to pressure test the tubing or replace the packers and/or gauges. All maintenance and workover operations will be monitored to ensure there is no loss of mechanical integrity. [redacted] will be used to ensure pressure is contained during the workovers. Each injection well is designed to allow the [redacted] at the bottom of the tubing to allow the tubing to be removed and replaced as needed while keeping a barrier in place. The [redacted] is set above the packer to allow for replacement, if needed, without removing the packer from the well.

The operational values detailed in **Table 1-53**, **Table 1-54,** and **Table 1-55** were obtained by constructing a hypothetical wellbore model that simulated multiphase fluid flow using [redacted], built to conduct a nodal analysis presented in section **1.6.1,** which was used to determine the range of possible injection rates. Using the analysis, an average injection rate of [redacted] for TCCSP_INJ-2 were assigned. Both wells will have a maximum rate of [redacted] of CO_2 per well. The expected wellhead pressure during injection operations will likely be between [redacted] psia.

The maximum allowable injection pressure was designed to be lower than [redacted] value of the fracture pressure at the shallowest point in the injection zone and is in compliance with EPA's requirements set forth in 40 CFR 146.88(a)). The maximum allowable surface pressure was estimated by using a [redacted] hypothetical wellbore model to calculate the wellhead pressure assuming the maximum allowed bottomhole pressure was attained bottomhole. This is likely possible when CO_2 is injected at the maximum single-well injection rate ([redacted]). The bottomhole pressure was set to [redacted] of the estimated hydraulic fracture pressure at the top perf depth for TCCSP_INJ-1, TCCSP_INJ-2 [redacted], and TCCSP_INJ-2 ([redacted]), values of which were [redacted], respectively. The results estimate each MASP for TCCSP_INJ-1, TCCSP_INJ-2 ([redacted]), and TCCSP_INJ-2 ([redacted]) to be [redacted], respectively. TCCSP, LLC. will ensure that the downhole pressures will not exceed [redacted] of the fracture pressure to ensure injection pressures never exceed the fracture pressure of the injection zone.

Operational parameters are expected to remain constant throughout the duration of the injection period. The only possible changes to operational parameters may stem from variations in the volume of the CO_2 source, which may lead to fluctuations in injection volumes.

Table 1-53. TCCSP_INJ-1 Injection Well Operational Parameters.

Parameters/Conditions	Limit or Permitted Value	Unit
Surface		psia
Downhole		psia
Surface		psia
Downhole		psia
Maximum Injection Rate		Metric tons/year
Average Injection Rate		Metric tons/year
Maximum Injection Volume and/or Mass (period)		Metric tons
Average Injection Volume and/or Mass (period)		Metric tons
Maximum Annulus Pressure		psia
Annular Fluid Weight		
Annulus Pressure/Tubing Differential at the Packer		psi

Table 1-54. TCCSP_INJ-2 ( ) Injection Well Operational Parameters.

Parameters/Conditions	Limit or Permitted Value	Unit
Surface		psia
Downhole		psia
Surface		psia
Downhole		psia
Maximum Injection Rate		Metric tons/year
Average Injection Rate		Metric tons/year
Maximum Injection Volume and/or Mass (period)		Metric tons
Average Injection Volume and/or Mass (period)		Metric tons
Maximum Annulus Pressure		psia
Annular Fluid Weight		ppg
Annulus Pressure/Tubing Differential at the Packer		psi

Table 1-55. TCCSP_INJ-2 ([redacted]) Injection Well Operational Parameters.

Parameters/Conditions	Limit or Permitted Value	Unit
	[redacted]	
Surface		psi
Downhole		psi
Surface		psi
Downhole		psi
Maximum Injection Rate		Metric tons/year
Average Injection Rate		Metric tons/year
Maximum Injection Volume and/or Mass [redacted] period)		Metric tons
Average Injection Volume and/or Mass ([redacted] period)		Metric tons
Annulus Pressure		psi
Annular Fluid Weight		ppg
Annulus Pressure/Tubing Differential		psi

1.8.2 Proposed Carbon Dioxide Stream [40 CFR 146.82(a)(7)(iii) and (iv)]

[redacted] will initially be the primary sources of CO_2 for TCCSP, but additional CO_2 sources throughout the life of the project will be added. The chemical composition of the CO_2 stream will be monitored to ensure it meets minimum composition specifications; these specifications will be refined when sources are finalized and capture equipment is operational. Table 1-56 below displays the chemical composition of the anticipated CO_2 stream. The CO_2 stream coming into the storage site is expected to have a CO_2 concentration of at [redacted] with other chemical constituents, including those listed in Table 1-56.

If the water content of the injectate or stream is higher than [redacted], then corrosion-resistant materials are suggested on all components of the injection well that would come into contact with the CO_2 stream [34]. Therefore, TCCSP_INJ-1 and TCCSP_INJ-2 will have corrosion-resistant materials present where CO_2 will be present. At INJ-2, on average, the CO_2 stream will be at an average of [redacted] and have an estimated density of [redacted] at the well head. After injection downhole into the reservoir zone, the CO_2 stream is anticipated to heat to near formation temperature with an estimated density of [redacted]. Upon injection into the reservoir formation, the CO_2 will remain in the supercritical phase, which will allow for minimal interaction with the formation.

Table 1-56. Specifications of the Anticipated CO_2 Stream Composition.

Component[1]	Specification	Unit
[redacted]	[redacted]	°F
		psi
		vol% dry
		ppmv
		ppmv
		ppmv
		ppmv
		ppmv
		ppbv
		ppmv

1.9 Testing and Monitoring Plan

Testing and Monitoring GSDT Submissions
GSDT Module: Project Plan Submissions ***Tab(s):*** Testing and Monitoring tab Please use the checkbox(es) to verify the following information was submitted to the GSDT: ☒ Testing and Monitoring Plan ***[40 CFR 146.82(a)(15) and 146.90]***

The **Testing and Monitoring Plan** describes how TCCSP, LLC. will monitor injection operations at the TCCSP site, pursuant to 40 CFR 146.90, for the duration of the [redacted] injection phase. The **Testing and Monitoring Plan** has been designed to evaluate project performance, verify compliance with permitted conditions, detect risks and demonstrate USDW non-endangerment, and if in the unlikely event of loss of containment from the storage complex, allow for detection of out-of-zone fluids so that impacts on groundwater may be mitigated. Additionally, testing and monitoring data collected will be used to validate and adjust geological models used to predict the movement of CO_2 and pressure within the storage zones to support AoR re-evaluations. The **Testing and Monitoring Plan** includes:

- CO_2 stream analysis
- Continuous recording of operational parameters
- Corrosion monitoring
- Above confining zone groundwater monitoring
- Mechanical integrity testing
- Pressure fall-off testing
- CO_2 plume and pressure front tracking
- Seismicity monitoring

TCCSP, LLC. plans to use [redacted] project wells to inject and monitor injection operations and groundwater resources. The project wells include two injection wells (TCCSP_INJ-1 and TCCSP_INJ-2), [redacted]. TCCSP_INJ-1 will be completed within the [redacted] whereas TCCSP_INJ-2 will first be completed within the [redacted] thereafter. Testing and monitoring activities including mechanical integrity testing, CO_2 stream analysis, continuous monitoring of operational parameters (i.e., injection rate, volume, temperature, pressure, annulus pressure, annulus fluid volume), corrosion monitoring, and [redacted] will be performed within the injection wells, on their well pad, or along the [redacted] wells will utilize [redacted] deployed within all injection zones and will be capable of directly monitoring the pressure and temperature of each storage reservoir. In addition to the injection and [redacted] monitoring wells collecting data from the storage reservoirs, [redacted] will be acquired across the TCCSP site to track the CO_2 plume throughout the subsurface. The [redacted] monitoring wells ([redacted]) will be completed in the [redacted] (first permeable zone above caprock and lowermost USDW), and [redacted] will be drilled into the [redacted] (shallow groundwater zone) for above confining zone groundwater monitoring (pressure/temperature monitoring within the [redacted]).

The site-specific methods, strategies, and resultant characterization data will inform the TCCSP model to better understand and predict future system changes due to CO_2 injection operations. The **Testing and Monitoring Plan** will be reviewed at a minimum of once every five years to comply with 40 CFR 146.90(j). The plan will be adjusted accordingly with the results of site testing, monitoring, and modeling to meet any changes to the facility of site conditions over time. All amended plans will be sent to the U.S. EPA Region 09 UIC Program Director for approval as outlined in the permit modification requirements under 40 CFR 144.39, 144.41, and 146.90(j). Should no amendment to the plan be required, TCCSP, LLC. will submit evidence to the UIC Program Director supporting the "no amendment" determination. Results of the activities described throughout the **Testing and Monitoring Plan** may trigger action according to the **Emergency and Remedial Response Plan**. Please refer to **Table 1-57** for a summary of the injection phase testing and monitoring program, and the **Testing and Monitoring Plan** for detailed information on the methods, locations, and frequencies of testing and monitoring activities.

Table 1-57. Summary of the Testing and Monitoring Methods for TCCSP.

Monitoring Category	Monitoring Parameter	Technology /Method	Purpose (40 CFR Section Reference)
CO_2 Stream Analysis	[redacted]		146.90(a) 146.91(a)(1) 146.91(a)(7)

Monitoring Category	Monitoring Parameter	Technology /Method	Purpose (40 CFR Section Reference)
Continuous Recording of Operational Parameters			146.88(e)(1) 146.90(b) 146.91(a)(2)
			146.88(e)(1) 146.90(b) 146.91(a)(2)
			146.88(e)(1) 146.90(b) 146.91(a)(2)
			146.88(e)(1) 146.90(b) 146.91(a)(2)
			146.88(e)(1) 146.90(b) 146.91(a)(6)
Corrosion Monitoring			146.90(c) 146.91(a)(7)
Above Confining Zone Groundwater Monitoring			146.90(d) 146.91(a)(7)
			146.90(d) 146.91(a)(7)
			146.90(d) 146.91(a)(7)
Mechanical Integrity Testing			146.88(d) 146.89(a)(1) 146.89(b) 146.91(a)(7) 146.91(b)(1)
			146.88(d) 146.89(a)(2) 146.89(c) 146.90(e) 146.91(a)(7) 146.91(b)(1)
Hydrogeologic Testing			146.90(f) 146.91(a)(7)
Indirect CO_2 Plume Tracking			146.90(g)(2) 146.91(a)(7)
Direct Pressure Front Tracking			146.90(g)(1) 146.91(a)(7)
Seismicity Monitoring			146.90(i) 146.91(a)(7)

Monitoring Category	Monitoring Parameter	Technology /Method	Purpose (40 CFR Section Reference)
		[redacted]	

[redacted]

1.10 Injection Well Plugging

Injection Well Plugging GSDT Submissions

GSDT Module: Project Plan Submissions
Tab(s): Injection Well Plugging tab

Please use the checkbox(es) to verify the following information was submitted to the GSDT:
☒ Injection Well Plugging Plan ***[40 CFR 146.82(a)(16) and 146.92(b)]***

Prior to plugging the injection wells, mechanical integrity will be demonstrated to ensure no pathway has been established between the injection zone and the USDWs or ground surface according to 40 CFR 146.82(a)(16) and 40 CFR 146.92(b).

After the [redacted] injection period, the injection wells [redacted] to ensure containment of the CO_2 in the injection zone. Prior to plugging the injection wells, bottom hole measurements will be taken from [redacted] to determine bottomhole reservoir pressure and the necessary fluid density to kill the well. Subsequently, the well will then be flushed with a brine fluid with sufficient kill weight [40 CFR §146.92]. The mechanical integrity of the wells will be determined to ensure no communication has been established between the injection zone and the USDWs or ground surface (per 40 CFR § 146.92). All casing in the wells will be cemented to the surface during construction [40 CFR §146.86] and will not be retrievable at abandonment.

Upon permanent cessation of well operations, the tubing and packer will be removed. After removal of the tubing and packer, the [redacted] to plug open perforations, along with the balanced-plug placement method, will be used to plug the well. If, after flushing, the tubing and packer cannot be released, an [redacted] will be used to cut off the tubing above the packer and the packer will be left in the well, and the [redacted] will be used for plugging the injection formation below the abandoned packer. After removal of the tubing and packer, the [redacted] will be used to plug the well. All the casing strings will be cut off at least [redacted] below the surface, below the plow line. A blanking plate with the required permit information will be welded to the top of the cutoff casing. All surface features associated with the plugged well and well-pad will be removed. A plugging report will be submitted within 60 days after plugging operations are completed to the U.S EPA Region 09 UIC Director [40 CFR §146.92].

For more specific information on well plugging procedures, please refer to the **Injection Well Plugging Plan.**

1.11 Post-Injection Site Care (PISC) and Site Closure

PISC and Site Closure GSDT Submissions
GSDT Module: Project Plan Submissions ***Tab(s):*** PISC and Site Closure tab Please use the checkbox(es) to verify the following information was submitted to the GSDT: ☒ PISC and Site Closure Plan ***[40 CFR 146.82(a)(17) and 146.93(a)]***
GSDT Module: Alternative PISC Timeframe Demonstration ***Tab(s):*** All tabs (only if an alternative PISC timeframe is requested) Please use the checkbox(es) to verify the following information was submitted to the GSDT: ☒ Alternative PISC timeframe demonstration ***[40 CFR 146.82(a)(18) and 146.93(c)]***

The PISC phase will begin when all CO_2 injection ceases and ends with site closure. TCCSP, LLC. proposes a [redacted] PISC period based on results from computational modeling as discussed in the **AoR and Corrective Action Plan** as well as the **PISC and Site Closure Plan**. Per 40 CFR 146.93(b), TCCSP, LLC. will monitor for CO_2 plume movement, pressure fall-off and groundwater quality to demonstrate non-endangerment of USDWs throughout the PISC phase and at site closure. The **PISC and Site Closure Plan** describes the post-injection modeling that was completed to determine the pressure differential, position of the CO_2 plume, and prediction of CO_2 migration. TCCSP, LLC. also provides information required under 40 CFR 146.93(c) to justify a [redacted] PISC period based on available modeling data. Additionally, there is a detailed description of the post-injection monitoring plan and the site-closure plan. The numerical reservoir model used for calculating the AoR was also used for the post-injection site-care and site-closure analysis.

Computer simulations indicate that the CO_2 plume expands from the injection wells in a [redacted]. Starting from the [redacted] year in the injection phase and onwards, the plume mainly moves in the direction of the [redacted] at TCCSP. During the post-injection period, the CO_2 plume mainly migrates [redacted] and its lateral movement is predictable and substantially slows with time. At the end of the [redacted] proposed PISC timeframe, the modeled simulations indicate that the CO_2 plume is contained inside the injection intervals, stabilized and estimated to be [redacted]. Additionally, the modeling results indicate that there is less than [redacted] in overall area of the CO_2 plume between [redacted]. Based on the model results the maximum pressure build-up declines to below [redacted], which is less than [redacted] of the pressure build-up during injection, within [redacted] after injection shut-in. Given the fast CO_2 plume stabilization and rapid pressure decrease in the injection formation predicted by the computational modeling, a [redacted] PISC is appropriate to ensure injected CO_2 poses no long-term threat to the overlying USDWs.

Following the cessation of injection, all injection wells will be [redacted] and will continue to contribute to the collection of data as part of the TCCSP, LLC. monitoring

program. [redacted] monitoring technologies are proposed to be added during the PISC phase of the project. The post-injection phase will include external mechanical integrity testing, groundwater monitoring above the confining zone, indirect CO_2 plume monitoring, and direct pressure monitoring. [redacted] during the post-injection phase of the project, the monitoring data will be incorporated into computational models and the monitoring plan will be reviewed and updated, if needed, based on modeling results.

Once TCCSP, LLC. demonstrates plume and pressure stabilization, as well as non-endangerment of local USDWs, well plugging and abandonment will commence. Abandonment shall be performed to prevent the movement of injection or formation fluids out of the storage complex. Prior to well plugging, the mechanical integrity of the wells will be verified by the [redacted] placed in the monitoring wells. The well plugging and abandonment will follow the methodology described in the **Injection Well Plugging Plan**, except that CO_2-resistant cement need not be utilized in wells that do not encounter CO_2 at depth. See the **PISC and Site Closure Plan** for more details.

1.12 Emergency and Remedial Response

Emergency and Remedial Response GSDT Submissions
GSDT Module: Project Plan Submissions ***Tab(s):*** Emergency and Remedial Response tab Please use the checkbox(es) to verify the following information was submitted to the GSDT: ☐ Emergency and Remedial Response Plan ***[40 CFR 146.82(a)(19) and 146.94(a)]***

The **Emergency and Remedial Response Plan (ERRP)** details actions that TCCSP, LLC. shall take to address movement of the injection fluid or formation fluid in a manner that may endanger a USDW during the construction, operation, or post-injection site care periods, pursuant to 40 CFR 146.82(a)(19) and 146.94(a). Examples of potential risks include: (1) injection or monitoring well integrity failure, (2) injection well monitoring equipment failure, (3) natural disaster, (4) fluid leakage into a USDW, (5) CO_2 leakage to USDW or land surface, or (6) an induced seismic event. In the case of one of the listed risks, site personnel, project personnel, and local authorities will be relied upon to implement this ERRP.

Prior to the start of CO_2 injection operations, TCCSP, LLC. will communicate to the public, including landowners within the AoR, about any event that requires an emergency response to ensure that the public understands what happened and whether there are any environmental or safety implications. This will include a detailed description of the event, any impacts to the environment or other local resources, how the event was investigated, what actions were taken, and the status of the remediation. Response personnel that service the area will be notified and provided with information of the nature of the operations, potential risks, and appropriate response approaches for the various emergency scenarios.

The ERRP will be reviewed at least once every five years following it approval, within one year of an AoR reevaluation, within the timeframe indicated by the U.S EPA Region 09 UIC Program

Director following any significant changes to the injection process or the injection facility, or an emergency event, or as required by the permitting agency. The Emergency Contact List provided in the ERRP will be updated annually. Periodic training will be provided to well operators, plant safety and environmental personnel, the plant manager, plant superintendent, and corporate communications to ensure that the responsible personnel have been trained and possess the required skills to perform their relevant emergency response activities described in the ERRP.

1.13 Injection Depth Waiver and Aquifer Exemption Expansion

Injection Depth Waiver and Aquifer Exemption Expansion GSDT Submissions
GSDT Module: Injection Depth Waivers and Aquifer Exemption Expansions ***Tab(s):*** All applicable tabs Please use the checkbox(es) to verify the following information was submitted to the GSDT: ☐ Injection Depth Waiver supplemental report ***[40 CFR 146.82(d) and 146.95(a)]*** ☐ Aquifer exemption expansion request and data ***[40 CFR 146.4(d) and 144.7(d)]***

Not Applicable for TCCSP.

1.14 Other Information

Not Applicable for TCCSP.

1.15 Environmental Justice

TCCSP is located in Tulare County, California. Tulare County is located south of Fresno and north of Bakersfield in Central California encompassing parts of the San Joaquin Valley and the Sierra Nevada Foothills. According to the 2020 census, the population is around 473,117 people [35]. **Figure 1-80** shows the demographic breakdown of the county.

[redacted]

Communities in the region are in Tulare County, California and are shown below in **Figure 1-82**. They are numerous environmental justice communities surrounding the project area such as Tule River Reservation, Matheny, Tipton, Woodville, Woodville Farm Labor Camp, East Porterville, Poplar Cotton Center, Porterville 101 and 102*, Alpaugh, Richgrove, Allensworth, Earlimart, Ducor, and Terra Bella (refer to **Figure 1-82:** Map of census tracts and census-designated places (CDP) in the project area).

Tulare County has the most disadvantaged communities in the San Joaquin Valley [39]. Additionally, according to a PolicyLink report that used the year 2000 census data, People of Color were more likely to live in census designated places and unincorporated areas than those identifying as white. Around 80% of the population living in the CDP are people of color and 67% identify as low-income (earning <34,999 per year). Additionally, around 82% of the population living in unincorporated areas identify as people of color, and 67% also identify as low income (earning <34,999 per year) [39]. These disparities are also found in environmental monitoring data, as according to the CalEnviroScreen 4.0 (see **Figure 1-82**), the majority of census-designated places and unincorporated areas are also within the 90th-100th percentile in linguistic isolation and education [38].

Table 1-58 presents projected benefits and impacts on the communities in the project area. It also displays the anticipated tracking methods to be employed for TCCSP, the quantification metric, and the term for realization.

The proposed project prioritizes engagement with and for the benefit of communities and to mitigate potential harms. Integrating economic and social data will help both the project team and local stakeholders understand potential benefits and disbenefits/burdens associated with TCCSP.

Figure 1-80. Demographics of Tulare County population according to the 2020 Census data [37].

Figure 1-81. Population demographics of [redacted], CA according to 2021 Census estimates [36].

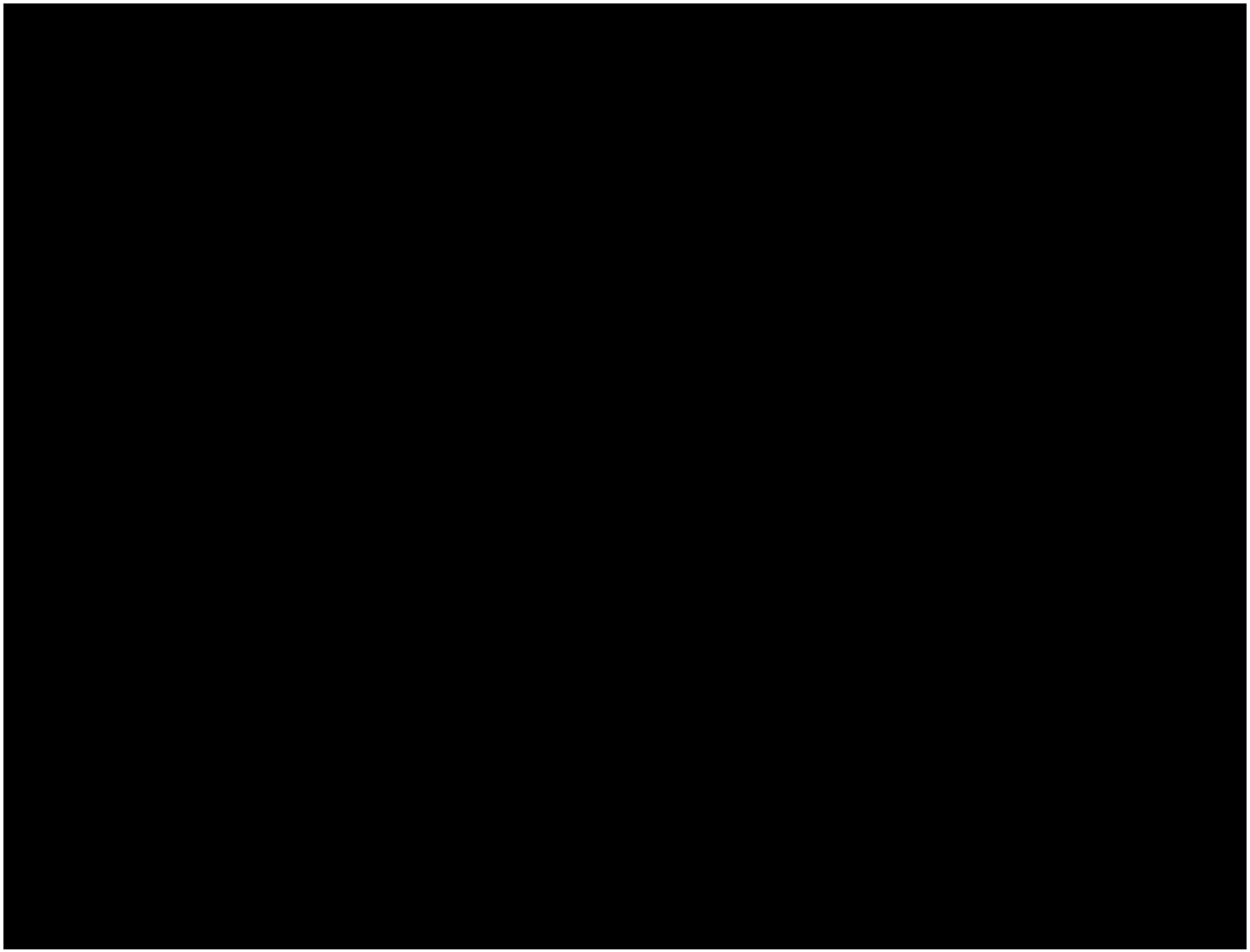

Figure 1-82. Map of communities (census-designated places) and census tracts (shown outlined in grey) surrounding the TCCSP project area. CalEnviroScreen 4.0 results for project area communities included [38], [39].

Table 1-58. Summary of TCCSP Benefits and Impacts (adapted from TCCSP J40 Initiative Plan Development Proposal).

Projected Benefits and Impacts	Anticipated Tracking Method	Anticipated Quantification Metric	Term for Realization of Benefit
Clean Energy Jobs	[redacted]		
Economic Stimulus			
Supplier Diversity			
Increased Traffic & Road Congestion			
Increased Generator & Tail Pipe Emissions			
Increased Dust & Noise Pollution			
Use of limited natural resources			
USDW Contamination			
Atmospheric Leak of Fugitive CO_2			
Asphyxiation (Catastrophic leak)			
Loss of species biodiversity in Pixley Wildlife Refuge			
Interfere/ impact on other land uses (e.g. recreational use of open space - Pixley Wildlife Refuge and Capinero Creek Restoration Site)			

1.16 References

[1] Bartow, J.A. 1991. "The Cenozoic Evolution of the San Joaquin Valley, California," U.S. Geological Survey Professional Paper 1501, p. 1–40.

[2] Scheirer, A.H. and Magoon, L.B., 2007, "Age, Distribution, and Stratigraphic Relationship of Rock Units in the San Joaquin Basin Province, California," Chapter 5: Petroleum Systems and Geologic Assessment of Oil and Gas in the San Joaquin Basin Province, California, p. 1-107.

[3] Johnson, C.L. Graham, S.A. 2007. "Middle Tertiary Stratigraphic Sequences of the San Joaquin Basin, California," USGS Chapter 6: Petroleum Systems and Geologic Assessment of Oil and Gas in the San Joaquin Basin Province, California.

[4] Hewlett, J. S., Phillips, S., and Bazeley, W. J. M. 2014, Middle Tertiary Sequence Stratigraphy, Southern San Joaquin Basin, California, Pacific Section American Association of Petroleum Geologists, https://doi.org/10.32375/2014-MP51

[5] Magoon, L.B., Lillis, P.G. and Peters, K.E. 2009. "Petroleum Systems Used to Determine the Assessment Units in the San Joaquin Basin Province, California," Petroleum Systems and Geologic Assessment of Oil and Gas in the San Joaquin Basin Prince, California, Chapter 8, p. 1-64.

[6] Tye, R.S., Hewlett, J.S., Thompson, P.R. and Goodman, D.K. 1993. "Integrated stratigraphic and depositional-facies analysis of parasequences in a transgressive systems tract, San Joaquin Basin, California,": AAPG Memoir 58, Siliciclastic sequence stratigraphy: recent developments and applications, Chapter 5, p. 99-133.

[7] Graham, S. and Johnson, C.L. 2004. "Stratigraphic Megasequences of the San Joaquin Basin: Origins, Characteristics, and Petroleum Occurrence," American Association of Petroleum Geologists Abstract.

[8] Bloch, R.B., 1991, "Studies of the Stratigraphy and Structure of the San Joaquin Basin, California," A Dissertation Submitted to the Dept. of Applied Earth Sciences and the Committee on Graduate Studies, Standford University, v. 1.

[9] Loken, K.P. 1959. "Gill Ranch gas field, in Summary of operations, California oil fields: San Francisco, Calif., Annual Report of the State Oil and Gas Supervisor," v. 45, no. 1, p. 27–32 [also available in California Division of Oil and Gas, Summary of Operations, 1915-1999: California Division of Conservation, Division of Oil, Gas, and Geothermal Resources, Publication No. CD-3, and at ftp://ftp.consrv.ca.gov/pub/oil/Summary_of_Operations/1959/].

[10] Bartow, J.A., McDougall, K., 1984, "Tertiary Stratigraphy of the Southeastern San Joaquin Valley, California", Geological Survey Bulletin 1529-J, p-J1–J38.

[11] Addicott, W.O. 1970. "Miocene gastropods and biostratigraphy of the Kern River area, California,": U.S. Geological Survey Professional Paper 642, p. 174.

[12] California Division of Oil, Gas, and Geothermal Resources. 1998. "California Oil & Gas Fields Volume 1 – Central California," v. 1, p. 1 – 499.

[13] California Geological Survey, Fault Traces from California Department of Conservation, http://maps.conservation.ca.gov/cgs/informationwarehouse/. Accessed 15 July, 2024.

[14] Timur, A., 1968. An Investigation of Permeability, Porosity, and Residual Water Saturation relationships[C]//SPWLA 9th Annual Logging Symposium. Society of Petrophysicists and Well-Log Analysts.

[15] Bent, J.V. 1985. "Petrographic Reconnaissance of Upper Oligocene-Middle Miocene Sandstones of the San Joaquin Basin, California,": Master's Thesis, Standford University, California.

[16] Pettijohn F.J., Potter P.E. and Siever R., 1987, Sand and sandstones, 2nd edition Springer-Verlag, New York.

[17] Unruh, S. 2016. "Diagenesis and Reservoir Quality of the Oligocene Vedder Sandstones, of the Rio Bravo Oil Field, Kern County, California," Msc Thesis, Dept. Geological Sciences, California State University, Bakersfield.

[18] Chevron, U.S.A., Inc., 2023, Chevron Kern River Eastridge CCS Project Underground Injection Control (UIC) Permit Application Class VI Pre-Construction Permit Application Nos. R9UIC-CA6-FY24-1.1-1.4

[19] Eaton, B.A. 1969. "Fracture Gradient Prediction and Its Application in Oilfield Operations," Journal of Petroleum Technology, October, 1969, v. 246, p. 1353-1360

[20] United States Geological Survey National Seismic Hazard Map, 2023, www.usgs.gov/media/images/hazard-map-2023-50-state-update-national-seismic-hazard-model-project.

[21] USGS (2019). ArcGIS Web Application. [online] Arcgis.com. Available at: https://usgs.maps.arcgis.com/apps/webappviewer/index.html?id=5a6038b3a1684561a9b0aadf88412fcf.

[22] Jennings, C.W. and Saucedo, G.J., 1999, Simplified Fault Activity Map of California, Revised 2002, Tousson Toppozado and David Branum, (Jennings and Sausedo, 1999)

[23] Amec Foster Wheeler Environment & Infrastructure, Inc (2017). GEOLOGY AND SOILS IMPACTS ANALYSIS, Pixley Groundwater Banking Project Tulare County, California. [online] usbr.gov, Amec Foster Wheeler Environment & Infrastructure, pp.1–19. Available at: https://www.usbr.gov/mp/nepa/includes/documentShow.php?Doc_ID=31385#:~:text=The%20Pond-Poso%20Creek%20fault%20consists%20of%20a%202%2F3,a%202-mile%20segment%20of%20the%20fault%20is%20active..

[24] United States Geological Survey Earthquake Hazards Program, accessed 2024, https://earthquake.usgs.gov/earthquakes/search/

[25] Tulare County, 2012, Revised Draft General Plan 2030 Update, Tulare County, Resource Management Agency, http://generalplan.co.tulare.ca.us/ (Tulare County, 2012).

[26] Luhdorff, Scalmanini. 2017, "Geologic and Stratigraphic Evaluation Pixley Groundwater Banking Project, Tulare County, California," Luhdorff & Scalmanini, Consulting Engineers, Woodland, CA. January 18, 2017.

[27] Kang, M., Perrone, D., Wang, Z., Jasechko, and Rohde, M.M. 2020. "Base of fresh water, groundwater salinity, and well distribution across California," PNAS, 32302-32307, v. 117, n. 51.

[28] United States Environmental Protection Agency (EPA), 1988, Survey of Methods to Determine Total Dissolved Solids Concentrations, Underground Injection Control Program, Washington D.C., EPA LOE Contract NO.68-03-3416, 87p.

[29] Bateman, R.M., 2012, Openhole Log Analysis and Formation Evaluation, second edition, Society of Petroleum Engineers, 688p.

[30] California Department of Water Resources "SGMA Data Viewer" 2024. https://sgma.water.ca.gov/webgis/?appid=SGMADataViewer#gwlevels.

[31] Lower Tule River Irrigation District. (n.d.). Lower Tule River Irrigation District. Retrieved August 10, 2024, from http://www.ltrid.org/

[32] Madalyn S. Blondes, Katherine J. Knierim, Mary R. Croke, Philip A. Freeman, Colin Doolan, and Amanda S. Herzberg, Jenna L. Shelton, 2023, U.S. Geological Survey National Produced Waters Geochemical Database (version 3.0, November 2023): U.S. Geological Survey, https://doi.org/10.5066/P9DSRCZJ.

[33] Rochelle, C., Czernichowski-Lauriol, I., and Milodowski, A., 2004, The impact of chemical reactions on CO_2 storage in geological formations: A brief review. Geological Society, London, Special Publications. 233. 87-106. 10.1144/GSL.SP.2004.233.01.07.

[34] Meyer, J.P. 2007. API Summary of Carbon Dioxide Enhanced Oil Recovery Injection Well Technology. Prepared for API

[35] "U.S. Census Bureau Quickfacts: Tulare County, California." QuickFacts Tulare County, California, U.S. Census Bureau, www.census.gov/quickfacts/fact/table/tularecountycalifornia/PST045222. Accessed 22 Dec. 2023.

[36] "Pixley, CA." Data USA, https://datausa.io/profile/geo/pixley-ca#demographics. Accessed 22 Dec. 2023.

[37] "Tulare County." Data USA, datausa.io/profile/geo/tulare-county#demographics. Accessed 22 Dec. 2023.

[38] CalEnviroScreen 4.0, California Office of Environmental Health Hazard Assessment, https://experience.arcgis.com/experience/11d2f52282a54ceebcac7428e6184203/page/CalEnviroScreen-4_0/. Accessed 22 Dec. 2023

[39] Flegal, C., Rice, S., Mann, J., Tran, J., 2013, "California Unincorporated: Mapping Disadvantaged Communities in the San Joaquin Valley, PolicyLink,policylink.org/sites/default/files/CA%2520UNINCORPORATED_FINAL.pdf.

[40] California Air Resources Board, "CARB Pollution Mapping Tool," 2024. https://ww2.arb.ca.gov/resources/carb-pollution-mapping-tool.

[41] V. N. Balashov, G. D. Guthrie, J. A. Hakala, C. L. Lopano, J. D. Rimstidt, and S. L. Brantley, "Predictive modeling of CO_2 sequestration in deep saline sandstone reservoirs: Impacts of geochemical kinetics," *Geochem. Asp. Geol. Carbon Storage*, vol. 30, pp. 41–56, Mar. 2013, doi: 10.1016/j.apgeochem.2012.08.016.

[42] A. Raza, R. Gholami, M. Rabiei, V. Rasouli, R. Rezaee, and N. Fakhari, "Impact of geochemical and geomechanical changes on CO2 sequestration potential in sandstone and limestone aquifers," *Greenh. Gases Sci. Technol.*, vol. 9, no. 5, pp. 905–923, Oct. 2019, doi: 10.1002/ghg.1907.

[43] T. D. Rathnaweera, P. G. Ranjith, and M. S. A. Perera, "Experimental investigation of geochemical and mineralogical effects of CO2 sequestration on flow characteristics of reservoir rock in deep saline aquifers," *Sci. Rep.*, vol. 6, no. 1, p. 19362, Jan. 2016, doi: 10.1038/srep19362.

[44] Geoactive Limited. (2024). *Interactive Petrophysics (IP) 2024 user/help guide* [Software documentation]. Geoactive Limited.

[45] Spooner, P. (2014, May). *Lifting the fog of confusion surrounding clay and shale in petrophysics* (Paper VV). Presented at the SPWLA 55th Annual Logging Symposium, Abu Dhabi, United Arab Emirates. Society of Petrophysicists & Well Log Analysts.

[46] Goodman, A., Sanguinito, S., Levine, J. (2016). *Prospective CO2 resource estimation methodology: Refinement of existing US-DOE-NETL methods based on data availability, International Journal of Greenhouse Gas Control,* v. 54, p. 952–965.

[47] Goodman, A.; Hakala, A.; Bromhal, G.; Deel, D.; Rodosta, T.; Frailey, S.; Small, M.; Allen, D.; Romanov, V.; Fazio, J.; Huerta, N.; McIntyre, D.; Kutchko, B.; Guthrie, G.. (2011). *U.S. DOE methodology for the development of geologic storage potential for carbon dioxide at the national and regional scale.* International Journal of Greenhouse Gas Control, v. 5, p. 242–249.

[48] Peck, W.D., Glazewski, K.A., Klenner, R.C.L., Gorecki, C.D., Steadman, E.N., and Harju, J.A. (2014). *A workflow to determine CO2 storage potential in deep saline formations*: Energy Procedia, v. 63, p. 5231–5238.

[49] Walters, R., Zoback, M. (2015). *Characterizing & Responding to Seismic Risk Associated with Earthquakes Potentially Triggered by Fluid Disposal and Hydraulic Fracturing,* doi:10.1785/0220150048 Seismological Research Letters Volume 86, Number 4

1.17 Appendix

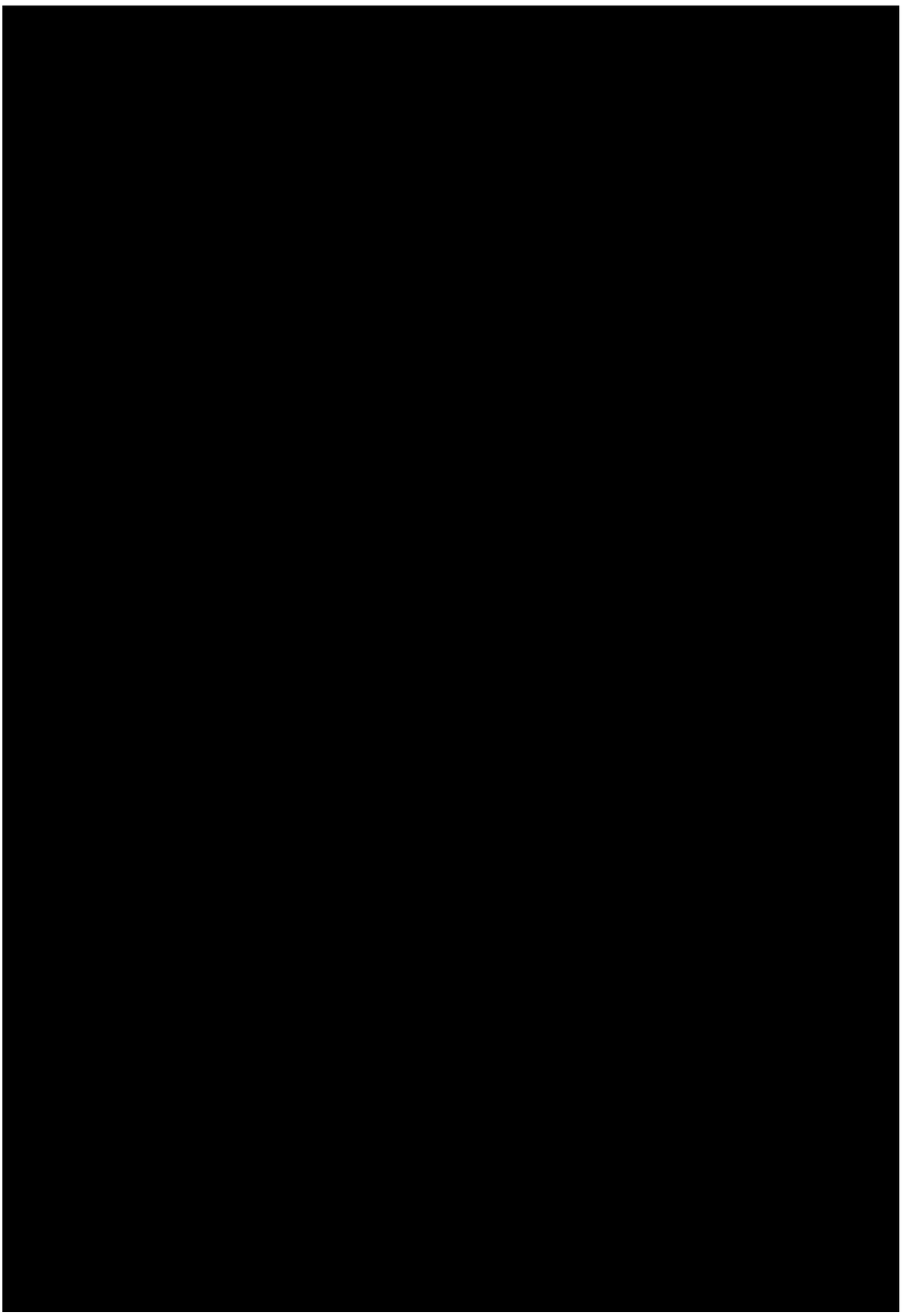

Appendix Figure 1-1. CO_2 stream analysis from [redacted].

Appendix Table 1-1. Groundwater well completion reports within the AoR and the [redacted] surrounding the AoR [30].

WCR Number*	Well Use	Latitude	Longitude	APN	Total Drilled Depth	Total Completed Depth	Top of Perforated Interval	Bottom of Perforated Interval
[redacted]								

*Blue highlighted WCR Numbers indicate wells within the [redacted] of the AoR.

Appendix Table 1-2. Legacy wells used in SEM structural modeling and petrophysics.

Name	Well ID (for Figure 1-44)	UWI	Latitude	Longitude	KB Datum	TD (TVDSS)	TD (MD)
[redacted]							